DYNAMIC MODELS OF BOF BASED O
SUBLANCE MEASUREMENTS

by

Chakravartula Gopi Krishna

DEPARTMENT OF MATERIALS AND METALLURGICAL ENGINEERING
INDIAN INSTITUTE OF TECHNOLOGY KANPUR

January, 2000

DYNAMIC MODELS OF BOF BASED ON SUBLANCE MEASUREMENTS

A Thesis Submitted
in Partial Fulfillment of the Requirements
for the Degree of
MASTER OF TECHNOLOGY
by

Chakravartula Gopi Krishna

to the

DEPARTMENT OF MATERIALS AND METALLURGICAL ENGINEERING
INDIAN INSTITUTE OF TECHNOLOGY KANPUR
JANUARY, 2000

Dedicated to

Priyamaina Amma Nanna mariyu Chelleliki

CERTIFICATE

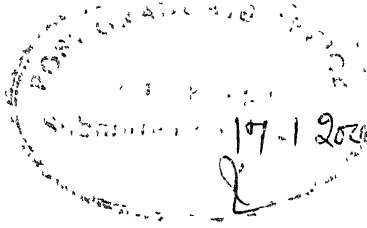

It is certified that the work contained in this thesis entitled **Dynamic Models of BOF Based on Sublance Measurements** has been carried out by **Mr. Chakravartula Gopi Krishna** under my supervision and that this work has not been submitted elsewhere for the award of a degree.

17.1.2000

Dr. Brahma Deo
Professor
Dept. of Materials and Metallurgical Engineering
Indian Institute of Technology, Kanpur

Acknowledgements

With immense pleasure I express my deep sense of gratitude to Dr. Brahma Deo, for his guidance and valuable suggestions through out the work, with out which this modest accomplishment of mine would not have been possible. I cherish the moments of working with him. I would also like to thank Mrs. Brahma Deo for her warmth and affection.

I am indebted to my parents, grandparents and sister for their constant encouragement and support through out my carrer. They have been by source of inspiration.

I am also thankful to my friends Anita, Lakshmi Narayana, Annaiah (hemasunder), M. Mahesh, G. K. Raju, P. Kumar, Krishna, Rohitashw Prasad, Srikanta Kundu, Mukut Sen and many more whose company made my stay at IIT-K a memorable one.

Last but not the least, I am thakful to many more whose list is never ending, for their cooperation.

Chakravartula Gopi Krishna
IIT Kanpur
Jan 2000

Contents

List of Figures

List of Tables

List of Symbols

a	radius of the droplet
a_0,a_i	regression constant and regression coefficients
a_c	activity of carbon in hot metal
A	interfacial area (cm^2)
A	sucked air or slopping gas volume
b_0,b_2	coefficient of heat balance
[%C]	carbon concentration in the both expressed in mass%
ΔC	amount of decarburization
C_c	mass % of carbon in the melt
C_s	bulk concentration of sulphur (mass %)
C^b, C^i	are bulk and interfacial concentration of carbon, mol/cc
C_o	Critical carbon content below which decarburization does not substantially occur
C_p	parameter derived statistically based on operational variables
C_{SL}	carbon content determined by sensor lance
C_{fa}	aimed carbon content
C_p	specific heat capacity of molten steel (Kcal / kg ^{0}C)
C_B	carbon content of charge (%)
C_r^d	carbon concentration of droplet at the time of falling in metal
C_o^d	droplet carbon concentration at the time of ejection of droplet
C_e	equilibrium carbon concentration
C_τ^d	carbon concentration of droplet at time of falling in metal

$C_b^{(t-\tau)}$	concentration of carbon in bulk metal at time $t-\tau$
C_b^+	bath concentration before fall,
C_b^-	bath concentration after fall
$(\%CaO)$	mass %CaO of slag
c_t	end point carbon
c_o	sublance carbon
c_t'	predictedend point carbon
D	diffusivity of carbon
dO_2	total oxygen
$dO_{2_{FeO}}$	amount of oxygen consumed for FeO formation
$dO_{2_{CO}}$	the amount of oxygen consumed for CO formation
dolo1	dolomite added during first blow
dolo2	dolomite added during second blow
e_t	the most recent error from forecasting
error(i)	error of the feedback model
f	activity coefficient of sulphur in the surface layer and in bulk metal
fi	input oxygen
fo	output oxygen
F	amount of coolant
F_{t+1}	forecast value for the next period
FO_2	amount of oxygen after sublance measurement
FB_c	adjustment of oxygen balance from the feedback
FB_T	adjustment of heat balance from the feedback
FB(i)	feedback value
$(\%Fe)$	mass %Fe in slag
G_{FB}	feedback gain
G	gain
ho	output carbon
hi	input carbon
ΔH_i	the heat produced from each reaction (Kcal / Nm^3 - O_2)

H	on-detective value
hlans2	lance height during second blow
i	intensity of blowing
k_c	mass transfer coefficient of carbon (m/sec)
k_d	mass transfer coefficient (cm/sec)
K_d	mass transfer coefficient within the droplet (cm/sec)
k_g	average mass transfer coefficient in gas film ($\frac{cm}{sec}$)
k_R	rate constant (mol/m2/sec/atm)
K	adsorption coefficient of Sulphur
K	Equilibrium constant
K*	smoothing factor
K'	capacity mass transfer coefficient
k_p	mass transfer coefficient for phosphorus
k_{Mn}	mass transfer coefficient for manganese
l_i	coefficient of statistical model
m	constant of sampling number
Mdlerror(i)	error of the model
Mg.dt	droplet fall in metal
Mn^b	concentration of manganese in the bulk
Mn^i	concentration of manganese at the interface
Mn'_t	end point manganese value predicted
N	number of historical data
n_c	concentration of carbon
O_2	input oxygen
ΔO_2	amount of blowing after sensing (Nm^3/ton of charge)
O_c	oxygen combined with carbon to form CO (Nm^3 - O_2)
O_{Fe}	oxygen combined with Fe to form FeO (Nm^3-O_2)
[O]	dissolved oxygen in metal (ppm)
ore1	ore added in first blow
ore2	ore added during second blow
$P^b_{co_2}$	bulk pressure of CO2. (atm)

$P^i_{co_2}$	interfacial pressure of CO_2
P_{co}, P_{co_2}	partial pressures of CO andCO_2, respectively
$[\%P]$	mass % of phosphorus in metal
$(\%P)$	mass % of phosphorus in slag
p^b	concentration of phosphorus in the bulk
p^i	concentration of phosphorus at the interface
p_t	end point phosphorus predicted
$p_{t_{act}}$	end point phosphorus
Q	top blow oxygen
QB	bottom blowing gas flow rate
Q_{eff}	effective volume flow rate of gas $\left(\frac{m^3}{s}\right)$ from top and bottom
P Q R	Parameters calculated from multiple regression analysis by using actual operational data such as lance height, slag volume , etc.
R_c	rate of carbon transfer (mol / sec)
Si_B	silicon content of charge (%)
s_1,s_2	are coefficients
slag1	slag added during first blow
slag2	slag added during second blow
(T.Fe)s	(T. Fe) at in - blow sublance
t	time in sec
t_{max}	the total time of second blow period
Δt	small time steps
T	absolute temperature of the bath
T_f	average gas film temperature (^oK)
T_f , C_f	temperature and carbon content of the bath at blowing end respectively
T_{SL} C_{SL}	temperature and carbon content of the bath measured by the sensor lance
T_s,T_e	temperature at sublance measurement and at the endpoint,
T_{sub}	cooling capacity of fluxes
T	end point temperature
T_o	sublance temperature
$V_{CO,\ CO_2}$	volume in exhaust gas

$V_{C,I}$	rate of carbon oxidation(%C/min)
V	volume of bulk metal (including droplets) (cm^3)
W_s	weight of slag in tons
W_{sub}	amount of flux
W_{ST}	weight of molten steel
W_t	bath weight in gms
WO_2	oxidation degree
W_{so}	Slag volume except (FeO), (MnO) , (P_2O_5)
Ws	slag volume
WM	Weight of steel
WOBS	waste oxide briquettes
x_i	operational variables
$\overline{X_i}$	Mean value of standard operational variables
x_{co}	represent the mole fraction of CO
x_{co_2}	represent the mole fraction of CO_2
x_{Inr}	represent the mole fraction of inert gas
X_t	most recent observation
Z_i	Operational variables
$\overline{Z_i}$	standard operational variables (mean values)
ρ	density of the melt ($\frac{g}{cm^3}$)
θ_u	fraction of the surface sites not available for the chemisorption of sulfur
ξ	theoretical maximum decarburization rate
γ_i, χ_i, ϵ_i	regression coefficient
γ_0, χ_0	regression Constant
λ_1, μ_1	coefficients
α, α_2, α_3, ζ	constants
β, γ	parameters
γ	coefficient of cooling capacity
α	decarburization efficiency
α_{max}	decarburization efficiency in maximum decarburization period
η	exponential factor

Abstract

latex \noindent\vspace*{0.75cm}

Oxygen steelmaking converter is the single most important unit process in a steel plant and is sometimes called the throbbing heart of a steel plant. Introduction of sublance technology in the early eighties to analyze carbon and temperature in an oxygen steelmaking converter during the blow, approximately 3-4 minutes before the end blow, proved to be an important step in the control of oxygen steelmaking processes. Since the introduction of sublance, the accuracy of end point prediction (hit rate) at most of steel plants has gradually increased from approximately 60% to 90%.

In the present work several new models are developed by using genetic algorithm and multiple linear regression to predict end point carbon, temperature, phosphorus, manganese and dissolved oxygen from sublance data for 3 plants collected from literature. Other operational parameters like slag basicity, ore added during first blow, ore added during second blow, lance life, lance height, dolomite added during first blow etc. are also considered in predicting the end point values.

Using the models developed in the present work, it is possible to predict end point carbon with an accuracy of σ=0.004% for Plant 1, σ =0.005% for Plant 2, σ =0.004% for Plant 3. Temperature can be predicted with σ = 5 ^{O}C for Plant 1, σ = 8 ^{O}C for Plant 2, σ =9 ^{O}C for Plant 3. Phosphorus can be predicted with σ = 0.007% for Plant 1, σ =0.001% for Plant 3. Manganese can be predicted with σ =0.0065% for Plant 1, σ = 0.012% for Plant 3. Dissolved oxygen can be predicted with σ = 34 ppm for Plant 1, σ =140 ppm for Plant 2, σ = 77 for Plant 3.

The variation of capacity mass transfer coefficient K' is studied by using the dynamic models developed . The dependence of K' on gas flow rate is $K' \propto Q^{0.23}$ which implies that variation is slow and, during the blow, K' gradually decreases with time due to fall in rate of decarburization. It is observed that the variation is very slow with time. It is furthur observed that capacity mass transfer coefficient decreases with converter capacity. For example, K' for 100 t converter is greater than that for 200 t and for 300 t converters.

Chapter 1

Introduction

Oxygen steel making process accounts for nearly 65% of the steel produced in the world. A typical diagram of the physical state of an oxygen steel making converter when a single hole lance is used, is shown in Fig 1.1. Most of the plants in world now use multi hole lance instead of a single hole lance.The pure oxygen jet emerging from the nozzle impinges on metal surface. A stream of metal droplets is ejected due to deflection of the jet in the impingment zone. The droplets eventually fall back to metal after their passage through slag or gas slag foam. The amount and size range of the droplets depend on lance nozzle design and lance height whereas the residence time of droplets in slag depends upon the properties of slag. The chemical reactions occur primarily in and around the jet impact zone and in the droplets falling through slag and rising gas bibbles.

In the early years of its development (1952-1962), oxygen steel making process itself was given several names like LD (Linz-Donavitz), BOF (Basic Oxygen Furnace), BOP (Basic Oxygen Steel making), etc. These names were modified in early seventies when bottom blowing process was adopted in which pure oxygen gas was blown through tuyeres located at the bottom of the converter. The tuyeres needed cooling because of the high temperature generated at the tuyere tip. Depending upon the nature of coolant used (viz. fuel oil or natural gas), the new breed of processes were named as Q-BOP, LWS, etc. As a further modification of bottom blowing practice, combined top and bottom blowing processes were invented and today more than 30 commercial names exist for the variety of oxygen steel making process. For the sake of simplicity, however, they all are now

grouped under a single name of 'Combined blown processes'.

The specific combination of top and bottom blowing(i.e. the flow rate and nature of gas through top and/or bottom) adopted at a particular plant depends upon the starting composition of hot metal, capacity of converter, quality of lime, refractory life, desired end point composition of steel, economics of operation, etc. As a result, the steel making process at each steel plant has its own unique features. The blowing time may vary from 15-22 minutes depending upon capacity, oxygen flow rate and nozzle design etc. The control models developed at one plant are rarely applicable to the situation at another steel plant. In a more recent development (since mid eighties), a separate lance called "Sublance" is introduced into the converter to measure temperature and take a sample of metal, only few minutes before the end of the blow. Corrective actions are then taken on the basis of analysis of sample obtained by sublance measurement and this has significantly improved the accuracy of control of obtaining desired end point temperature and carbon of liquid steel. The fine tuning models based on sublance measurement, as also developed in this work, are called "sublance models".

The present work is organized into 7 chapters. Chapter 1 is the present one. Chapter 2 briefly reviews the models published in literature as summarized else where [1], for end point carbon, temperature, dissolved oxygen, phosphorus and manganese, followed by the sublance models developed in the present work. Experimental data used in the present work are given in Chapter 3 and Chapter 4 discusses models for optimal control of end point windows. Chapter 5 presents results and discussion on the sublance models developed in this work and Chapter 6 presents results and discussion of the optimization models. Conclusions and suggestions for further work are presented in chapter 7.

Chapter 2

Review of Models for End Point Carbon, and Temperature Prediction using Sublance Data

2.1 Introduction

Sublance is used in oxygen steelmaking to take a sample and also determine instantaneously the steel composition 3-4 minutes before the end of blow. This analysis is used to determine the amount of oxygen to be blown in remaining part of the blow so as to arrive at a predefined carbon and temperature at the end. Thus, we are concerned with the modelling of trajectory of process during the last few minutes of converter operation. Metal sample is also taken at the end of blow to verify carbon, phosphorus, manganese, dissolved oxygen and temperature achieved. While the blow is in progress, adjustment of lance height can be done and judicious additions of iron ore, raw dolomite and solidified slag (return slag from converter) can be made to control the trajectory of carbon as well as temperature. Since the concentrations of carbon and oxygen are related to each other carbon may also predicted using the dissolved oxygen content of the bath and vice versa. Hence, the models for prediction of end point carbon, temperature, phosphorus, manganese and oxygen from sublance data play an important role in determining the amount

of oxygen to be blown during second blow period and thereby achieve the aim composition of steel.

This chapter briefly reviews the models published in literature. Models developed in the present work are discussed in chapter 3.

2.2 Review of models of decarburization, temperature and dissolved oxygen during end blow period

One of the key objectives during end blow period (i.e. the period after sublance measurement) is the control of decarburization rate and a great deal of research has been done in this area. Several models, both static and dynamic, have been proposed which are suited to specific steel plant conditions. The fundamental basis of various models, adapted from an earlier work [1] are discussed in section 2.2 to section 2.4.

2.2.1 Model by Lee and Rao

Lee and Rao [2] have developed a mixed control model for decarburization in levitated droplets assuming gas phase mass transfer and dissociative adsorption of CO_2 (or interfacial chemical reaction) by studying the kinetics of decarburization in high carbon regime (0.911 - 2.479 wt % C) at 1973 K. The rate equation assuming mass transfer control in the gas phase as

$$-\frac{dc}{dt} = \frac{1200 \cdot A}{\rho V} \cdot \frac{k_g}{RT_f} \ln\left(1 + P^b_{co_2}\right) \tag{2.1}$$

where C_c is wt % of carbon in the melt, A is interfacial area (cm^2), ρ is density of the melt ($\frac{g}{cm^3}$), V is Volume of the melt (cm^3), k_g is average mass transfer coefficient in gas film ($\frac{cm}{sec}$), T_f is average gas film temperature (^oK), $P^b_{co_2}$ is bulk pressure of CO2. (atm).

If interfacial chemical reaction control is assumed as a rate controlling step,then

$$-\frac{dC_c}{dt} = \frac{1200 \cdot A}{\rho V} \cdot k_R \left(\frac{1 + K\theta f C_s}{1 + K f C_s}\right) P^i_{co_2} \tag{2.2}$$

where k_R is rate constant (mol/m2/sec/atm), K is adsorption coefficient of Sulphur, θ_u is the fraction of the surface sites not available for the chemisorption of sulfur, $f = \frac{\gamma_s^b}{\gamma_s^k}$ is activity coefficient of sulphur in the surface layer and in bulk metal, C_s is bulk concentration of sulphur (wt %), $P_{co_2}^i$ is interfacial pressure of CO_2.

On assuming mixed control of mass transfer and interfacial chemical reaction, the decarburization rate is

$$-\frac{dC_c}{dt} = \frac{1200 \cdot A}{\rho V} \cdot \left(\frac{k_g^0 k_R (1 + K\theta f C_s)}{\left(k_g^0 + k_R\right) + \left(k_g^0 + k_R\theta_u\right) K f C_s} \right) \ln\left(1 + P_{co_2}^b\right) \qquad (2.3)$$

where $k_g^0 = \frac{k_g}{RT_f}$.

The experimental results of Lee and Rao showed that

•Liquid phase mass transfer is not a rate controlling step in the high carbon regime. The initial carbon concentration has no discernible effect on the decarburization kinetics.

•Sulphur has a clear and reproducible retarding effect on decarburization. This effect is most pronounced in the range of 0 to 0.05 mass % sulphur.

•The P_{co_2} of the gas mixture has a marked effect on the decarburization kinetics.

•The flow rate of the gas mixture has a small but finite effect on the rate of decarburization.

In low carbon range (C< 0.4 mass %) equation assuming liquid phase mass transfer as control step is

$$R_c = \frac{k_c A}{V}\left(n^b c - n^i c\right) \qquad (2.4)$$

where R_c is rate of carbon transfer (mol / sec), k_c is mass transfer coefficient of carbon (m/sec), n_c is concentration of carbon (b=bulk, i=interface).

Distin, Hallett and Richardson [3] have assumed in their study on the decarburization of liquid Fe-C alloys with O_2 and CO - CO_2 mixtures that the concentration of carbon at the surface becomes virtually zero at the instant of oxide formation. When the oxide appears on the surface Eq. (2.4) is reduced to

$$R_c = \frac{k_c A}{V}\left(n^b c\right)$$

Or

$$-\frac{d[\%C]}{dt} = \frac{k_c A}{V}\left(\%C^b\right) \tag{2.5}$$

where A is surface area of droplet (m^2), V is Volume of droplet (m^2).

For spherical droplets [2]

$$k_c = \frac{5D}{a} \tag{2.6}$$

where D is diffusivity of carbon, a is radius of the droplet.

Lee and Rao calculated the k_c for their experimental conditions as follows:

T = 1973K

$C^b = 0.1\%$

a = 0.2875 cm

D = 3.24 X 10-3 $\frac{cm^2}{sec}$

$$k_c = \frac{5D}{a} = \frac{5*3.24*10^{-3}}{0.2875} = 56.348 * 10^{-5}\frac{m}{sec}$$

They found that mass transfer in the liquid phase is enhanced by about ten times due to electromagnetic levitation as compared to that at stationary condition. This enhancement is brought about as a consequence of motion in the liquid phase. A situation, similar to those for levitated droplets, may be assumed to prevail during decarburization in converter where droplets are ejected from jet impact zone at high velocity.

2.2.2 Model by Chou et al.

Chou, Pal and Reddy [4] have developed a general model for the decarburization process. If it is assumed that hot metal at 1400^0C with a high carbon content is initially charged (for instance, liquid iron containing 4% carbon) in the converter with some scrap, then for the sake of simplicity bath temperature may be approximated to vary linearly with carbon content as follows:

$$T = 1873 - 50[\%C] \tag{2.7}$$

where T is the absolute temperature of the bath, [%C] is carbon concentration in the both expressed in wt. pct.

In an actual converter, bath temperature can be predicted at each time step by dynamic heat and mass balance. When oxygen blows into the liquid metal, the carbon in hot metal will be oxidized by oxygen to form carbon dioxide. At an elevated temperature, the CO_2 will react again with bath carbon according to the Boudouvard reaction

$$CO_2 + [C] = 2CO \tag{2.8}$$

where [C] is the carbon dissolved in the hot metal. In accordance with the mass action law, we have

$$K = \frac{P_{co}^2}{P_{co_2} \cdot a_c} \tag{2.9}$$

where P_{co}, P_{co_2} are the partial pressures of CO andCO_2 respectively, a_c is activity of carbon in hot metal. K, the Equilibrium constant, is a function of temperature and can be derived in terms of standard Gibbs free energy data.

$$K = exp(15.30 - 16759/T) \tag{2.10}$$

Substituting Eq (2.7) into Eq (2.10) and combining with Eq (2.9) yield

$$\exp\left[15.30 - \frac{16759}{1873 - 50\,[\%C]}\right] = \frac{P_{co}^2}{P_{co_2} \cdot a_c} \tag{2.11}$$

If the oxygen blowing into the converter bath is not pure but contains some inert gases such as nitrogen, argon etc. and the total pressure is assumed to be P, we would have

$$P_{co} = P \cdot x_{co} \tag{2.12}$$

$$P_{co} = P \cdot x_{co_2} \tag{2.13}$$

$$P_{co} = P \cdot x_{Inr} \tag{2.14}$$

Where x_{co}, x_{co_2}, x_{Inr}represent the mole fractions of CO, CO_2 and inert gas in the decarburization zone, respectively, and

$$x_{co} + x_{co_2} + x_{Inr} = 1 \tag{2.15}$$

On the other hand, the activity of carbon can be expressed in terms of the products of [%C] and activity coefficient, f_c i.e.

$$a_c = [\%C]\, f_c \tag{2.16}$$

Substituting Eqs (2.12) to (2.16) into Eq (2.11) generate as

$$\exp\left[15.30 - \frac{16759}{1873 - 50\,[\%C]}\right] = \frac{P \cdot x_{co}^2}{(1 - x_{Inr} - x_{co})\,[\%C] \cdot f_c} \tag{2.17}$$

Let two other quantities be defined as X_{co} *and* X_{co_2} (which are relative contents of CO and CO_2 in CO + CO_2)

X_{co}=x_{co}/(x_{co}+x_{co_2})=x_{co}/(1-x_{Inr})

X_{co_2}=x_{co_2}/(x_{co}+x_{co_2})=x_{co_2}/(1-x_{Inr})

Substituting X_{co} *and* X_{co_2} into Eq (2.17) we obtain

$$\exp\left[15.30 - \frac{16759}{1873 - 50\,[\%C]}\right] = \frac{P \cdot X_{co}^2\,(1 - x_{Inr})}{(1 - X_{co})\,[\%C] \cdot f_c} \tag{2.18}$$

The above relation gives the dependence of relative content of the carbon monoxide on the carbon concentration in the hot metal during the BOP operation. Based on this solution the relative mole fraction of CO can be calculated if carbon content and f_c are known.

Bensel et al [5] have used the following expression for f_c.

$$f_c = \alpha[\%C] \tag{2.19}$$

where $\alpha = 0.167$ when [% C] > 1%, $\alpha = 0.2$ when [% C] < 1%

These are approximation formulae and they completely neglect the effect of temperature on f_c. Rist and Chipman [6] have given a Equation, which explains the effect of temperature on activity coefficient of carbon

$$\log f_c = 0.1666\ [\%\ C] - 0.01585\ [\%\ C]^2 + 9.9613\ X\ 10^{-7}\ [\%\ C]^3 \cdot (T\text{-}273)$$
$$+3.0246X10^{-5}[\%\ C]^4 \cdot (T\text{-}273)$$

The decarburization rate depends on the oxygen blow rate into the furnace. If the rate of oxygen blow is $\frac{dn_{o_2}}{dt}\left(\frac{mol}{min}\right)$ and the decarburization rate $\frac{dn_c}{dt}$, then from mass balance considerations

$$(1 - x_{Inr})\frac{dn_{o_2}}{dt} = -\frac{dn_c}{dt}\left(X_{co_2} + \tfrac{1}{2}X_{co}\right)$$

Where the factor (1 - X_{Inr}) reflects the purity of oxygen. The negative sign stems from the decreasing carbon content during decarburization. It is implicitly assumed that oxidation of other elements like P, Mn, Fe, S is negligible in high carbon regime and this is approximately so.

Expressing in terms of [%C] and the flow rate Q_0 (Nm^3/ton) the above equation becomes

$$\frac{d[\%C]}{dt} = \frac{-Q_0(1 - x_{Inr})}{1.87 \cdot 10^{-5}(1 - 0.5X_{co})W_t} \tag{2.20}$$

where W_t is bath weight in gms, [%C] is weight percent of carbon.

When carbon content is less then 0.3 , the decarburization will be controlled by mass transfer of carbon in the melt instead of oxygen and it can be expressed as

$$\frac{dn_c}{dt} = -k_d \cdot A \cdot \left(C^b - C^i\right) \tag{2.21}$$

where, C^b, C^i are bulk and interfacial concentration of carbon, mol/cc, k_d is mass transfer coefficient (cm/sec), A is bath / oxygen interface area (cm^2).

Since the reaction between carbon and oxygen at high temperature is very fast, C^i is

negligible (except towards end of the blow) and hence Eq (2.21) can be written as:

$$\frac{dn_c}{dt} = -k_d \cdot A \cdot \left(C^b - C^i\right)$$

or

$$\frac{d\,[\%C]}{dt} = -\frac{k_d \cdot A}{V}\,[\%C] \tag{2.22}$$

where V= melt volume

2.2.3 Exponential Model

2.2.3.1 Model by Bessho et al.

Bessho et al.[7] have developed a dynamic model, based on exponential dependence of decarburization rate on carbon content . This model has been applied to estimate carbon content and temperature of Q -BOP heats after sublance measurement.

Exponential model is expressed as

$$-\frac{dC}{dO_2} = \xi + \tau \exp\left(\phi C\right) \tag{2.23}$$

where

$$\tau = -\xi \exp\left[\frac{C_o}{C_p - C_o}\right]$$

$$\phi = \frac{-1}{C_p - C_o}$$

Then Eq (2.28) becomes

$$-\frac{dC}{dO_2} = \xi\left[1 - \exp\left(\frac{C_o - C}{C_p - C_o}\right)\right] \tag{2.24}$$

where ξ is theoretical maximum decarburization rate, C_o=Critical carbon content below

which decarburization does not substantially occur and is found to be 0.01% for Q- BOP, C_p = a parameter derived statistically based on operational variables.

Value of 'ξ' can be calculated for a converter with oxygen flow rate Q_0 = 600 Nm3/min and weight of bath W_t = 300 tons as follows:

$$\xi = \frac{\frac{600}{22.4} * 12 * 2}{300 * 1000} = -.214\%C/min$$

By integrating the Equation (2.24)

$$-\int \frac{dC}{\left[1-\exp\left(\frac{C_o-C}{C_p-C_o}\right)\right]} = \int \xi dO_2$$

$$-\int \frac{dC}{\left[1-\exp\left(\frac{C_o-C}{C_p-C_o}\right)\right]} = \xi \triangle O_2$$

$$\Delta O_2 = \frac{(C_o - C_p)}{\xi}\left[\ln\left(\frac{1-\exp\frac{C_o-C_{fa}}{C_p-C_o}}{1-\exp\frac{C_o-C_{SL}}{C_p-C_o}}\right) + \frac{C_{fa}-C_{SL}}{C_p-C_o}\right] \tag{2.25}$$

where C_{SL} is carbon content determined by sensor lance,

C_{fa} is the aimed carbon content,

ΔO_2 is the amount of oxygen required (per ton of charge) to reduce the carbon content from C_{SL} to C_{fa} .

End point carbon content at any arbitrary time after the measurement by the sensor lance can be calculated, by simplifying the above equation to

$$C_{fa} = (C_o - C_p)\ln\left[\frac{R}{1-\exp\frac{C_o-C_{SL}}{C_p-C_o} + R\exp\frac{C_o}{C_p-C_o}}\right] \tag{2.26}$$

where,

$$R = \exp\frac{\xi \cdot \triangle O_2 - C_{SL}}{C_p - C_o}$$

where $\triangle O_2$ (Nm^3 /ton of charge) is the amount of oxygen blown after the measurement by sensor lance. The value of Cp in the above equations is estimated from multiple linear regression (MLR) analysis which involves the carbon content and temperature of the bath monitored by the sensor lance.The MLR equation to estimate C_p can be expressed as

$$C_p = a_o + \sum_{i=1}^{m} a_i \cdot x_i \tag{2.27}$$

where a_0, a_i = regression constant and regression coefficients, x_i = operational variables as shown below.

The operational variables used by Bessho et al. For regression analysis are

x_i	meaning
1	real carbon content at blowing end
2	real bath temperature at blowing end
3	hot ratio (=wt of bath /wt. of scrap)
4	carbon content by sensor lance
5	bath temperature by sensor lance
6	amount of lime used after one point check by sensor lance.
7	total amount of lime and dolomitic lime used
8	calculated basicity

Bessho et al. used a semi empirical equation to estimate the temperature rise.

$$T_f = T_{SL} + P \cdot \Delta O_2 + Q\left[\frac{1}{C_f} - \frac{1}{C_{SL}}\right] + R \tag{2.28}$$

where T_f , C_f is the temperature and carbon content of the bath at blowing end respectively,

T_{SL} ,C_{SL} is the temperature and carbon content of the bath measured by the sensor lance,

ΔO_2 is amount of blowing after sensing (Nm^3/ton of charge),

P, Q, R = Parameters calculated from multiple regression analysis by using actual operational data such as lance height, slag volume , etc.

2.2.3.2 Model by Byun et al.

Byun et al. [8] employed a simplified form of exponential model Eq. (2.24), as:

$$-W_{st}\frac{d[C]}{dO_2} = \alpha[1 - \exp -\beta(c - c_o)] \tag{2.29}$$

W_{st} = Weight of molten steel (kg). Here the term β is same as $1/(C_p - C_o)$ and α is same as ξ in Eq (2.24).It is implied that β represents combined effect of C_p and C_o on decarburization.

Integrating Eq (2.29) from sublance carbon content C_s to aimed carbon C_e gives the oxygen consumption from the in - blow sublance measurement to the blow end

$$\Delta O_{2,cal} = -\int_{c_s}^{c_e} dO_2 = -\int_{c_s}^{c_e} \frac{W_{st}}{[1-\exp -\beta\,(c-c_o)]} d\,[C] \tag{2.30}$$

Eq (2.30) can be simplified to

$$\Delta O_{2,cal} = \frac{W_{st}}{\alpha\beta}\left[\beta\,(C_e - C_s) - \ln\left[\frac{1-\exp -\beta\,(C_e - C_s)}{1-\exp -\beta\,(C_s - C_e)}\right]\right] \tag{2.31}$$

The effect of other operational variables on oxygen consumption can be incorporated through multiple linear regression as

$$\Delta O_{2,cal} = \frac{W_{st}}{\alpha\beta}\left[\beta\,(C_e - C_s) - \ln\left[\frac{1-\exp -\beta\,(C_e - C_s)}{1-\exp -\beta\,(C_s - C_e)}\right] + \sum_i \gamma_i \left(X_i - \overline{X_i}\right) + \gamma_0\right] \tag{2.32}$$

where γ_i = regression coefficient, γ_0= regression Constant, X_i = operational variables, $\overline{X_i}$= Standard operational variables.

2.2.3.3 Temperature calculation model

Temperature at the end of blow can be calculated by considering the heats evolved in various reactions

$$[C] + \frac{1}{2}O_2(g) = CO(g) \qquad \Delta H_1 \tag{2.33}$$

$$CO(g) + \frac{1}{2}O_2(g) = CO_2 \qquad \Delta H_2 \tag{2.34}$$

$$Fe + \frac{1}{2}O_2(g) = (FeO) \qquad \Delta H_3 \tag{2.35}$$

$$\frac{1}{2}O_2 = [O] \qquad \Delta H_4 \tag{2.36}$$

Vhere, ΔH_i is the heat produced from each reaction (Kcal / Nm^3 - O_2)

Over all heat balance (excluding heat losses) can be written as

$$C_p W_{st} dT = \Delta H_1 dO_c + \Delta H_2 dO_{co} + \Delta H_3 dO_{Fe} + \Delta H_4 dO_{dis} \tag{2.37}$$

'here C_p is specific heat capacity of molten steel (Kcal / kg ^{0}C),O_c = oxygen combined 'ith carbon to form CO (Nm^3 - O_2), O_{co} = oxygen combined with CO to form CO2 (Nm^3 O_2), O_{Fe} = oxygen combined with Fe to form FeO (Nm^3-O_2),O_{dis} = oxygen dissolved ı liquıd steel (Nm^3-O_2).

In Eq(2.35), the heat of Fe oxidation and the heat produced by oxidation of CO to CO_2 e not greatly different at steel making temperature, i.e. $\Delta H_2 \approx \Delta H_3$. In the later stage `BOF blowing process , it is generally accepted that the product of dissolved carbon and ;ygen in liquid steel is constant.

$$[C] \times [O] = K_4'$$

Therefore, the amount of dissolved oxygen can be expressed as a function of carbon ntent in steel.

$$dO_{dis} \cdot \frac{22.4 \cdot W_{st}}{3200} = -\frac{22.4 \cdot W_{st}}{3200} \frac{K_4'}{[C]^2} d[C] = -\frac{K_4}{[C]^2} d[C] \tag{2.38}$$

Assuming that the carbon removal from steel melt mainly occurs by Eq(2.33), the 'gen consumption for decarburization can be obtained as

$$dO_c = -\frac{11.2 \cdot W_{st}}{1200} d[C] = -K_1 d[C] \tag{2.39}$$

f an assumption is made that all lance oxygen is consumed by reactions (2.33) to) ,

$$dO_2 = dO_c + dO_{co} + dO_{dis}$$

e term $dO_{Fe} + dO_{co}$ is expressed as follows.

$$dO_{Fe} + dO_{co} = dO_2 - (dO_c + dO_{dis}) = dO_2 + K_1 d[c] + K_4 d[c]/[c]^2 \qquad (2.40)$$

If H_ii are assumed to be independent of temperature , the following differential equation can be obtained from Eq(2.37) through (2.40).

$$\mathrm{dT} = ((\delta_1 + (\delta_2 / [\mathrm{C}]^2)\, \mathrm{d[C]} + \delta_3 \mathrm{dO_2}$$

where $\delta_1 = (\Delta H_2 - \Delta H_1)\mathrm{K_1}/(\mathrm{C}_p\, \mathrm{W}_{st})$, $\delta_2 = (\Delta H_2 - \Delta H_4)\, \mathrm{K_4} /(\mathrm{C}_p\, \mathrm{W}_{st})$,$\delta_3 = \Delta H_2 / (\mathrm{C}_p$. $\mathrm{W}_{st})$. Integration of the above equation from in blow measurement(T_s) to the end blow (T_e) gives a linear function of temperature rise.

$$\Delta T_{cal} = \delta_1 (C_s - C_e) + \delta_2 \left(\frac{1}{C_e} - \frac{1}{C_s}\right) + \delta_3 \Delta O_2 \qquad (2.41)$$

where O_2 is total oxygen blow between these measurements.

In order to fit this model better to the actual temperature data, parameters δ_i in Eq(2.41) are modified by the multiple regression analysis as discussed in the decarburization model. In the present work operational variables other than the amount of oxygen and carbon content were also included in this model such as the steel temperature at sublance measurement, slag volume, HMR, lining life, lance height and the amount of iron ore used. Therefore, the equation for the temperature increase can be rewritten as:

$$\Delta T_{actual} = \epsilon_1 (C_s - C_e) + \epsilon_2 \frac{1}{C_e - C_s} + \epsilon_3 \Delta O_2 + \sum_i \chi_i \left(Z_i - \overline{Z_i}\right) + \chi_0 \qquad (2.42)$$

where χ_i, ϵ_i is regression coefficients, χ_0 is constant, Z_i is Operational variables and$\overline{Z_i}$ is standard operational variables (mean values)

2.2.3.4 Feedback model

There will always be deviation of oxygen quantity and temperature rise for a heat which are not accounted for by the explanatory relationships such as Eq. (2.32), (2.41) and thus some part of those deviations will remain unpredictable. In order to minimize the error various steps can be taken. The model can be modified to include the perturbing

factor which may be explained by the selected model parameter. The model parameter for upcoming heat can be adjusted by a time series analysis of the posterior calculation of actual turn down data of preceding heats. In other words the new model parameters for upcoming heat can be expressed as a function of old parameter of preceding heats.

One of the most important concerns in developing feedback model is how to select the adapted model parameters. In this work, various model parameters, θ_i for decarburization model and ϕ_i for temperature calculation model were employed and the general form of equations used are

$$\Delta O_2 = \theta_1 \left[\frac{W_{st}}{\theta_2 \theta_3} \ln \left[\frac{1 - \exp \theta_3 (C_s - C_0)}{1 - \exp \theta_3 (C_e - C_0)} \right] + \sum_i \gamma_i \left(X_i - \overline{X_i} \right) + \theta_4 \right] \tag{2.43}$$

$$\Delta T = \phi_1 \left[\epsilon_1 (C_s - C_e) + \epsilon_2 \left(\frac{1}{C_e} - \frac{1}{C_s} \right) + \phi_2 \Delta O_2 + \sum_i \chi_i \left(Z_i - \overline{Z_i} \right) + \phi_3 \right] \tag{2.44}$$

In addition to above, the following time - series forecasting methods can be tested to obtain appropriate feed back model.

Method 1 : Single moving average This technique consists of taking a set of observed values, finding the average of those values, then using that average as the forecast for the next period.

$$F_{t+1}=(X_t+X_{t-1}+\text{———}+X_{t-N-1}) / N$$

where F_{t+1} = the forecast value for the next period, X_t = the most recent observation, N = the number of historical data.

Method 2 : Exponential smoothing method. This forecasting is based on weighting the most recent observation with a weight of value,K* whose value is between 0 and 1 and weighting the most recent forecast with a weight of value, (1 - K*).

$$F_{t+1}=K^*X_t+(1-K^*)F_t$$

where K* = Smoothing factor

Method 3 : ARMA method In this model, the series to be forecast is expressed as a function of both previous values of the series (anti regressive term) and previous error values from forecasting (moving average term) . ARMA (2, 1) model used in Byun et al. model was

$$F_{t+1}=\lambda_1 X_t+\lambda_2 X_{t-1}-\mu_1 e_t$$

where λ_1, μ_1 are coefficients, e_t is the most recent error from forecasting .

Of the above three methods, the exponential smoothing method has been reported to give the best result with a K* value of 0.1. The procedure for On-line application of the model is as follows:

The in- blow sublance measurement is made when 80% of total oxygen amount, presumed by the static, model has been blown. At this point, the decarburization model starts a calculation of the oxygen amount to be blown for the aimed carbon content. The temperature increment in this dynamic period is then calculated based on the amount of oxygen to be blown. If the calculated end- point temperature is higher than the aimed one, the amount of coolant to be added is determined. If the calculated temperature is lower than the aimed one, the heat has to be over blown. The bath temperature and the carbon content in steel at turn down are used for adapting the model parameters for the next heat.

2.2.4 Model by Szegedi et al.

Szegedi et al [9] have developed a model for the adjustment of carbon content of steel by dividing the decarburization process into 3 periods, namely

I . Thermodynamic period

II . Reaction kinetic period

III . Chemical period

as shown in Fig. 1.1. V_c in the figure represents decarburization rate given by

$$V_c = \frac{-d\,[\%C]}{ct}$$

The formulae to calculate the decarburization rate and time taken for the blow for each

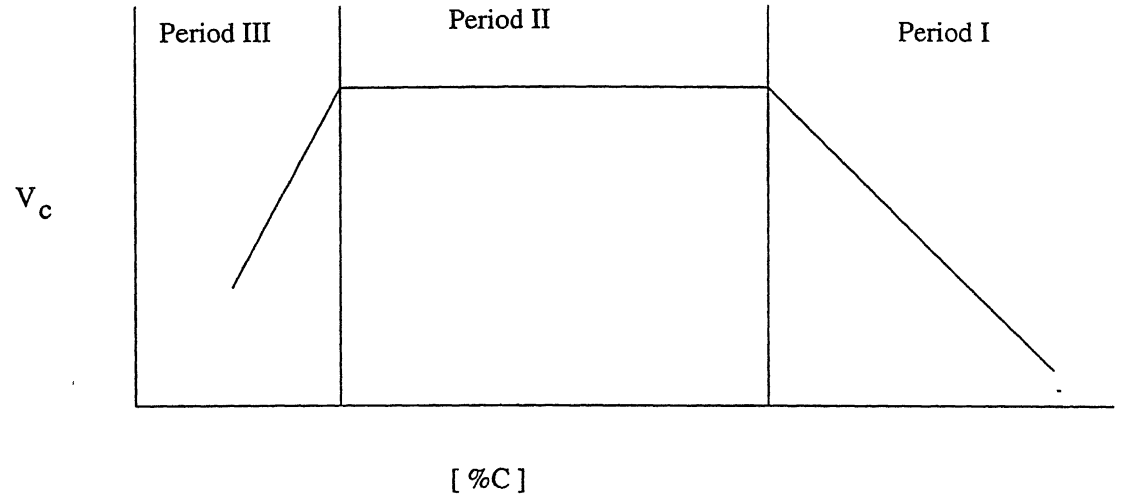

Figure 2.1: Schematic representation of decarburization process.

period are as follows.

The decarburization rate for the period I is obtained on the basis of operational data as

$$V_{C,I}=0.1071.i.[-0.1421.C_B-0.7366.Si_B - 0.0425.i + 1.4987]$$

where $V_{C,I}$ is rate of carbon oxidation(%C/min), i intensity of blowing (m3 o2/t s-teel.min), C_B carbon content of charge (%), Si_B is silicon content of charge (%).

Time taken for computing the period I is given by

$$t_I=100\cdot Si_B[i\cdot(2.031\cdot C_B+7\cdot Si_B + 0.106 \cdot i - 6)] \text{ min}$$

Similarly for the reaction kinetic period II

$$V_{C,II}=0.1071\cdot i$$

and time necessary for second period is

$$t_{II}=9.375(C_B-0.046)/(-1.942-Si.A/(i\cdot B))$$

where $A= C_B +5.1728.Si_B + 0.2981. i -10.52426$

and $B = 0.4217 - 0.1426. C_B - 0.4918 - Si_B -0.00744.i$

The third period is chemical period for which the rate of carbon oxidation is

$$V_{C,III}=12.89[\%C]\cdot\exp(-6590.73/T)$$

The regression analysis of operational data has shown that

$$t_{III} = \frac{\exp\frac{7323}{21422-[\%C]}}{1289} \ln\frac{0.208i+0.046}{[\%C]}, \text{ min}$$

The activation energy of the reaction is

$$G^T = -R \cdot 6590.73 \text{ J/mole.}$$

Total time for blowing $t = t_I + t_{II} + t_{III}$

By equating the decarburization rates periods II and III (i.e. $V_{C,II} = V_{C,III}$) they have derived a formula to calculate the critical carbon constant [C_k].

$$C_k = 0.208.(i) + 0.046$$

They have experimented this model in the range of 0.01 -4.0 C wt % .and have shown that the adjustment and the more exact control of carbon content ensure a significant saving of time and material costs.

2.2.5 Models Based on Exhaust Gas Composition

2.2.5.1 Model by Fukumi et al

Fukumi et al [10] have developed a refining control model based on exhaust gas information measured by mass spectrometer. This model consists of calculation models that use sublance information to estimate various values as follows.

- Calculation and estimation of the oxidation degree (WO2)
- Estimation of (T.Fe)
- Estimation of decarburization
- Estimation of temperature in steel
- Estimation of oxygen content in steel.

2.2.5.2 Calculation and estimation of oxidation degree (WO_2)

WO_2 is defined as Eq(2.45) based on oxygen balance calculated by refining conditions (top and bottom gas flow rate, amount of flux, etc.) and exhaust gas information (analysis, flow rate)

$$WO_2 = \left[\int (fi(Q,F) - fo(V,A))\, dt \right] / WM \qquad (2.45)$$

where fi is input oxygen, fo is output oxygen, WO_2 is oxidation degree, Q is top blow oxygen, F is amount of coolant,V is O_2,CO, CO_2 volume in exhaust gas, A is sucked air or slopping gas volume.

WO_2 indicates oxygen in slag and steel, and this value is the most important parameter in this model. The volume of air sucked from the converter mouth and slopping gas volume are evaluated with reference to bottom blowing gas, balance of air, Ar and N_2. Analyzed values of exhaust gas have a time lag behind the actual reactions because of gas transport time. At the final stage of blowing when WO2 is rapidly increased, this time lag must not be neglected. Thus, reacted volume can be calculated at real time by the estimation of WO2 from Eq(2.46) which is calculated from actual data.

$$dWO_2/dO_2 = \alpha\,[1 - \exp WO_2/\beta] \tag{2.46}$$

where WO_2 is degree oxidation, O_2 is input oxygen, α constant, β is parameter.

2.2.5.3 Estimation of total iron

Since WO_2 indicates oxygen in slag and steel , WO_2 has a close relationship with total iron (T.Fe) in slag. In other words, the change of (T.Fe) can be known from the change of WO_2. Therefore, from (T.Fe) at the first sublance and the increasing amount of WO_2 after the first sublance, the value of (T. Fe) at the final stage can be estimated in real time from the equations given below.

$$\text{(T.Fe)s=f(QB,FO}_2\text{,Cs)}$$

$$\text{Ws(t)=}\alpha\text{WO}_2\text{(t)+}W_{so}/\{1\text{-}\beta\text{(T.Fe)s/100}\}$$

$$\text{(T.Fe)(t)=(T.Fe)s+}\gamma\text{WO}_2\text{(t)/Ws}\sim\text{t}$$

where, (T.Fe)s is (T. Fe) at in - blow sublance, QB is bottom blowing gas flow rate, Cs is [C] in steel at in - blow sublance, WO_2 is oxidation degree, W_{so} is Slag volume except (FeO), (MnO) , (P_2O_5), Ws is slag volume, t is time in sec, α, β, γ are parameters.

2.2.5.4 Estimation and prediction of the amount of decarburization

The amount of decarburization utilized for the estimation of steel temperature and prediction of slopping is calculated based on carbon balance from refining conditions and exhaust gas information, from the equation

$$\Delta C\text{=[}\int f\text{(ho(V.A)-hi(F)dt]/WM}$$

where, ho is Output carbon, hi= Input carbon, ΔC is Amount of decarburization, V is CO, CO_2 volume in exhaust gas, A is sucked air volume or slopping gas volume, F is amount of coolant and flux.

At the final stage of blowing , the estimation of decarburization , amount that contains time lag is calculated according to the efficiency of oxygen for decarburization.

2.2.5.5 Estimation of steel temperature

The heating of the steel at the final stage of blowing has a close relationship with the generated amount of (T.Fe) namely the increased amount of WO_2 and amount of decarburization.

Therefore, heating after sublance is estimated by

$$dT/dO_2 = \alpha \cdot dWO_2 / dO_2 - \beta \cdot dC / dO_2 - \gamma\, WsWM + \delta$$

where T is temperature in steel, O_2 is input oxygen (gas + coolant), WO_2 is oxidation degree, C is carbon content in steel, Ws is slag volume except (FeO) , (MnO) , (P_2O_5), WM is Weight of steel, α, β, γ, δ are parameters.

2.2.5.6 Estimation of dissolved oxygen content in steel

Oxygen content in steel is estimated from the oxygen balance Eq (2.47) calculated from (T.Fe) which is evaluated from exhaust gas information and the steel temperature.

$$\log[O] = \log[\alpha\,(T.Fe)] + b/T + \gamma \tag{2.47}$$

where, [O]= Oxygen in steel, T is temperature in steel, α, β, γ are parameters.

2.2.6 Model by Iwamura et al

Iwarmura et al.[11] have developed a new endpoint control system of BOF with an autotuning function for the model parameter based on the measured exhaust gas composition. This system can accurately estimate the steel temperature and the carbon content at the blow-end through one campaign without changing of the model parameter. The dynamic

control model consist of an oxygen balance equation and heat balance equation. The amount of oxygen required in a heat is expressed by the sum of the amount of oxygen based on the change of carbon.

$$\frac{Fo_2 + \eta \sum W_s \cdot O_2}{W_{ST}} = a_0 (C_s - C_e) + a_1 \ln \frac{C_{SL}}{C_{EP}} + a_2 + \sum l_i \left(X_i - \overline{X_i}\right) + FB_c \quad (2.48)$$

where a_0,a_1 are coefficients of oxygen balance, C_s, C_e are carbon contents at sublance measurement and endpoint, FO_2 is the amount of oxygen after sublance measurement, η is coefficient of oxygen in fluxes, W_{sub} is amount of flux, O_2 is the amount of oxygen fluxes, W_{ST} is weight of molten steel, X_i is factor i of operating condition, $\overline{X_i}$ is mean value of X_i, l_i is coefficient of statistical model, FB_c is adjustment of oxygen balance from the feedback.

In the heat balance model, the fundamental equation has been changed from the carbon content to the oxygen basis . In situations where the carbon content of the metal at the endpoint has little variation, temperature variation has stronger relation with the amount of oxygen than the change of carbon content. The heat balance is represented by the following equation.

$$T_e - T_s = b_0 \frac{Fo_2 + \eta \sum W_s \cdot O_2}{W_{ST}} + b_2 + \gamma \sum W_s T_{sub} + \sum l_i \left(X_i - \overline{X_i}\right) + FB_T \quad (2.49)$$

where T_s,T_e is temperature at sublance measurement and at the endpoint, b_0, $b_2$is coefficient of heat balance, γ coefficient of cooling capacity, l_i is coefficient of statistical model, $T_{sub}$is cooling capacity of fluxes, FB_T is adjustment of heat balance from the feedback.

2.2.6.1 Auto-Parameter -Tuning function

Usually the decarburization efficiency is changed during blowing for each heat. This fact shows that in the oxygen balance equation with a fixed parameter it is difficult to obtain a highly accurate estimate of steel carbon content and temperature at endpoint through one

campaign . To solve this problem, Iwamura et al. have added an auto-parameter -tuning function of parameters in oxygen balance Eq.(2.48) using exhaust gas information from a mass spectrometer. The parameters of a_0 and a_i are adjusted according to the following Equations.

First of all, Eq(2.50) is altered to the following Equation .

$$-W_{ST}\frac{dC}{dt} = \frac{1}{\left(a_0 + \frac{a_1}{c}\right)} \tag{2.50}$$

The decarburization efficiency is expressed with the parameter of a_0 and a_i and the estimated steel carbon content . On the other hand, the actual decarburization efficiency is calculated by

$$\alpha = G\frac{W_{ST}\,\triangle\, C_i}{\triangle o_i} \tag{2.51}$$

where G is gain, α is decarburization efficiency, i is sampling number from sublance measuring time to blow-end.

$\triangle C_i$ is the change of steel carbon content and $\triangle O_i$ is the amount of oxygen during the sampling period $\triangle t$ as shown below. .

$$\triangle C_i = C_i - C_{i-1}$$

$$\triangle o_i = \int_{t'}^{t'+\triangle t} Fo_2(\tau)\, d\tau \tag{2.52}$$

The amount of decarburization in the exhaust gas during (t is calculated from the following expression using the exhaust gas information.

$$\triangle W_{c,i} = \int_{t'}^{t'+\triangle t} \frac{\{CO(\tau) + CO_2(\tau)\}\, Q(\tau)\, 12}{3600 \cdot 22.4 \cdot 1000} d\tau \tag{2.53}$$

From Eq. (2.51) and .(2.53) we can obtain

$$\alpha_i = G\frac{\triangle W_{c,i}}{\triangle o_i}100 \tag{2.54}$$

when C is infinity, the term of 1/C in the Eq.(2.50) can be neglected and the parameter of a_0 is expressed from Eq.(2.50) and (2.51) can be shown as,

$$a_0 = \frac{1}{\alpha_i} \tag{2.55}$$

In on-line operation, the parameter of a_0 is decided by the average of the actual decarburization efficiency during the maximum decarburization period before sublance measuring time as shown in the following equation

$$a_0 = \frac{1}{\sum \alpha_{max,i}/m} \tag{2.56}$$

where, α_{max}= decarburization efficiency in maximum decarburization period, m is constant of sampling number.

On real time after sublance measurement, the parameter of a_1 in Eq.(2.50) is calculated as.

$$a_1 = \frac{(1 - a_0 - \alpha_i)}{\alpha_i}C \tag{2.57}$$

The parameter of a_1 changes in proportion to the decrease of the decarburization efficiency and this function can accurately estimate the steel carbon content.

2.2.6.2 Feedback calculation model

The feed back calculation model has been developed in order to adjust the errors in the dynamic control model. The amount of feedback is calculated by considering the trend in the errors of the dynamic control model in past some heats measured by sublance at blowing and endpoint. The rule of feedback is classified with three cases by the trend of

the error as shown below.

Case	The trend of the error of the model	The amount of feedback
1	Mdlerror(i-1)·Mdlerror(i)≥0	FB(i) = FB(i-1)+G_{FB}error(i)+error(i-1)/2
2	Mdlerror(i-1)·Mdlerror(i)<0 and |error(i)|-|error(i-1)>H	FB(i) = FB(i-1)+G_{FB}.error(i)
3	Mdlerror(i-1)·Mdlerror(i<0) and |error(i)|-|error(i-1)|≤H	FB(i) = FB(i-1)

where, FB(i) is feedback value, Mdlerror(i) is error of the model, error(i) is error of the feedback model, G_{FB} is feedback gain, H is on-detective value.

In the oxygen balance equation, the feedback value is adjusted according to the condition of the sublance measured carbon content at end point in addition to the above rule of the feedback. This is because the sensitivity of the carbon content for the amount of oxygen varies with the sublance measured carbon content in the blowing.

The relationship between carbon content and amount of oxygen can be defined in the following equation

$$C_{EP} = s_1 \log \frac{\Delta o_2}{W_{ST}} + s_2 \tag{2.58}$$

where s_1, s_2 are coefficients.

The sensitivity of the carbon content to the amount of oxygen is related to the following equation.

$$\epsilon = \frac{d \triangle o_2}{dC_{EP}} = \frac{1}{s_1} \exp \frac{C_{EP} - s_2}{s_2} \tag{2.59}$$

where ϵ is the sensitivity

The actual feedback value is adjusted with the sensitivity as shown in the following equation.

$$FB'(i)=h \cdot FB(i)$$

where

$$h = \frac{\epsilon'}{\epsilon_{base}}$$

and

$$\epsilon' = \frac{d\Delta o_2}{dC_{EP}} = \frac{1}{s_1} \exp \frac{C_{sim} - s_2}{s_2}$$

2.2.7 Droplet Decarburization Model

This model was developed by Divyesh Dixit [12].The metal droplets are ejected from jet impact zone and eventually return to metal via slag phase. The dissolved carbon in these droplets reacts with FeO present in the slag(or FeO formed on the surface of droplets) according to the following reaction

$$[C] + Feo = (CO)_g + Fe$$

If the droplets spend on average τ time (residence time in slag foam) then

$$\ln \left[\frac{C_\tau^d - C_e}{C_o^d - C_e} \right] = -\frac{K_d A}{V} \tau \tag{2.60}$$

Where C_τ^d is the carbon concentration of droplet at the time of falling in metal, C_o^d is droplet carbon concentration at the time of ejection of droplet, C_e is equilibrium carbon concentration, A is surface area of the droplet, V is volume of the droplet and K_d is the mass transfer coefficient within the droplet.

From the above equation,

$$C_\tau^d = C_e \left[1 - \exp -\frac{K_d A}{V} T \right] + C_o^d \exp -\frac{K_d A}{V} \tau \tag{2.61}$$

where C_τ^d is carbon concentration of droplet at time of falling in metal

For the droplets joining the metal bath between time t and $t + \Delta t$,

$$C_o^d = C_b^{(t-\tau)}$$

where $C_b^{(t-\tau)}$is the concentration of v\carbon in bulk metal at time $t - \tau$.

Hence Eq. (2.61) can be written as

$$C_\tau^d = C_e \left[1 - \exp -\frac{K_d A}{V} T \right] + C_b^{(t-\tau)} \exp -\frac{K_d A}{V} \tau \tag{2.62}$$

where

$$C_b^{(t-\tau)} = C_b^t - \frac{dC_b}{dt}\tau$$

If iron conversion is defined ad Kg/s of the droplet thrown in to the slag, then the mass of droplets produced between time t and $t + \Delta t$ is Mg.dt. From carbon mass balance,

$$W_b C_b^+ + Mg \cdot dt C_\tau^d = (W_b + Mg \cdot dt)\, C_b^- \tag{2.63}$$

this can be simplified to

$$\ln\left[\frac{C_b^o - C_e}{C_b^t - C_e}\right] = \frac{Mg\left[1 - \exp -\frac{K_d A}{V}\tau\right]}{W_b + Mg \cdot \exp -\frac{K_d A}{V}\tau} \tag{2.64}$$

where, W_b is bath weight, Mg.dt is droplet fall in metal,$C_b^+$is bath concentration before fall, $C_b^-$is bath concentration after fall.

2.2.8 Quadratic Model

This model, proposed by Besso et al [7], postulates that at a later stage of blowing oxygen gas is consumed in three different ways: (1) formation of CO, (2) formation of FeO and (3) formation of other oxides and stray oxygen. Assuming that consumption of oxygen for (3) is very small, we can write

$$dO_2 \simeq dO_{2_{FeO}} + dO_{2_{CO}} \tag{2.65}$$

where dO_2 is the total oxygen, $dO_{2_{FeO}}$ is the amount of oxygen consumed for FeO formation and $dO_{2_{CO}}$ is the amount of oxygen consumed for CO formation.

The concentration of FeO in the slag is assumed to be inversely proportional to the concentration of carbon in the bath i.e.,

$$(FeO) = \frac{\beta}{c} + \gamma$$

where β and γ are constants and statistically determined.

Suppose percentage of oxygen which forms FeO is represented as η_{FeO} (oxygen efficiency for FeO formation), and the percentage of oxygen which forms CO is represented as η_{CO} (oxygen efficiency for CO formation). Both η_{FeO} and η_{CO} are related by a parameter α as

$$\eta_{FeO} = \alpha\,(100 - \eta_{CO}) \tag{2.66}$$

where $0 < \alpha < 1$. The parameter α in eq. (2.66) is introduced to take care of the approximation in eq. (2.65). The value of this parameter can be calculated from experimantal data. Theoritical amount of oxygen required for CO and FeO formation can be calculated as given below.

$$\begin{aligned} dO_{2_{CO}} &= -d\left[\tfrac{W_m}{100}c\right] * 1000000 * 22.4 * 10^{-3} * \tfrac{1}{2*12} \\ &= -9.33 * W_m * dc \end{aligned}$$

where W_m is the weight of metal in tons, and

$$\begin{aligned} dO_{2_{FeO}} &= \tfrac{1}{\alpha} d\left[\tfrac{W_s(FeO)}{100}\right] \cdot \tfrac{1000000*22.4*10^{-3}}{72} \\ &= \tfrac{1\,556}{\alpha} W_s d\,[(FeO)] \end{aligned}$$

where W_s is the weight of slag in tons. Substituting (FeO) in the above equation, we get

$$dO_{2_{FeO}} = -\frac{1.556 * \beta}{\alpha * c^2} dc$$

Substituting $dO_{2_{CO}}$ and $dO_{2_{FeO}}$ in eq. (2.65) we get

$$dO_2 = -\left[\frac{1.556 * \beta}{c^2 * \alpha} + 9.33 W_m\right] dc \tag{2.67}$$

since the rate of decarburization $-\frac{dc}{dO_2}$ in the eq. (2.67) is expressed as quadratic funciton of carbon content in the bath, this model is denoted as quadratic model. Upon integration

in the limits c_{SL} ans c_{Fa} we get

$$\Delta O_2 = 9.33 W_m \left(c_{SL} - c_{Fa}\right) + 1.556 W_s \frac{\beta}{\alpha} \left(\frac{1}{c_{SL}} - \frac{1}{c_{Fa}}\right) \tag{2.68}$$

where ΔO_2 is total oxygen blown, c_{SL} is sublance carbon and c_{Fa} is end point carbon.

One of the limitations of this model is that it neglects the oxygen required for oxidation of P, Mn etc, also neglects the oxygen for oxidation of CO to CO_2. The percentage of CO_2 in waste gas can be as high as 15-25% towards end of the blow.

Chapter 3

Models Developed for End Point Carbon, Temperature, Phosphorus, Manganese and Dissolved Oxygen

3.1 Introduction

The flux of carbon in metal, assuming mass transport of carbon in metal to be the rate controlling step, is given by

$$\frac{dc}{dt} = -k\frac{A}{V}(c^b - c^i) \tag{3.1}$$

or

$$\frac{dc}{dt} = -K'(c^b - c^i)$$

where A is the area of interface, V is the volume of bulk metal, t is time in seconds, c^b is concentration of carbon in the bulk, c^i is the concentration of carbon at the interface and K' is capacity mass transfer coefficient (or rate constant). Capacity mass transfer coefficient K' depends essentially on stirring energy imparted to metal by impinging jets and stirring energy due to gas evolution within bath and bottom stirring. In a small time interval (for constant lance height and gas evolution rate) if k is assumed to be constant

then eq. (3.1) can be integrated to give

$$\ln \frac{c_t - c_e}{c_o - c_e} = -kt\frac{A}{V}\frac{c_o}{c_o - c_e} = -K'\frac{c_o t}{c_o - c_e} \tag{3.2}$$

where c_t is end point carbon, c_o is sublance carbon and c_e is the equilibrium concentration.

It may also be noted that, besides gas flow rate, K' may also dependent upon operational parameters such as basicity, hot ratio, ore added in first blow (ore1), dolomite added during first blow (dolo1), slag added during first blow (slag1), lance height during second blow (hlans2), ore added during second blow (ore2), dolomite added during second blow (dolo2) and slag added during second blow (slag2) etc. For small concentrations of c^a in comparison with c^b eq. (3.1) can be simplified to

$$\frac{dc}{dt} = -K'c \tag{3.3}$$

It can be shown that stirring energy density $\left(\dot{\epsilon},\ \frac{W}{m^3}\right)$ is directly proportional to gas flow rate[13] through metal and the capacity mass transfer coefficient is proportional to $\dot{\epsilon}^{\eta}$.

$$\dot{\epsilon} \propto \text{(gas flow rate)}$$

Thus $K\prime$ can be written as

$$K' \propto \left[-\frac{dc}{dt}\cdot\beta_1 + Q_{eff}\right]^{\eta}$$

where $-\frac{dc}{dt}\beta_1$is rate of decarburization i.e., gas (CO) evolution rate and Q_{eff} is effective volume flow rate of gas $\left(\frac{m^3}{s}\right)$ from top and bottom (see appendix 1) and η is exponential factor. The magnitude of exponent η can either be assumed to be constant through out the process or made to depend upon gas flow rate itself (as reported in literature [13]). If it is assumed to be constant then on substituting $K\prime$ in eq. (3.3) we get

$$\frac{dc}{dt} = -\alpha_1 \cdot \left[-\beta_1 \cdot \frac{dc}{dt} + Q_{eff}\right]^{\eta} \cdot c \tag{3.4}$$

The values of α_1 and η in eq. (3.4) are process dependent and can be obtained by evalua-

tion of experimental data. Alternately, if η is made to depend on gas flow rate itself then we get

$$\frac{dc}{dt} = -\alpha_1 \cdot \left[-\beta_1 \cdot \frac{dc}{dt} + Q_{eff}\right]^{\alpha_2\left[-\beta_1 \frac{dc}{dt} + Q_{eff}\right]} \cdot c \tag{3.5}$$

The values of α_1 and α_2 in eq. (3.5) are also process dependent and can be obtained by evaluation of experimental data.

In order to determine the best fitting values of α_1, α_2 and η in eq. (3.4)-(3.5) the following approaches have been adopted in the present work for evaluation and/or simplification.

1. Simplification of eq. (3.4) by neglecting the contribution of top jet and bottom gas to mass transfer (hereafter referred to as CO-gas evolution model)
2. Simplification of eq. (3.4) to a non-linear algebraic equation and subsequent evaluation (hereafter referred to as Non-Linear model)
3. Simplification of eq. (3.4) to a linear algebraic equation and subsequent evaluation (hereafter referred to as Linear model)
4. Optimization of various models using genetic algorithms (hereafter referred to as GA-decarb models)
5. Purely emperical approach where K' is assumed to be some function of blowing time or amount of oxygen blown (hereafter referred to as emperical model)
6. Statistical models using multiple linear regression (hereafter referred to as Regression Models)

The fundamental basis of each of the above models is described below.

3.2 CO-Gas evolution model

If it is assumed that carbon mono oxide gas (CO) evolution rate in the bath is very high when compared to the effective top and bottom gas flow rate then the Q_{eff} term in eq.

(3.4) can be neglected to give

$$\frac{dc}{dt} = -\alpha \cdot \left(\frac{dc}{dt}\right)^{\eta} \cdot c$$

or

$$-\left(\frac{dc}{dt}\right)^{1-\eta} = \alpha \cdot c$$

or

$$-\left(\frac{dc}{dt}\right) = \beta \cdot c^{\frac{1}{1-\eta}}$$

on integrating,

$$\int_{c_o}^{c_t} \frac{dc}{c^{\frac{1}{1-\eta}}} = -\beta \int_0^t dt$$

and assuming that η is constant, we get

$$c_t = (c_o^{\mu} + \gamma t)^{\frac{1}{\mu}} \tag{3.6}$$

where $\mu = -\frac{\eta}{1-\eta}$and optimum value of μ can be calculated from experimental data by using a suitable numerical technique (see chapter 5).

3.3 Non-Linear model

Non-Linear model is based on the simplification of decarburization equation (3.4) to a non-linear algebraic equation. If it is assumed that stirring energy due to top and bottom gas evolution rates is proportional to the stirring energy due to CO evolution[1] through out the process, eq. (3.4) can be simplified to

[1]This is also supported by the fact that CO evolution takes place mainly near the impinging spots in the hot metal and hence can be assumed to be of similar magnitude to effective stirring energy from top and bottom gases .

$$\frac{dc}{dt} = -\alpha_2 \cdot \left[1 - \beta_2 \cdot \frac{dc}{dt}\right]^{\eta} \cdot c. \tag{3.7}$$

Since $\left|\beta_2 \cdot \frac{dc}{dt}\right| < 1$ eq. (3.7) can be simplified using binomial expansion to

$$\frac{dc}{dt} = -\alpha_2 \cdot \left[1 - \eta \cdot \beta_2 \cdot \frac{dc}{dt}\right] \cdot c$$

Upon readjusting the terms

$$\frac{dc}{dt}\left[1 - \alpha_3 c\right] = -\alpha_2 c$$

Upon integration in the limits c_o and c_t we get

$$\int_{c_o}^{c_t} \left[\frac{1}{c} - \alpha_3\right] dc = -\alpha_2 \int_0^t dt$$

or

$$\ln\left(\frac{c_t}{c_o}\right) - \alpha_3 \cdot [c_t - c_o] = -\alpha_2 \cdot t \tag{3.8}$$

Above equation can be further simplified using logarithmic expansion $for -1 < \left(\frac{c_t}{c_o} - 1\right) \leq 1$ to give

$$\frac{c_t}{c_o} - 1 - \alpha_3 \cdot [c_t - c_o] = -\alpha_2 \cdot t$$

or

$$c_t = -\frac{\alpha_2 \cdot c_o}{1 - \alpha_3 \cdot c_o} \cdot t + c_o \tag{3.9}$$

where α_2 and α_3 are constants which can be determined by a suitable numerical procedure (see chapter 5). Eq. (3.9) represents a non-linear dependence of c_t on c_o and t and hence the name Non-Linear model.

3.4 Linear model

Linear model is based on simplification of decarburization equation (3.4) to linear algebraic equation. Equation (3.8) can be rewritten as

$$\ln c_t - \alpha_3 \cdot [c_t - c_o] = -\alpha_2 \cdot t + \ln c_o$$

Above equation can be further simplified by using logarithmic expansion $for\ -1 < (c_t - 1) \leq 1$ and $-1 < (c_o - 1) \leq 1$ to

$$c_t - \alpha_3 \cdot [c_t - c_o] = -\alpha_2 \cdot t + c_o$$

or

$$c_t = -\frac{\alpha_3}{[1 - \alpha_2]} \cdot t + c_o \tag{3.10}$$

where α_2 and α_3 are constants which can be determined by a suitable numerical procedure (see chapter 5). Eq. (3.10) represents a linear dependence of c_t on c_o and t and hence the name Linear model.

3.5 GA-decarb models

These models use genetic algorithms [18] to dynamically evaluate the optimum mass transfer coefficient at each time step. Two methods can be followed to dynamically optimize eq. (3.4).

Method 1

In this method, η is assumed to be constant through out the process. Eq. (3.4) can be written as

$$\Delta c = \Delta t \cdot \alpha_1 \cdot \left(-\frac{dc}{dt}\beta_1 + Q_{eff}\right)^{\eta} \cdot c \tag{3.11}$$

For small time steps of Δt, the parameters to be optimized are α_1 and η and are determined by using GA (as explained in chapter 5). Carbon at the present time step, c_t, is calculated as

$$c_t = c_o - \Delta c$$

where c_o is the carbon content at previous time step.

Optimization is done successively for time steps (say $\Delta t = 0.01 sec$) until $t \leq t_{max}$ where t_{max} is the total time of second blow period.

Method 2

Since the gas flow rate during the process is changing substantially, η can be made to depend on the gas flow rate itself. The governing equation for optimization becomes

$$\Delta c = \Delta t \cdot \alpha_1 \cdot \left(-\frac{dc}{dt}\beta_1 + Q_{eff}\right)^{\alpha_2 \cdot \left(-\frac{dc}{dt}\beta_1 + Q_{eff}\right)} \cdot c \tag{3.12}$$

For small time steps of Δt, the parameters to be optimized are α_1 and α_2. These are determined by using GA (as explained in chapter 5).

3.6 Emperical model

Since gas evolution rate slows down with time and time of second blow is short, capacity mass transfer coefficient K' in eq. (3.3) can be made to depend inversely on the time of second blow period t as

$$K' \propto \frac{1}{t}$$

or

$$K\prime = \frac{\zeta}{t}$$

where, ζ is a proportionality constant. Upon substitution of k in (3.3) , we get

$$\frac{dc}{dt} = -\zeta \frac{c}{t}$$

On integration,

$$\int_{c_0}^{c_t} \frac{dc}{c} = -\zeta \int_1^t \frac{dt}{t}$$

or

$$\frac{c_o}{c_t} = t^{\zeta}$$

or

$$c_t = \frac{c_o}{t^{\zeta}} \tag{3.13}$$

Optimum value of ζ can be calculated from experimental data (see chapter 5).

3.7 Regression models

The models discussed above can be further subjected to multiple linear regression (MLR) to incorporate the effect of other operational variables on the end point carbon prediction. For example, for the case of Linear model, the equation for end point carbon prediction can be written as

$$c_t' = \mu_o + \mu_1 c_o + \sum_{i=2}^{n-1} \mu_i \cdot X_i \tag{3.14}$$

where, c_t' is the predictedend point carbon and c_o is the carbon value at sublance from actual model and μ_i 's are coefficients (to be determined by MLR) of operational variables X_i 's such as basicity, ore1[2], dolo1, hlans2, ore2, dolo2, slag2 etc. It may be noted that

[2]These variables are explained earlier.

regression model is nothing but a special case of Linear model discussed earlier (Section 3.4).

Regression models can also be developed for prediction of temperature and dissolved oxygen by incorporating all the variables which affect the process

$$\tau = \mu_o + \sum_{i=1}^{n-1} \mu_i \cdot X_i \tag{3.15}$$

where $\tau = T$ for Temperature prediction models

$\tau = [O]$ for oxygen prediction models.

μ_i 's are coefficients (to be determined by MLR) of operational variables X_i 's such as basicity, ore1, dolo1, T_1 , hlans2, ore2, dolo2, slag2 etc. For details of variables see List of Symbols.

3.8 Models for phosphorus prediction

At the end of blow in BOF steel making only a quasi static (or pseudo thermodynamic) equilibrium is approached between slag and metal with a separating interface. Since the slag only approximates to equilibrium with metal and gas[CO, CO_2] at the end of blow, the application of thermodynamics for direct estimation of phosphorus distribution at end point has not been straight forward. The models developed to predict endpoint phosphorus distribution have been generally based on regression analysis of actual plant data by assuming a pseudo thermodynamic equilibrium at the end of process. In the present work, however, a kinetic model has also been tried.

3.8.1 Thermodynamics of phosphorus distribution

The molecular theory of slag stipulates the formation of tricalcium phosphate in lime rich slags

[P]+5/2[FeO]+3/2CaO = 1/2{Ca_3 $(PO_4)_2$}+5/2(Fe)

$$K_p = \frac{a_{Ca_3(PO_4)}}{a_{CaO}^{1.5} \cdot a_{FeO}^{2.5} \cdot a_P} \tag{3.16}$$

This process can be vied as a multi step process involving several stages

i) $[P_M] \rightarrow p_g\,(gas)$, at slag/metal interface

ii) $P_{(g)} + O_{(g)} \rightarrow P_2O_{5(g)}$ at slag/metal interface

ii) $P_2O_{5(g)} + (CaO) \rightarrow (CaO.P_2O_5)$

Step (ii) in the gas-slag (transitory intermediate) reaction introduced by Wagner[17] as

$(P_2)_g + 5/2\,(O_2)_g + 3\,(O) \rightarrow 2\,(PO_4)^{-3}$

and is the basis of the term phosphate capacity, a measure of dephosphorising capability of slag under a given oxygen potential and is related to oxygen activity in slag by

$\frac{(P)}{[a_P]} = C\,(PO_4)^{-3} \cdot (a_{FeO})^{2.5}$

where, $C(PO_4)^{-3}$ is the phosphate activity which is strongly influenced by temperature and slag composition. The conversion of P to P_2O_5 takes place at slag metal interface and is related to activity of P in metal and other active parameters of slag as implied above. The rate determining stage of the reaction is activity of [P] at the slag metal interface and is decided by the rate of transport of phosphorus to the slag metal boundary for oxidation. If manganese is present in appreciable concentrations then dephosphorization process is hindered.

Balajiva et al [14] proposed dephosphorisation reaction as

2P[metal]+5Feo[slag] = P_2O_5[slag]+Fe[metal]

for which the apparent equilibrium constant can be written as

$$K = \frac{wt\%P_2O_5}{[wt\%P]^2[wt\%FeO]^5}$$

Regression analysis of the above equation on data obtained during laboratory experiments yielded

log K = 10.78%CaO-0.089T-6.425 where T is Deg C.

In the above study the three important variables identified for dephosphorisation were

(i) FeO content of slag which represents oxidation potential of slag,

(ii) CaO content of slag which is directly related to basicity and

(iii) Turn-down temperature [T], deg C and a negative coefficient for temperature implies poorer dephosphorization as temperature rises.

The simultaneous effect of temperature, lime and FeO content of slag on phosphorus distribution has been described by Healy [14] by using ionic theory of slag

$$\log \frac{(\%P)}{[\%P]} = \frac{22350}{T} + 0.08(\%CaO) + 2.5\log(\%Fe) - 16.0 \qquad (3.17)$$

where $[\%P]$=mass % of phosphorus in metal

$(\%P)$=mass % of phosphorus in slag

$(\%Fe)$=mass %Fe in slag

$(\%CaO)$=mass %CaO of slag

T=temperature in ^oK

Healy's equation is widely used in steel industry by adapting it to the plant data.

Since temperature at tap varies in a small range, Deo et al [15] proposed a dephosphorization model in terms of basicity only (on the basis of plant data),

log(%P)/[P] = 0.43·Basicity + 0.55

where, basicity = %CaO/%SiO_2

3.8.2 Phosphorus prediction models developed in the present work

Phosphorus prediction is done using

1. Kinetic model of mass transfer

2. Regression model

3.8.2.1 Kinetic model of mass transfer

Similar to the decarburization equation (3.1), flux of phosphorus in metal is given by

$$\frac{dp}{dt} = -k_p \frac{A}{V}(p^b - p^i) \qquad (3.18)$$

or

$$\frac{dp}{dt} = -K'(p^b - p^i)$$

where k_p is mass transfer coefficient for phosphorus, A is area of slag-metal interface, V is volume of bulk metal (including droplets), p^b is concentration of phosphorus in the bulk and p^i is the concentration of phosphorus at the interface and K' is capacity mass transfer coefficient. If it is assumed, as also done in the previous works[ ], that mass transfer coefficient is nearly constant through out the process then eq. (3.18) can be integrated to give

$$\ln \frac{p_t - p_e}{p_o - p_e} = -kt\frac{A}{V}\frac{p_o}{p_o - p_e} \tag{3.19}$$

where t is time in seconds, p_t is end point phosphorus, p_o is sublance phosphorus and p_e is the equilibrium concentration of phosphorus. Eq. (3.19) can be simplified to

$$\ln \frac{p_t - p_e}{p_o - p_e} = -K't \tag{3.20}$$

However, K' is dependent upon operational parameters such as basicity, hot ratio, ore1, dolo1, slag1, hlans2, ore2, dolo2, slag2 etc. The effect of other variables affecting phosphorus distribution can be incorporated by MLR and hence above equation can be written as

$$-\ln \frac{p_t - p_e}{p_o - p_e} = \mu_o + \sum_{i=1}^{n-1} \mu_i \cdot X_i \tag{3.21}$$

where μ_i 's are coefficients of operational variables X_i such as basicity, hot ratio, ore1, dolo1, slag1, hlans2, ore2, dolo2, slag2 etc.

3.8.2.2 Regression model

This model is similar to the one developed for carbon (eq. (3.14)). Here end point phosphorus is predicted as a function of operational variables.

$$p_t' = \mu_o + \mu_1 p_o + \sum_{i=2}^{n-1} \mu_i \cdot X_i \tag{3.22}$$

where, p'_t is the end point phosphorus value predicted from MLR, p_o is sublance phosphorus and μ_i 's are coefficients (to be determined by MLR) of operational variables X_i such as basicity, hot ratio, orel, dolo1, slag1, hlans2, ore2, dolo2, slag2 etc. It may be noted that regression model is only a special case of eq. (3.21).

3.9 Models for manganese prediction

The FeO and MnO exchange reaction involving the oxidation of manganese in steel can be formulated as

$$(FeO) + [Mn] = (MnO) + [Fe]$$

The equilibrium relation can therefore described in terms of the mass concentration of oxides

$$K''_{FeMn} = \frac{(\%MnO)}{(\%FeO)[\%Mn]}$$

where the equilibrium relation K'' depends on temperature and slag composition.

3.9.1 Thermodynamics of manganese distribution

Turkdogan[16] proposed the relationship for manganese partition as

(MnO%)/[%Mn] = 6(%Feo)*SiO_2/CaO,

where combined effect of slag FeO and basicity of Mn partition have been considered. Two new relations for estimating Mn partition have also been proposed in which

(i) hot metal Si is considered, since it remarkably affects basicity (slag route) and FeO in slag.

(ii) residual oxygen activity of the steel, which is related to the end point carbon, has been introduced. This residual oxygen does not participate in any of the oxidation reactions in the melt, but it may activate the manganese atoms effectively such that the kinetics of Mn + FeO = MnO + Fe and subsequent removal of MnO to slag phase is

enhanced at the slag/metal interface. In other words, higher the oxygen activity of the bath, larger will be Mn partition to slag i.e., Mn recovery will be less.

Deo et al[15] proposed a model for manganese partition as

(Mn)/[Mn] = 2.1864(%Fe_2O_3+%FeO)-23.728

and since at the quasi-static stage (Fe_2O_3+FeO)t can be expressed in terms of FeOt, the manganese partition is expressed as

(Mn)/[Mn] = 2.1864%FeO-23.728,

where the only variable is slag FeO. This equation is, however, applicable only to a narrow and specific range of operation.

3.9.2 Models developed for manganese prediction in the present work

Manganese prediction was done using

1. Kinetic model of mass transfer
2. Regression model

3.9.2.1 Kinetic model of mass transfer

Similar to decarburization equation (3.1), flux of manganese in metal is given by

$$\frac{dMn}{dt} = -k_{Mn}\frac{A}{V}(Mn^b - Mn^i) \tag{3.23}$$

or

$$\frac{dMn}{dt} = -K'(Mn^b - Mn^i)$$

where k_{Mn} is mass transfer coefficient for manganese, A is area of slag-metal interface, V is volume of bulk metal (including droplets), Mn^b is concentration of manganese in the bulk and Mn^i is the concentration of manganese at the interface and K' is capacity mass transfer coefficient. If it is assumed , as done in the previous works[17], that K' is constant through out the process then eq. (3.23) can be integrated to give

$$\ln \frac{Mn_t - Mn_e}{Mn_o - Mn_e} = -k_{Mn} t \frac{A}{V} \frac{Mn_o}{Mn_o - Mn_e} \tag{3.24}$$

where Mn_t is end point manganese, Mn_o is sublance manganese and Mn_e is the equilibrium concentration of manganese. Eq. (3.24) can be simplified to

$$\ln \frac{Mn_t - Mn_e}{Mn_o - Mn_e} = -K't \tag{3.25}$$

However, K' is dependent upon operational parameters such as basicity, hot ratio, orel, dolol, slagl, hlans2, ore2, dolo2, slag2 etc. Other variables affecting manganese distribution can incorporated by MLR and hence above equation can be written as

$$-\ln \frac{Mn_t - Mn_e}{Mn_o - Mn_e} = \mu_o + \sum_{i=1}^{n-1} \mu_i \cdot X_i \tag{3.26}$$

where μ_i 's are coefficients of operational variables X_i such as basicity, hot ratio, orel, dolol, slagl, hlans2, ore2, dolo2, slag2 etc.

3.9.2.2 Regression model

This model is similar to the one developed for carbon (eq. (3.14)). Here end point manganese is predicted as a function of operational variables.

$$Mn'_t = \mu_o + \mu_1 Mn_o + \sum_{i=2}^{n-1} \mu_i \cdot X_i \tag{3.27}$$

where, Mn'_t is the end point manganese value predicted from MLR, Mn_o is the sublance manganese and μ_i 's are coefficients of operational variables X_i such as basicity, hot ratio, orel, dolol, slagl, hlans2, ore2, dolo2, slag2 etc. It may be noted that regression model is only a special case of eq. (3.26).

Chapter 4

Experimental Data

Experimental data was collected for three converters of 300, 200 and 100ton capacity from literature and is classified as plant1[18], plant2[19] and plant3[20], respectively. The following section explains the data and classification.

4.1 Plant 1

Table 3.1 shows a sample set of heats for a 300 ton converter consisting of parameters basicity, hotratio, hot ratio*initial phosphorus (p), slag volume, ore added during first blow, slag added during first blow, dolomite added during first blow, sublance temperature (T_o), sublance carbon (c_o), oxygen blown during second blow (O22), slag added during second blow (slg2), dolomite added during secon blow (dolo2), lance height during second blow (hlans2), end point carbon (c_t), sublance phosphorus (p_o), end point temperature (T), end point manganese (Mn_t), end point phosphorus (p_o), sublance manganese (Mn_o) and end point dissolved oxygen ([O]) used in tuning the models. Oxygen gas flow rate is 750 $\frac{m^3}{min}$. The parameters calculated from actual heat are defined below, for a typical heat with hot metal weight (HMwt) = 295400 kg, scrap weight = 56700 kg, Silicon content of hot metal (%Si) = 0.359%, lime added during first blow (lime 1) = 11956 kg, dolomite added in the first blow (dolo1)=413 kg and phosphorus content of hot metal (%p)=0.056 %,

$$SiO_2 = HMwt \star \frac{\%Si}{100} \star \frac{60}{28}$$
$$= 295400 \star \frac{0.359}{100} \star \frac{60}{28} \quad = 2272.47 \quad Kg.$$

Slag volume = SiO_2 +lime 1+slg1 = 2272.47+11956+2980 = 17208.47 Kg

$$hot\,ratio = \frac{HMwt}{scrapwt} = \frac{295400}{56700} = 5.2098$$

$$basicity = \frac{lime1 + dolo1}{SiO_2} = \frac{11956 + 413}{2272.47} = 5.443$$

The actual data is divided into 3 case studies.

4.1.1 Case study 1

Number of heats in this case study are 273. For all the modes developed on these 273 heats, it is referred to as case study 1(273 heats). Two subsets of this data are created by subjecting it to the overall restriction that end point carbon should be in the range of 0.035%-0.075% and whether ore is added or dolo2 is added during second blow.

4.1.2 Case study 2

End point carbon is in the range of 0.035-0.075% and ore 2 is not added in the heats of this case study. Number of heats in this case study are 156. For the models tuned on these 156 heats, it is referred to as case study 2 (156 heats).

In 33 heats Ore2 is added in place of dolo 2 in the heats. Since number of heats in this group are only 33 no models are tested on this set.

Table 4.1 Sample data set of Plant 1

Heat No.	Basicity	hot ratio	ore1 (kg)	slg1 (kg)	dolo1 (kg)	T_o (^oC)	c_0 (wt%)	O22 m^3	Ore 2 (Kg)	slg2 (kg)	dolo2 (kg)
M9170	3.746	4.563	5864	4021	0	1599	0.369	2220	0	0	1
M9172	4.384	5.185	5407	3149	0	1600	0.464	2253	0	0	496
M9175	4.531	4.107	5979	3124	0	1587	0.381	2022	0	0	331
M9177	4.749	4.783	5445	3046	0	1596	0.390	2152	0	0	1281
M9181	5.043	4.533	6233	2849	0	1578	0.449	2324	0	0	1188
M9182	5.254	4.569	5710	2719	0	1618	0.235	1744	0	0	1027
M9184	5.322	5.437	5008	3404	0	1612	0.470	2262	0	0	2805
M9187	4.661	4.435	5384	3640	0	1584	0.457	2434	0	0	1506
M9189	5.505	6.086	4529	2906	0	1610	0.455	2233	0	0	1190
M9190	5.220	4.939	4960	2972	0	1557	0.537	2960	0	0	991
M9193	4.876	4.568	7270	3000	0	1536	0.481	2720	0	0	238
M9195	5.364	4.805	178	4446	994	1611	0.338	2310	0	0	737
M9198	5.358	5.005	5045	3121	1002	1616	0.252	1583	0	0	531
M9199	4.778	5.970	6986	2934	0	1607	0.304	1961	0	0	874
M9201	4.436	5.178	5515	3115	0	1594	0.451	2088	0	0	633
M9208	3.918	5.165	4935	3289	0	1617	0.407	2096	612	0	0
M9227	4.646	6.504	2975	3870	0	1645	0.169	1401	513	0	0
M9250	6.400	8.38	4785	4294	1010	1647	0.310	2162	992	418	601
M9319	5.443	5.210	3994	2980	413	1607	0.517	2464	0	1508	1501
Mean	5.054	5.305	4782	3021	223	1603	0.412	2149	116	91	540
σ	0.831	0.979	1627	819	626	17	0.082	304	283	372	553

Table 4.1 (contd. ...)

Heat No	Slag volume (kg)	$hotratio * p^*$ (kg)	p_o wt%	T (^oC)	p_t wt%	Mn_o wt%	Mn_t wt%	[O] ppm	hlans2 cm	c_t wt%
M9170	21850.768	0.287	0.022	1675.000	0.008	0.337	0.168	469.000	192	0.044
M9172	18818.600	0.316	0.027	1668.000	0.011	0.315	0.187	398.000	191	0.060
M9175	18249.875	0.246	0.015	1654.000	0.007	0.313	0.170	416.000	189	0.062
M9177	17943.504	0.287	0.021	1653.000	0.007	0.334	0.162	407.000	184	0.059
M9181	16569.447	0.267	0.020	1643.000	0.007	0.314	0.153	426.000	188	0.057
M9182	15853.072	0.256	0.020	1651.000	0.009	0.304	0.179	395.000	216	0.064
M9184	17041.258	0.321	0.030	1646.000	0.008	0.352	0.161	365.000	211	0.061
M9187	18895.980	0.257	0.019	1644.000	0.008	0.327	0.167	401.000	193	0.063
M9189	16649.943	0.365	0.025	1664.000	0.010	0.351	0.205	331.000	189	0.073
M9190	17119.346	0.301	0.012	1643.000	0.006	0.310	0.153	403.000	192	0.063
M9193	17575.758	0.283	0.013	1632.000	0.005	0.286	0.136	509.000	191	0.049
M9195	22300.977	0.308	0.018	1679.000	0.006	0.287	0.146	505.000	194	0.046
M9198	17678.311	0.285	0.014	1651.000	0.007	0.272	0.164	359.000	209	0.061
M9199	17099.869	0.358	0.018	1650.000	0.008	0.298	0.171	381.000	210	0.058
M9201	18163.229	0.326	0.020	1652.000	0.009	0.313	0.192	306.000	208	0.074
M9208	19711.025	0.315	0.030	1684	0.010	0.337	0.178	503	185	0.048
M9227	18016.832	0.390	0.023	1676	0.011	0.282	0.176	473	199	0.063
M9250	25058.34	0.528	0.023	1702	0.008	0.290	0.140	595	180	0.046
M9319	17208.47	0.292	0.027	1662.000	0.008	0.326	0.174	413	187	0.050
Mean	17886.256	0.309	0.022	1665	0.009	0.316	0.176	426	194	0.059
σ	1857.449	0.041	0.005	14	0.002	0.029	0.026	89	22	0.011

4.2 Plant 2

Table 3.2 shows a sample set of heats for a 200 ton converter consisting of SiO_2, O22, scrap added during first blow, sublance temperature (T_o), end point temperature (T), sublance carbon (c_o), flux added, waste oxide briquettes (WOBS), chill scrap, end point carbon (c_t) and end point dissolved osygen ([O]). SiO_2 is calculated as explained earlier for plant 1. Oxygen gas flow rate is $600\frac{m^3}{min}$. Heats are selected with end point carbon lying in the range of 0.02 to 0.075% only. There is a total of 321 heats. Parameter SiO_2 is calculated as already shown for plant 1.

4.3 Plant 3

Table 3.3 shows a sample set of heats for a 100 ton converter consisting of parameters basicity, slag volume, sublance temperature (T_o), sublance carbon (c_o), oxygen blown during second blow (O22), raw dolomite added during second blow (raw dolo2), burnt dolomite added during second blow (burnt dolo2), lance height during second blow (lance level), end point carbon (c_t), sublance phosphorus (p_o), end point temperature (T), end point manganese (Mn_t), end point phosphorus (p_o), sublance manganese (Mn_o) and end point dissolved oxygen ([O]) used in tuning the models. End point carbon range for these heats are 0.03 to 0.09% only. Oxygen gas flow rate is $340\frac{Kg}{min}$. Heats are selected with end point carbon lying in the range of 0.03 to 0.07% only. There is a total of 297 heats. Method of calculation of parameters such as basicity, slag volume is same as for plant 1.

Comparison of mean and σ values for the variables of Plant 1, Plant 2 and Plant 3 is shown in Table 4.4.

Table 4.2 Sample data set for Plant 2

Heat No	SiO_2	O22	scrap	T_o	T	c_o	flux	wobs	chill scrap	c_t	[O]
928262	2213.529	2127	44574	1534	1670	0.450	12450	4180	0	0.029	1432.000
915061	2730.810	2140	61305	1529	1656	0.499	14000	2110	0	0.027	1411.000
915062	2454.671	1227	50700	1589	1679	0.151	12620	2070	0	0.026	1517.000
928264	2593.470	1228	34100	1600	1650	0.365	9230	4190	0	0.056	594.000
915063	1945.671	1631	50902	1553	1662	0.228	12110	2100	0	0.027	1401.000
915070	2676.472	1156	16000	1596	1628	0.056	14870	2100	0	0.035	1010.000
928270	2729.546	1701	50800	1566	1660	0.217	14960	4190	0	0.026	1457.000
915071	2592.165	1482	46800	1605	1677	0.525	11560	2100	2033	0.048	713.000
928271	2247.429	1778	50300	1564	1673	0.307	14160	4220	0	0.026	1508.000
915073	2786.713	1800	43983	1568	1644	0.499	13140	4090	1903	0.037	972.000
915074	2555.698	1052	49102	1605	1667	0.206	10490	2080	0	0.030	1200.000
928273	1511.807	2122	40000	1542	1662	0.655	11050	4120	1546	0.027	1381.000
915075	1227.861	1336	35100	1583	1668	0.330	7000	2090	1577	0.040	878.000
915076	1588.371	1385	45300	1581	1658	0.228	9990	3680	0	0.035	1013.000
928275	2276.100	1718	44500	1593	1686	0.589	9500	1610	0	0.040	892.000
Mean	2083.849	1402	35407	1584	1661	0.362	9878	4774	335	0.044	893
σ	575.331	361	9492	25	16	0.182	1954	2001	799	0.019	296

Table 4.3 Sample data set for Plant 3

Heat No	Basicity	T_o (^oC)	c_o (wt%)	O22 (Kg)	raw dolo2 (Kg)	Burnt dolo2 (Kg)	lance level (cm)	c_t (wt%)
1	6955.128	1679.000	0.321	610.000	370.000	180.000	158.000	0.054
2	13888.889	1621.000	0.349	480.000	0.000	230.000	151.000	0.049
3	7879.155	1581.000	0.499	650.000	0.000	250.000	144.000	0.048
4	8964.781	1589.000	0.564	780.000	0.000	280.000	142.000	0.066
5	9053.954	1637.000	0.340	480.000	0.000	1670.000	168.000	0.048
6	8115.942	1641.000	0.218	250.000	0.000	400.000	169.000	0.063
7	8311.137	1654.000	0.392	490.000	0.000	280.000	167.000	0.058
8	7553.048	1650.000	0.200	210.000	0.000	220.000	167.000	0.054
9	6584.022	1631.000	0.336	440.000	0.000	280.000	160.000	0.057
10	7798.069	1634.000	0.460	750.000	520.000	0.000	165.000	0.055
11	3850.853	1629.000	0.549	740.000	650.000	0.000	148.000	0.050
12	4579.349	1639.000	0.419	650.000	390.000	0.000	152.000	0.067
13	5074.187	1554.000	0.478	1600.000	270.000	0.000	149.000	0.069
14	9772.999	1623.000	1.009	680.000	620.000	0.000	148.000	0.043
15	7733.225	1617.000	0.476	700.000	600.000	0.000	148.000	0.047
16	8173.829	1606.000	0.535	700.000	360.000	0.000	150.000	0.049
Mean	7193.807	1629	0.385	557	247	12	159	0.051
σ	1461.411	21	0.134	156	310	106	3	0.010

Table 4.3 Sample data set for Plant 3 (Contd....)

Heat No	T (^oC)	slag volume (Kg)	lance life	p_o (wt%)	Mn_t (wt%)	p_t (wt%)	Mn_o (wt%)	[O] ppm
1	1741.000	2880.802	224.000	0.016	0.160	0.011	0.240	710.000
2	1676.000	2640.356	177.000	0.015	0.140	0.008	0.180	568.000
3	1664.000	3320.779	178.000	0.007	0.120	0.005	0.160	535.000
4	1674.000	2600.502	183.000	0.012	0.140	0.007	0.190	382.000
5	1688.000	3340.696	158.000	0.014	0.170	0.008	0.260	581.000
6	1664.000	3500.808	161.000	0.022	0.170	0.013	0.210	372.000
7	1706.000	3620.819	162.000	0.016	0.200	0.009	0.270	394.000
8	1672.000	3760.949	115.000	0.009	0.170	0.009	0.190	514.000
9	1701.000	2550.726	24.000	0.015	0.150	0.010	0.210	597.000
10	1708.000	2500.608	219.000	0.019	0.180	0.012	0.280	697.000
11	1702.000	2871.444	6.000	0.018	0.120	0.009	0.190	680.000
12	1692.000	3631.546	22.000	0.023	0.140	0.010	0.190	495.000
13	1706.000	3711.411	24.000	0.020	0.150	0.012	0.190	579.000
14	1690.000	2150.418	50.000	0.020	0.130	0.009	0.210	911.000
15	1672.000	2110.524	54.000	0.018	0.150	0.009	0.260	661.000
16	1684.000	2020.475	73.000	0.023	0.140	0.012	0.210	629.000
Mean	1689	3137.791	124	0.015	0.144	0.008	0.202	602
σ	19	460.325	70	0.004	0.026	0.002	0.0041	161

Table 4.4: Comparison of Mean and σ for operational variables of Plant 1, Plant 2 and Plant 3.

Operational	Plant 1		Plant 2		Plant 3	
Variavles	Mean	σ	Mean	σ	Mean	σ
Basicity	5.054	0.831	-	-	7193.807	1461.411
hot ratio	5.305	0.979	-	-	-	-
orel (kg)	4782	1627	-	-	-	-
slg1 (kg)	3021	223	-	-	-	-
dolo1 (kg)	819	626	-	-	-	-
T_o (^oC)	1603	17	1584	25	1629	21
c_0 (mass%)	0.412	0.082	0.362	0.182	0.385	0.134
O22 m^3	2149	304	1402	361	557	156
Ore 2 (Kg)	116	283	-	-	-	-
slg2 (kg)	91	372	-	-	-	-
dolo2 (kg)	540	553	-	-	-	-
Slag volume (kg)	17886.256	1857.449	-	-	3137.791	460.325
$hotratio * p$ (kg)	0.309	0.041	-	-	-	-
$p_o$mass%	0.022	0.005	-	-	0.015	0.004
T (^oC)	1665	14	1661	16	1689	19
p_t mass%	0.009	0.002	-	-	0.008	0.002
Mn_o mass%	0.316	0.029	-	-	0.202	0.0041
Mn_t mass%	0.176	0.026	-	-	0.144	0.026
[O] ppm	426	89	893	296	602	161
hlans2 cm	194	22	-	-	159	3
c_t mass%	0.059	0.011	0.044	0.019	0.051	0.010
SiO_2	-	-	2083.849	575.331	-	-
scrap	-	-	35407	9492	-	-
chill scrap (Kg)	-	-	335	799	-	-
wobs (Kg)	-	-	4774	2001	-	-
flux (Kg)	-	-	9878	1954	-	-
raw dolo2 (Kg)	-	-	-	-	247	310
Burnt dolo2 (Kg)	-	-	-	-	12	106
Lance life	-	-	-	-	124	70

Chapter 5

Results and Discussion for End point Carbon, Temperature, Dissolved oxygen, Phosphorus and Manganese Models

5.1 Introduction

This chapter discusses the results obtained for various end point carbon, temperature, phosphorus, manganese and dissolved oxygen models presented in chapter 3. The experimental data for Plant 1, Plant2 and Plant3, on which models heve been tested and tuned, are already presented in chapter 4.

5.2 Results of Plant 1

Two separate data sets have been considered for Plant 1. As described earlier, for Plant 1 the set of 273 heats is designated as Case Study 1. A sub set consisting of 156 heats, where only those heats in which raw dolomite is added as a coolant during second blow, is called Case Study 2. The results of all models for Plant 1 are summarized in Table 5.1

and results obtained with each model is are presented below, individually.

5.2.1 End point carbon prediction models for Plant 1

Fundamental aspects of development of end point carbon prediction models are discussed in chapter 3.

5.2.1.1 CO-Gas Evolution model (model 5.1)

CO-Gas evolution model is given by eq. (3.6)

$$c_t = (c_o^{\mu} + \gamma t)^{\frac{1}{\mu}} \tag{5.1}$$

where $\mu = -\frac{\eta}{1-\eta}$. This model is developed for Case Study 2 (156 heats) of Plant 1.

By using Gauss-Newton method the sum of square of errors (SSE) ($\sum$(actual−predicted)^2) was obtained for different values of μ in the range -1.5 to -0.33 (i.e. η in the range of 0.25-0.6). The optimum value of μ calculated from the graph of sum of square of errors (SSE) vs μ (Fig. 5.1, corresponding to minimum in SSE is) -0.41. The corresponding η value can be back calculated as 0.291. The γ value, corrsponding to minimum SSE, is 0.010292. Fig 5.2 shows the graph of actual vs predicted carbon. From the statistics of regression performed on actual vs predicted carbon (see Table 5.1, model 5.1), it can be observed that σ value is ±0.007 (0.0066)%C and correlation coefficient R is 0.59 (0.5852). Therefore model 5.1 is able to explain only 34% of variation. For a typical heat with

c_o = 0.517%, 022 = 2462, t = 197s, we obtain by substituting in eq. (5.1)

$c_t = (0.517^{-0.14} + 0.01029 * 197)^{\frac{-1}{0.41}}$

= 0.052.

Actual end point carbon value for this particular heat is 0.050.

5.2.1.2 Non-Linear model (model 5.2)

Nonlinear model is given by eq. (3.9)

$$c_t = -\frac{\alpha_2 \cdot c_0}{1 - \alpha_3 \cdot c_0} \cdot t + c_0 \tag{5.2}$$

Table 5.1 Summary of results for carbon prediction obtained for Plant 1

S. No	Model No	Model equation	Parameters used	Parameters optimized	Statistics of regression, y=mx+c			Remarks
					Dependent variable	Independent variable	Statistics	
1	5.1	$c_t = (c_o^{\mu} + \gamma t)^{\frac{1}{\mu}}$	c_o , t	μ, γ	c_t (0.052)	$c_{t_{act}}$ (0.050)	m=0.5694 c=0.0251 R=0.59 σ=0.007 F=80.207	Case study 2
2	5.1 (reg)	$c_t' = \mu_o + \mu_1 c_t + \sum_{i=2}^{n-1} \mu_i \cdot X_i$	Ore1 dolo1 c_o, t	μ_i	c_t' (0.055)	$c_{t_{act}}$ (0.050)	m=0.4294 c=0.033 R=0.66 σ=0.004 F=116.998	Case study 2
3	5.2	$c_t = \frac{-\alpha_2 c_0 t}{1-\alpha_3 c_0} + c_o$	c_o, t	α_2,α_3	c_t (0.055)	$c_{t_{act}}$ (0.050)	m=2.4337 c=-0.0775 R=0.66 σ=0.02449 F=109.368	Case study 2
4	5.2 (reg)	$c_t' = \mu_o + \mu_1 c_t + \sum_{i=2}^{n-1} \mu_i \cdot X_i$	Ore1 dolo1 c_o, t	μ_i	c_t' (0.057)	$c_{t_{act}}$ (0.050)	m=0.498 c=0.0315 R=0.68 σ=0.004 F=127.98	Case study 2

Table 5.1 Summary of results for carbon prediction obtained for Plant 1 (contd...)

S. No	Model No	Model equation	Parameters used	Parameters optimized	Statistics of regression (y=mx+c)			Remarks
					Dependent variable	Independent variable	Statistics	
5	5.3	$c_t = \frac{-\alpha_2 \cdot t}{[1-\alpha_3]} + c_0$	c_o, t	α_2,α_3	c_t (0.11)	$c_{t_{act}}$ (0.050)	m=2.8140 c=-0.0936 R=0.49 σ=0.04 F=41.847	Case study 2
6	5.3 (reg)	$c'_t = \mu_o + \mu_1 c_t + \sum_{i=2}^{n-1} \mu_i \cdot X_i$	Ore1 O22 hlans2 dolo1 co	μ_i	c'_t (0.059)	$c_{t_{act}}$ (0.050)	m=0.5796 c=0.0245 R=0.76 σ=0.004 F=212.882	Case study 2
7	5.3 (a) (reg)	$c'_t = \mu_o + \mu_1 c_t + \sum_{i=2}^{n-1} \mu_i \cdot X_i$	ore1, T_o c_o, Mn_o p_o, O22	μ_i	c'_t (0.055)	$c_{t_{act}}$ (0.050)	m=0.6708 c=0.0192 R=0.82 σ=0.004 F=308.958	Case study 2
8	5.4 (method 1)	$\Delta c = \Delta t \alpha_1 \epsilon^\eta c$ $\epsilon = (-\frac{dc}{dt}\beta_1 + Q_{eff})$	c_o, t	α_1 , η	c_t (0.054)	$c_{t_{act}}$ (0.050)	m=0.4987 c=0.0302 R=0.55 σ=0.008 F=120.748	Case study 1
9	5.4 (reg, method 1)	$c'_t = \mu_o + \mu_1 c_t + \sum_{i=2}^{n-1} \mu_i \cdot X_i$	Ore1 dolo1 hot ratio Ore2,T_o co, t	μ_i	c'_t (0.056)	$c_{t_{act}}$ (0.050)	m=0.4469 c=0.0322 R=0.67 σ=0.005 F=220.129	Case study 1

Table 5.1 Summary of results for carbon prediction obtained for Plant 1 (contd...)

S. No	Model No	Model equation	Parameters used	Parameters optimized	Statistics of regression (y=mx+c)			Remarks
					Dependent variable	Independent variable	Statistics	
10	5.4 (method 1)	$\Delta c = \Delta t \alpha_1 \epsilon^{\eta} c$ $\epsilon = (-\frac{dc}{dt}\beta_1 + Q_{eff})$	c_o, t	α_1 , η	c_t (0.052)	$c_{t_{act}}$ (0.050)	m=0.6292 c=0.0216 R=0.60 σ=0.007 F=87.292	Case study 2
11	5.4 (reg, method 1)	$c_t' = \mu_o + \mu_1 c_t + \sum_{i=2}^{n-1} \mu_i \cdot X_i$	Ore1 dolo1 c_o, t	μ_i	c_t' (0.056)	$c_{t_{act}}$ (0.050)	m=0.4333 c=0.0331 R=0.66 σ=0.004 F=118.963	Case study 2
12	5.4 (method 2)	$\Delta c = \Delta t \alpha_1 \epsilon^{\alpha_2 \epsilon} c$ $\epsilon = (-\frac{dc}{dt}\beta_1 + Q_{eff})$	c_o, t	α_1 ,α_2	c_t (0.055)	$c_{t_{act}}$ (0.050)	m=0.6898 c=0.0182 R=0.62 σ=0.010 F=167.455	Case study 1
13	5.4 (reg, method 2)	$c_t' = \mu_o + \mu_1 c_t + \sum_{i=2}^{n-1} \mu_i \cdot X_i$	Ore1 dolo1 hot ratio Ore2 c_o, t	μ_i	c_t' (0.058)	$c_{t_{act}}$ (0.050)	m=0.4751 c=0.0308 R=0.69 σ=0.005 F=224.079	Case study 1

Table 5.1 Summary of results for carbon prediction obtained for Plant 1 (contd...)

S. No	Model No	Model equation	Parameters used	Parameters optimized	Statistics of regression (y=mx+c)			Remarks
					Dependent variable	Independent variable	Statistics	
14	5.4 (method 2)	$\Delta c = \Delta t \alpha_1 \epsilon^{\alpha_2 \epsilon} c$ $\epsilon = (-\frac{dc}{dt}\beta_1 + Q_{eff})$	c_o, t	α_1 , α_2	c_t (0.055)	$c_{t_{act}}$ (0.050)	m=0.8781 c=0.0076 R=0.67 σ=0.008 F=124.988	Case study 2
15	5.4 (reg, method 2)	$c'_t = \mu_o + \mu_1 c_t + \sum_{i=2}^{n-1} \mu_i \cdot X_i$	Ore1 dolo1 c_o, t	μ_i	c'_t (0.056)	$c_{t_{act}}$ (0.050)	m=0.4962 c=0.0291 R=0.71 σ=0.004 F=153.313	Case study 2
16	5.5	$C_t = \frac{C_0}{t\zeta}$	c_o, t	ζ	c_t (0.068)	$c_{t_{act}}$ (0.050)	m=0.4120 c=0.0340 R=0.37 σ=0.009 F=23.868	Case study 2
17	5.5 (reg)	$c'_t = \mu_o + \mu_1 c_t + \sum_{i=2}^{n-1} \mu_i \cdot X_i$	dolo2 dolo1, T_o hlans2 c_o, t	μ_i	c'_t (0.060)	$c_{t_{act}}$ (0.050)	m=0.550 c=0.0261 R=0.74 σ=0.004 F=182.483	Case study 2

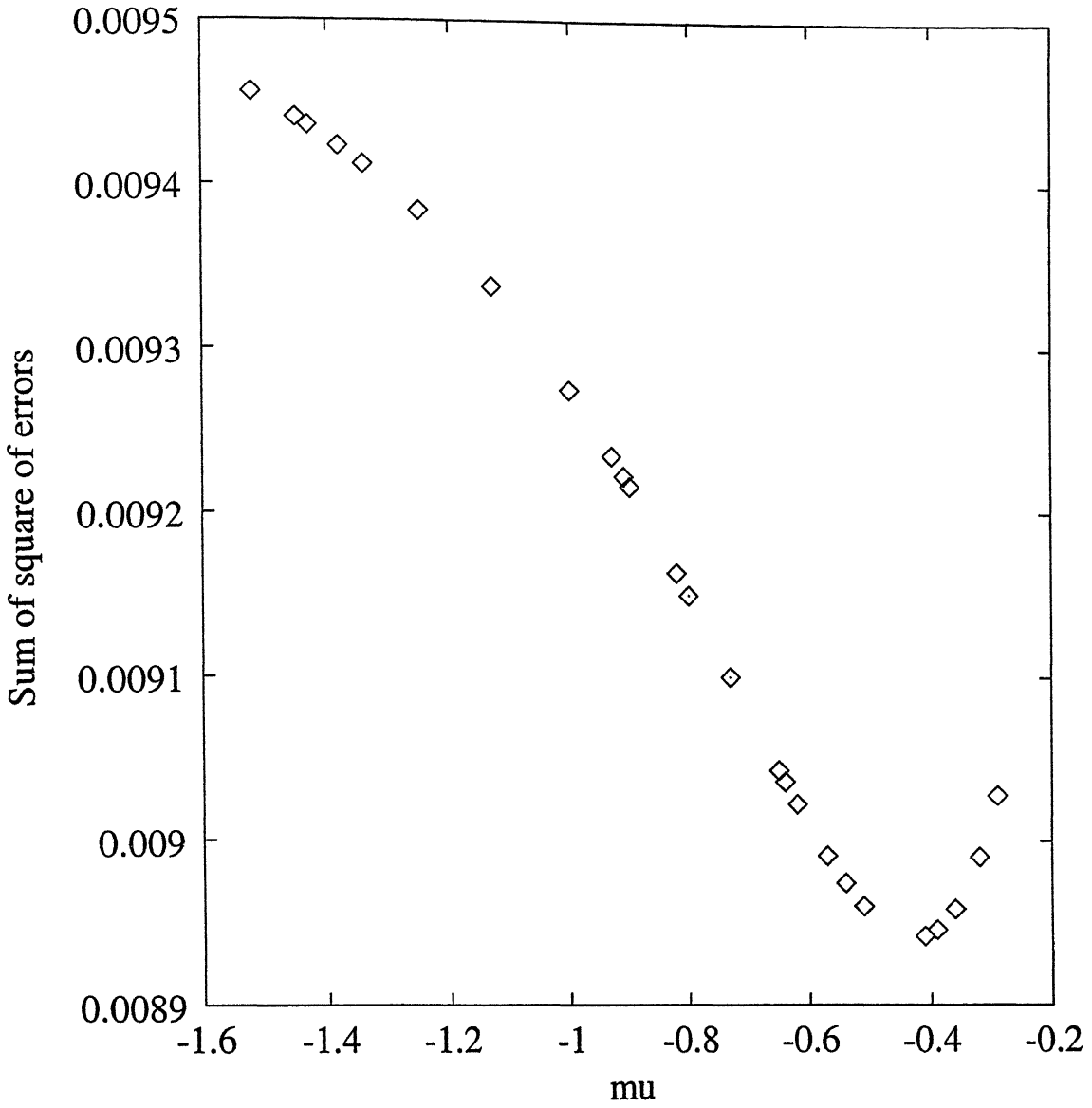

Figure 5.1: mu (μ) vs sum of square of errors for CO-Gas evolution model (model 5.1); minimum SSE occurs at μ = -0.41.

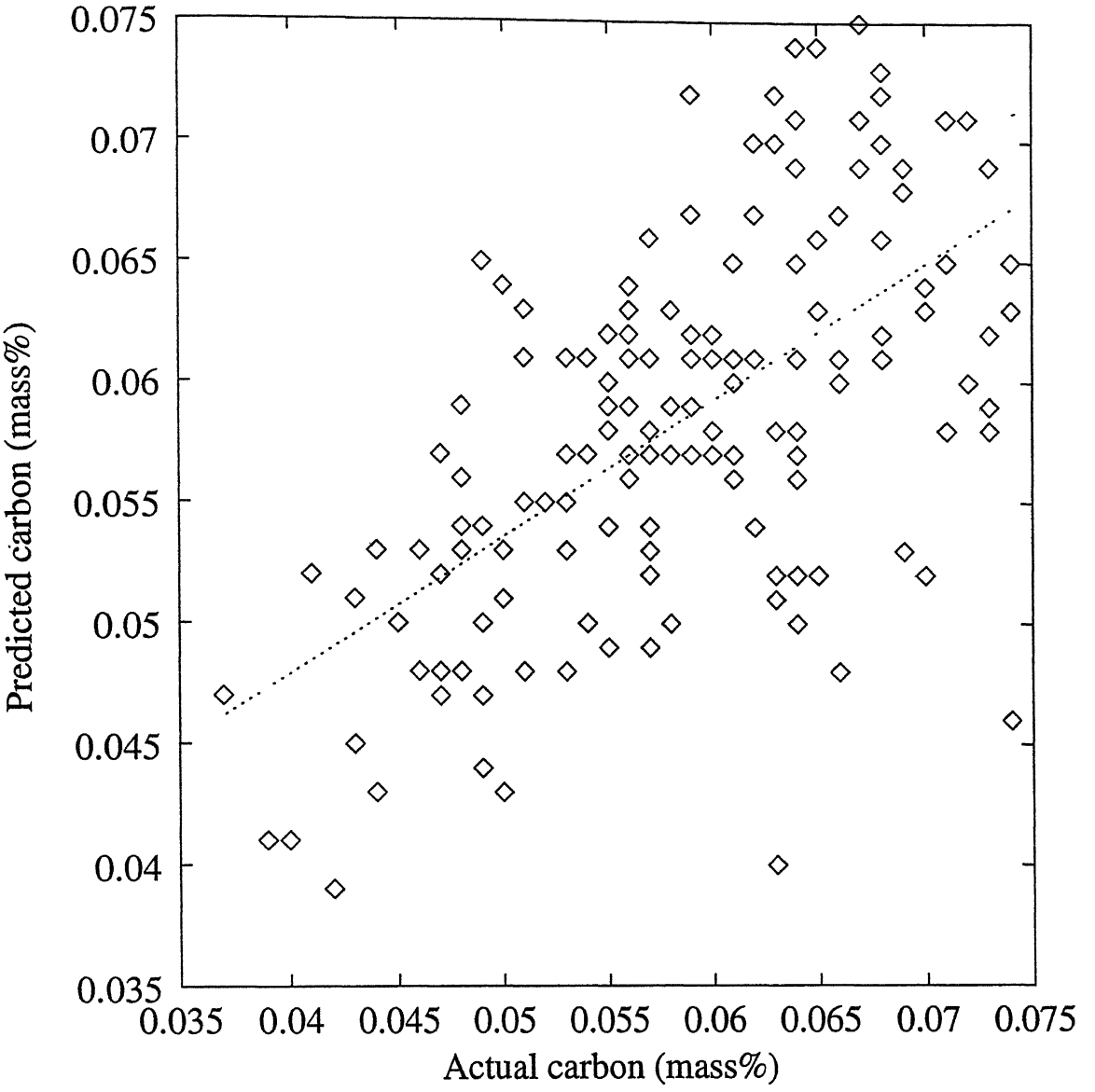

Figure 5.2: Data from Plant 1, Case Study 2 (156 heats): Actual vs predicted carbon for CO-Gas evolution model (model 5.1), best fit line is y=0.5694x+0.0251. Statistics are n=156, R=0.59, std. error=0.007.

where α_2 and α_3 are constants to be tuned. This model is tuned for Case Study 2 (156 heats) of Plant 1. Constants α_2 and α_3, again determined by applying Gauss-Newton method on 156 heats, are found to be 0.0075 and -1.2654 , respectively. From the statistics of regression performed on actual versus predicted carbon it can be observed that σ=0.024 (0.02449)%C and R=0.66 (0.6557) (see Table 5.1, model 5.2). Thus, this model is able to explain 43% of variation. For a typical heat with $c_0 = 0.517\%$, t = 197 s we get

$c_t = \frac{-0.0075*0.517*197}{1+1.2654*0\ 517} + 0.517$

= 0.055.

Actual end point carbon value for this particular heat is 0.050.

5.2.1.3 Linear model (model 5.3)

Linear model is given by eq. (3.10)

$$c_t = -\frac{\alpha_2}{[1-\alpha_3]} \cdot t + c_0$$

where α_2 and α_3 are constants. The above equation can be simplified into the form

$$c_t = -\beta \cdot t + c_0 \tag{5.3}$$

where the constant β is determined by performing linear regression on eq. (5.3) as 0.002062. When this model is tuned for 156 datasets of Plant 1,it can be observed from the statistics of regression performed on actual versus predicted carbon that σ=0.04 (0.0397)%C and R=0.4935 (0.49) (see Table 5.1, model 5.3). Thus, this model is able to explain only 24.35% of variation. For a typical heat with t=197 s, $c_0 = 0.517\%$, we get from eq. (5.3)

c_t =- 0.002062 * 197 + 0.517

= 0.11.

Actual end point carbon value for this particular heat is 0.050.

5.2.1.4 GA-decarb models (model 5.4)

GA-decarb models have been discussed earlier in section 3.5. In these models, genetic algorithm (GA) technique is used to optimize the parameters. After trail and error runs,

the GA parameters used for optimization of these models are: micro GA(Yes) [?], Cross over probability (0.9), Creep probability (0.004), Mutation probability (0.00001), Number of generations (300), Population size (10), Chromosome size (10). GA code developed by David L. Carroll of University of Illinois[?] was used for optimizing the models.

Method 1

The governing equation for optimization is given by eq. (3.11)

$$\Delta c = \Delta t \cdot \alpha_1 \cdot \left(-\frac{dc}{dt}\beta_1 + Q_{eff}\right)^{\eta} \cdot c \tag{5.4}$$

The parameters to be optimized are α_1 and η. Optimization is done successively for small time steps (say $\Delta t = 0.01sec$) until $t \leq t_{max}$ where t_{max} is the total time of second blow period. Range of α_1 is 0.005-0.007 and range of η is 0.20-0.65. Optimum values of α_1 and η are selected corresponding to minimum sum of square of errors (SSE) between actual and predicted carbon.

Case Study 1 (273 heats)

Eq. (5.4) was optimized for 273 data sets. Optimized values of α_1 and η corresponding to minimum SSE are 0.006771 and 0.2247, respectively. Table 5.1, model 5.4 (Case Study 1) shows the statistics of regression performed on actual vs predicted carbon. It can be observed from regression statistics (Table 5.1, model 5.4) that σ=0.008 (0.00806)% and R=0.55 (0.5552), thus explaining 30.8% of variation. Fig. 5.3 shows graph of actual vs predicted carbon. The significance of variation of mass transfer coefficient (K'), where $K' = \alpha_1 \cdot \left(-\frac{dc}{dt}\beta_1 + Q_{eff}\right)^{\eta}$, is discussed later.

Case Study 2 (156 heats)

Eq. (5.4) was optimized for 156 data sets. Optimized values of α_1 and η corresponding to minimum SSE are 0.006501 and 0.2477. The statistics of regression performed on actual versus predicted carbon Table 5.1, model 5.4 (Case Study 2) shows that σ=0.007 (0.0071)

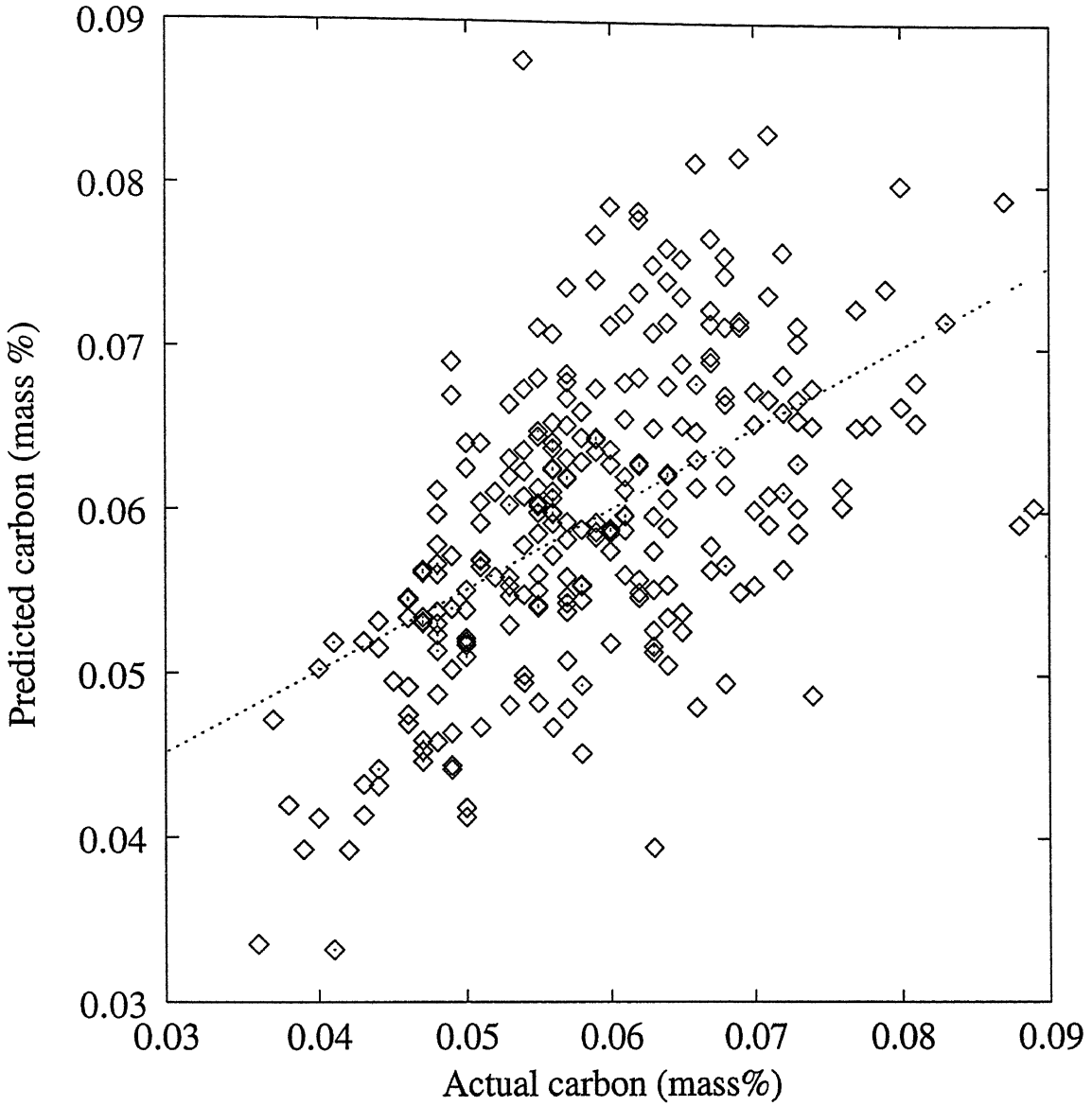

Figure 5.3: Data from Plant 1, Case Study 1(273 heats): Actual vs predicted for model 4 (Case Study 1), best fit line is y=0.4987x+0.0302. Statistics are n=273, R=0.55, std. error=0.008.

%C and R= 0.60 (0.6015), thus explaining 36.2% of variation. Fig. 5.4 shows graph of actual vs predicted carbon.

Method 2

In this method, η is made proportional to gas flow rate, because gas flow rate changes substantially with time. The governing equation for optimization is given by eq. (3.12) i.e.,

$$\Delta c = \Delta t \cdot \alpha_1 \cdot \left(-\frac{dc}{dt}\beta_1 + Q_{eff}\right)^{\alpha_2\left(-\frac{dc}{dt}\beta_1 + Q_{eff}\right)} \cdot c \tag{5.5}$$

The parameters to be optimized are α_1 and α_2. Optimization is done successively for time steps (say $\Delta t = 0.01sec$) until $t \leq t_{max}$ where t_{max} is the total time of second blow period. Range of α_1 is 0.01-0.016 and range of α_2 is 0.0005-0.0013. Optimum values of α_1 and α_2 are selected corresponding to minimum sum of square of errors (SSE) between actual and predicted carbon for all heats.

Case Study 1 (273 heats)

Eq. (5.5) was optimized for 273 data sets. Optimized values of α_1 and α_2 corresponding to minimum SSE are 0.01109 and 0.0006283, respectively.The statistics of regression performed on actual vs predicted carbon, Table 5.1, model 5.4 (method 2, Case Study 1) shows that σ=0.010 (0.00947)% and R=0.62 (0.6180), thus explaining 38.2% of variation. Fig. 5.5 shows graph of actual vs predicted carbon.

Case Study 2 (156 heats)

Eq. (5.5) was optimized for 156 data sets. Optimized values of α_1 and α_2 corresponding to minimum SSE are 0.01105 and 0.0007495. From the statistics of regression it can be observed that σ=0.008 (0.00826)%C and R=0.67 (0.6693) (see Table 5.1 model 5.4 (method 2, Case Study 2)), thus explaining 44.8% of variation. Fig. 5.6 shows the graph of actual vs predicted carbon.

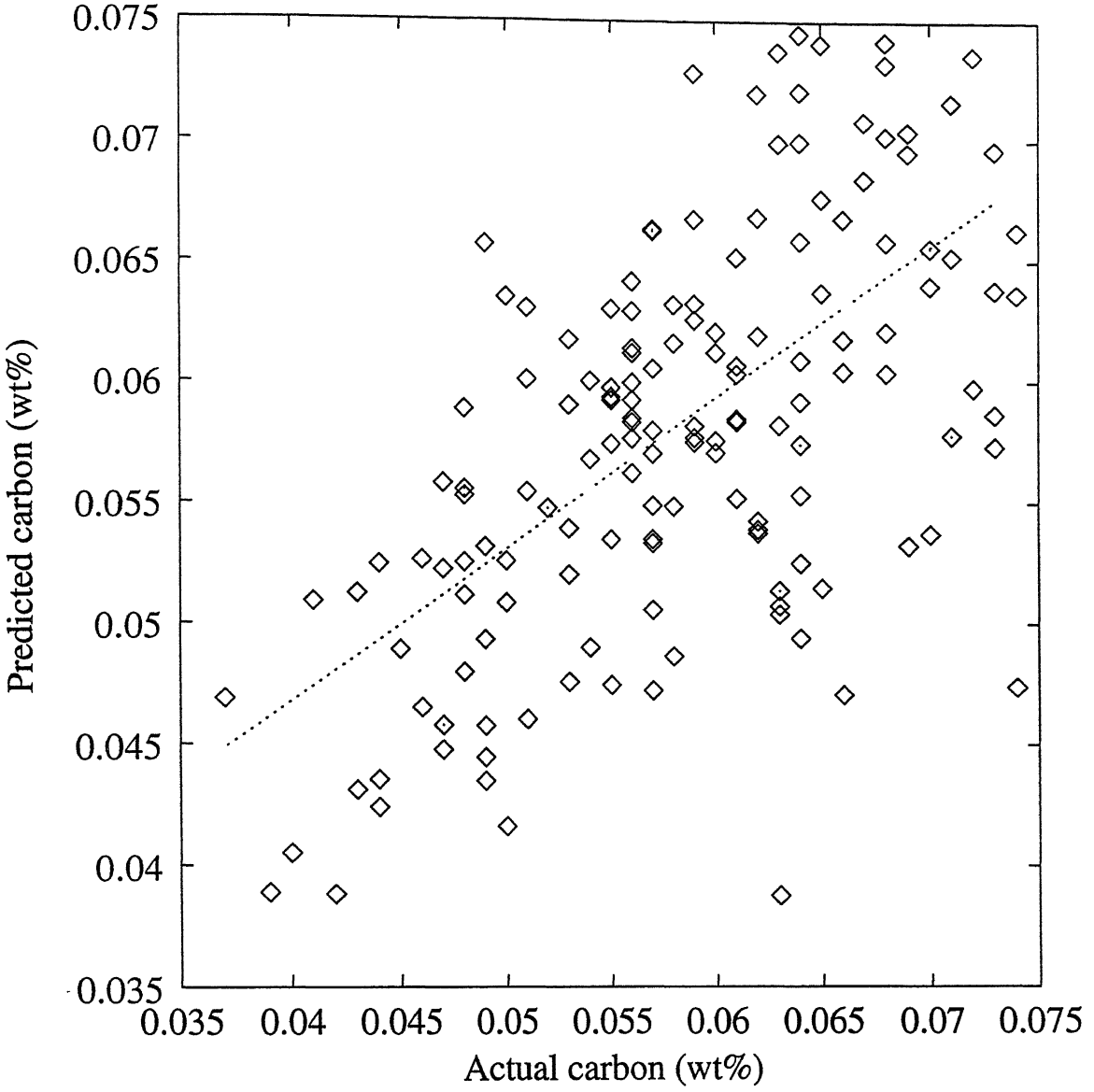

Figure 5.4: Data from Plant 1, Case Study 2 (156 heats): Actual vs predicted graph for model 5.4 (method 1, Case Study 2), best fit line is 0.6292x+0.0216. Statistics are n=156, R=0.60, std. error=0.007.

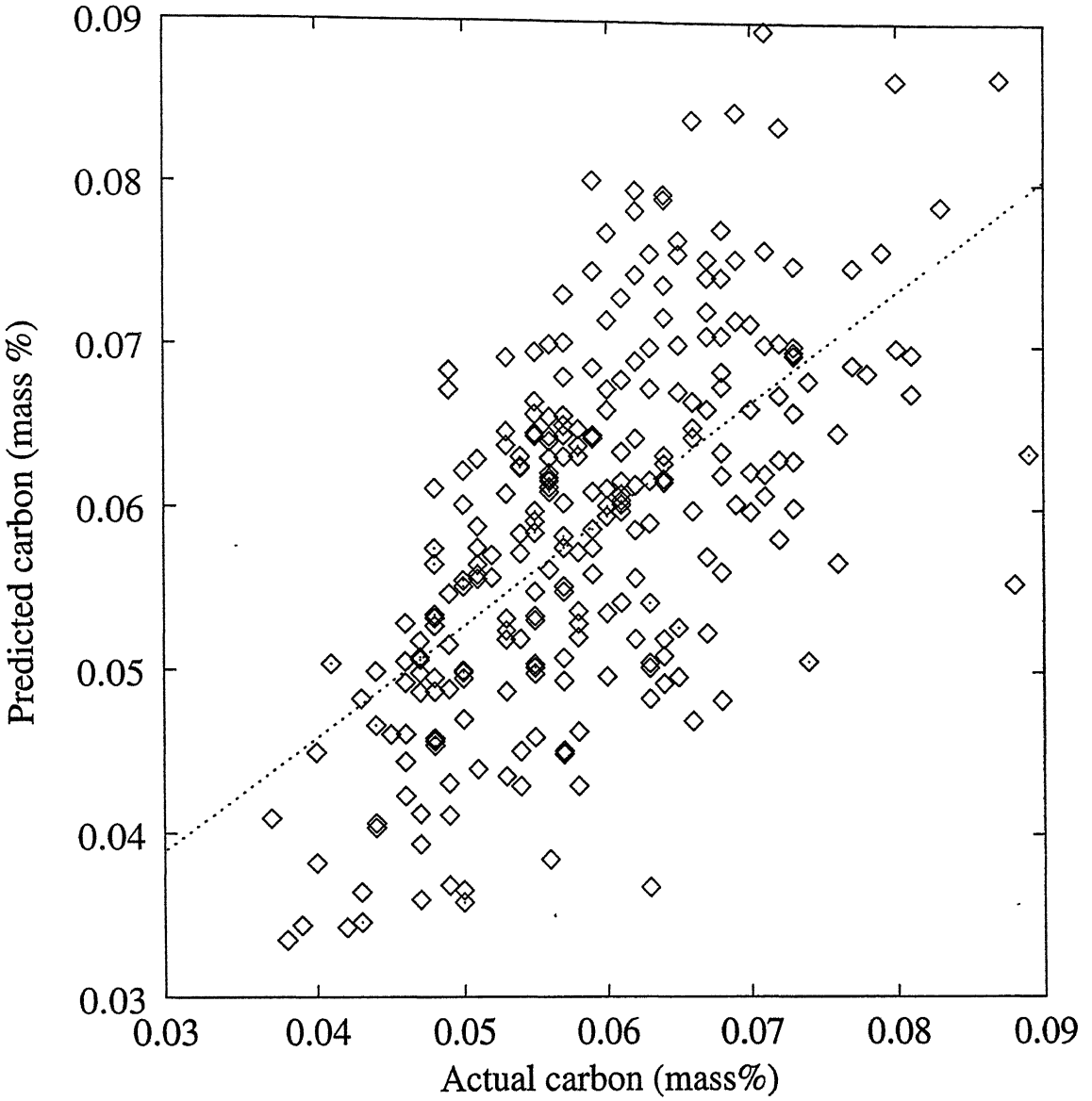

Figure 5.5: Data from Plant 1, Case Study 1(273 heats): Actual vs predicted carbon for model 5.4 (method 2, Case Study 1). Best fit line is y=0.6898x+0.0182. Statistics are n=273, R=0.62, std. error=0.010.

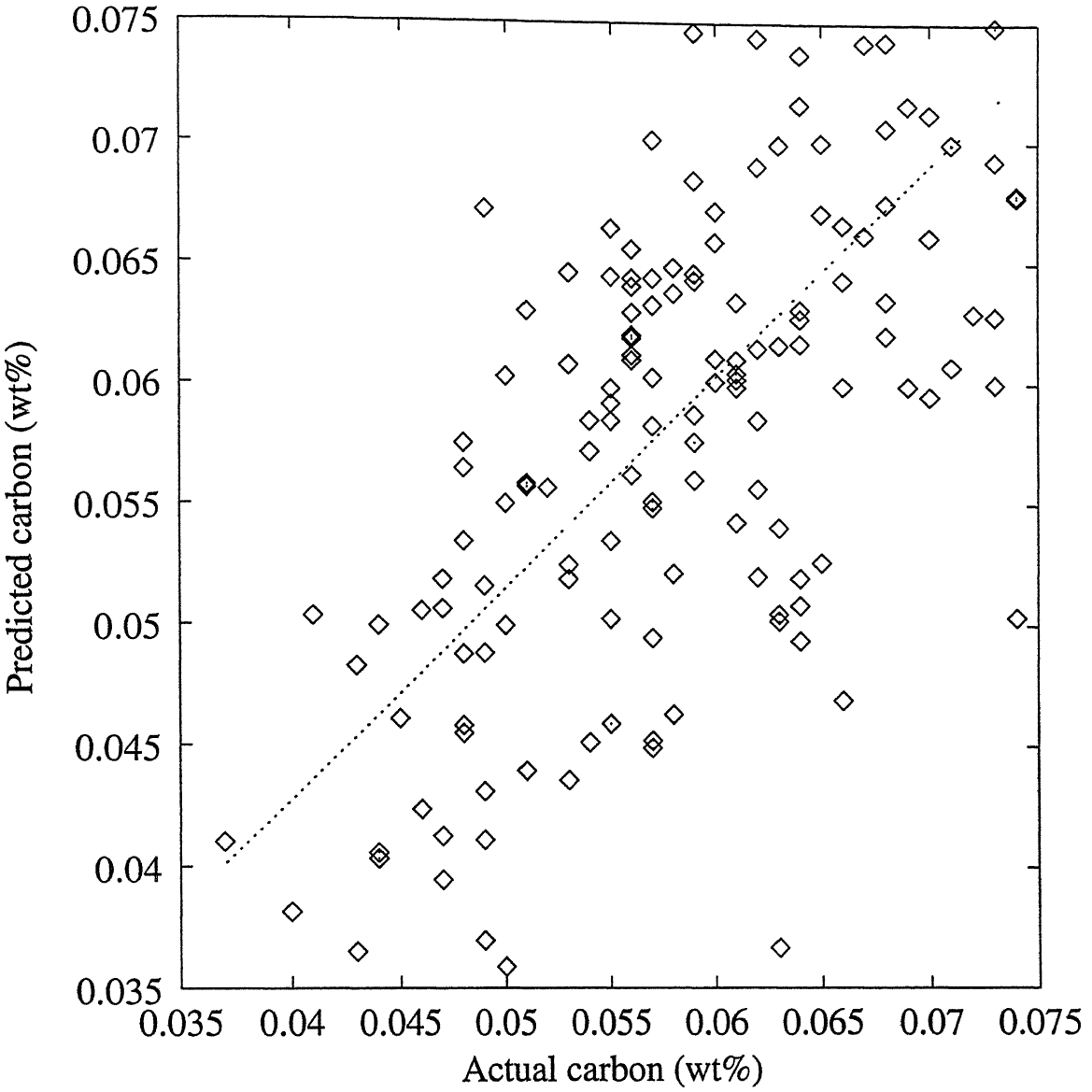

Figure 5.6: Data from Plant 1, Case Study 2(156 heats): Actual vs predicted graph for model 5.4 (method 2, Case Study 2), best fit line is y=0.8781x+0.0076. Statistics are n=156, R=0.67, std. error=0.008.

5.2.1.5 Empirical Model (model 5.5)

Empirical model is given by eq. (3.13) i.e.,

$$c_t = \frac{c_o}{t^{\zeta}} \tag{5.6}$$

Optimum value of ζ is calculated from the graph of sum of square of errors (SSE) vs ζ. A typical graph of SSE versus ζ is shown in Fig. 5.7. From the graph it can be observed that optimum value of ζ corresponding to minimum SSE is 0.382. From the statistics of regression it can be observed that σ=0.009 (0.0089)% and R=0.37 (0.3663) (see Table 5.1 model 5.5), thus explaining only 13.4% of variation. Fig 5.8 shows the actual vs predicted carbon. For a typical heat with c_O = 0.517% and t=197 s, we get

$c_t = \frac{0.517}{(197)^{.382}}$

=0.068.

Actual end point carbon for this particular heat is 0.050.

5.2.1.6 Regression models

As an attempt to improve upon the prediction of models developed so far, the effect of other variables is incorporated in regression models. Regression models as discussed in section 3.7 are given by eq. (3.14) i.e.,

$$c'_t = \mu_o + \mu_1 c_o + \sum_{i=2}^{n-1} \mu_i \cdot X_i \tag{5.7}$$

where, c'_t is the end point carbon and c_o is the sublance carbon value, μ_i 's are coefficients of operational variables X_i. These models are developed using multiple linear regression (MLR) technique. The units of the operational variables are as shown in Table 4.1

Model 5.1 (reg)

Model 5.1 (reg) is regression model for CO-Gas evolution model (model 5.1). Variables accepted and corresponding coefficients in this model are Ore1 (-0.0000009), dolo1(-

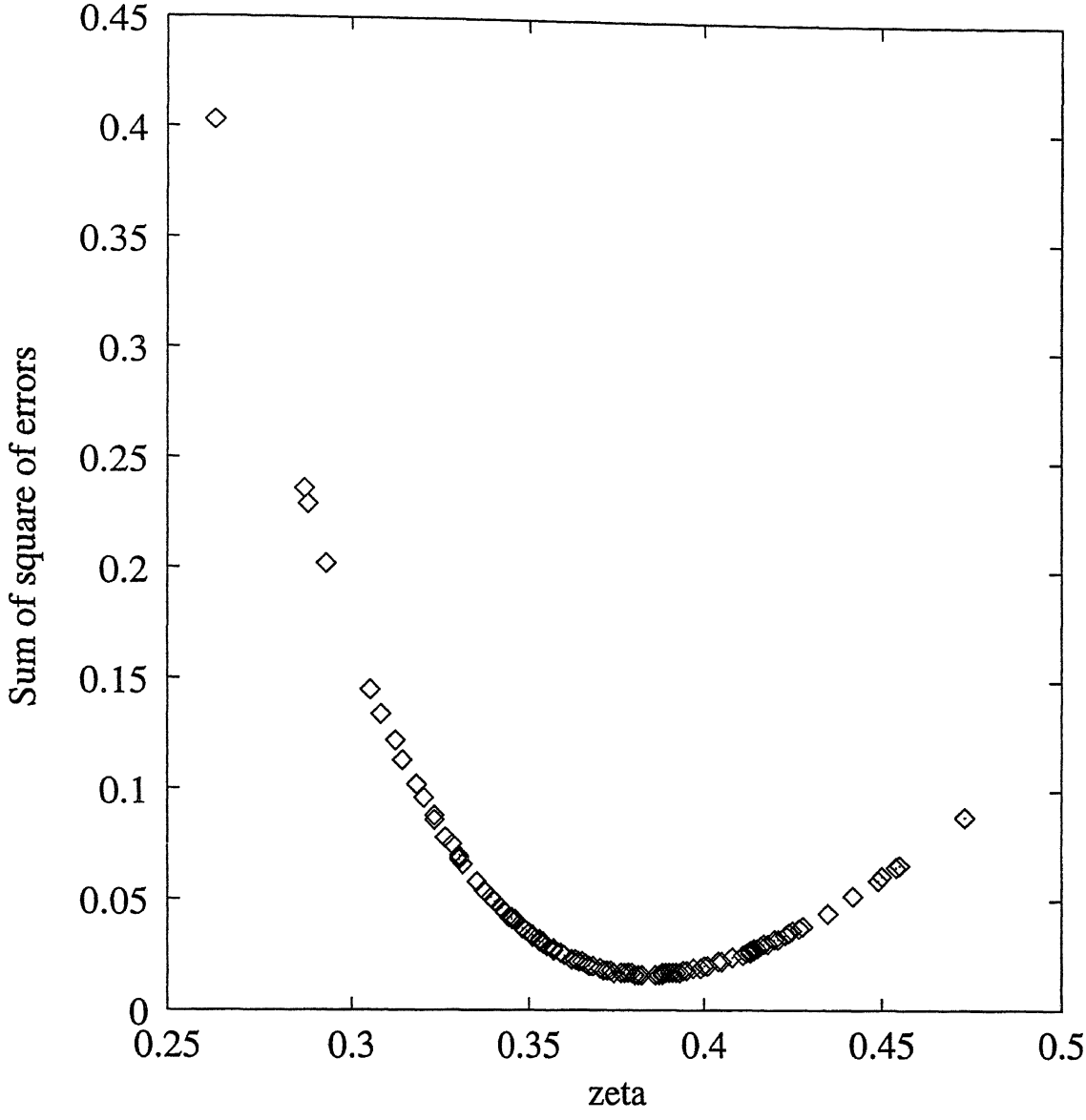

Figure 5.7: zeta (ζ) vs sum of square of errors for model 5.5; minimum error occurs at ζ =0.382.

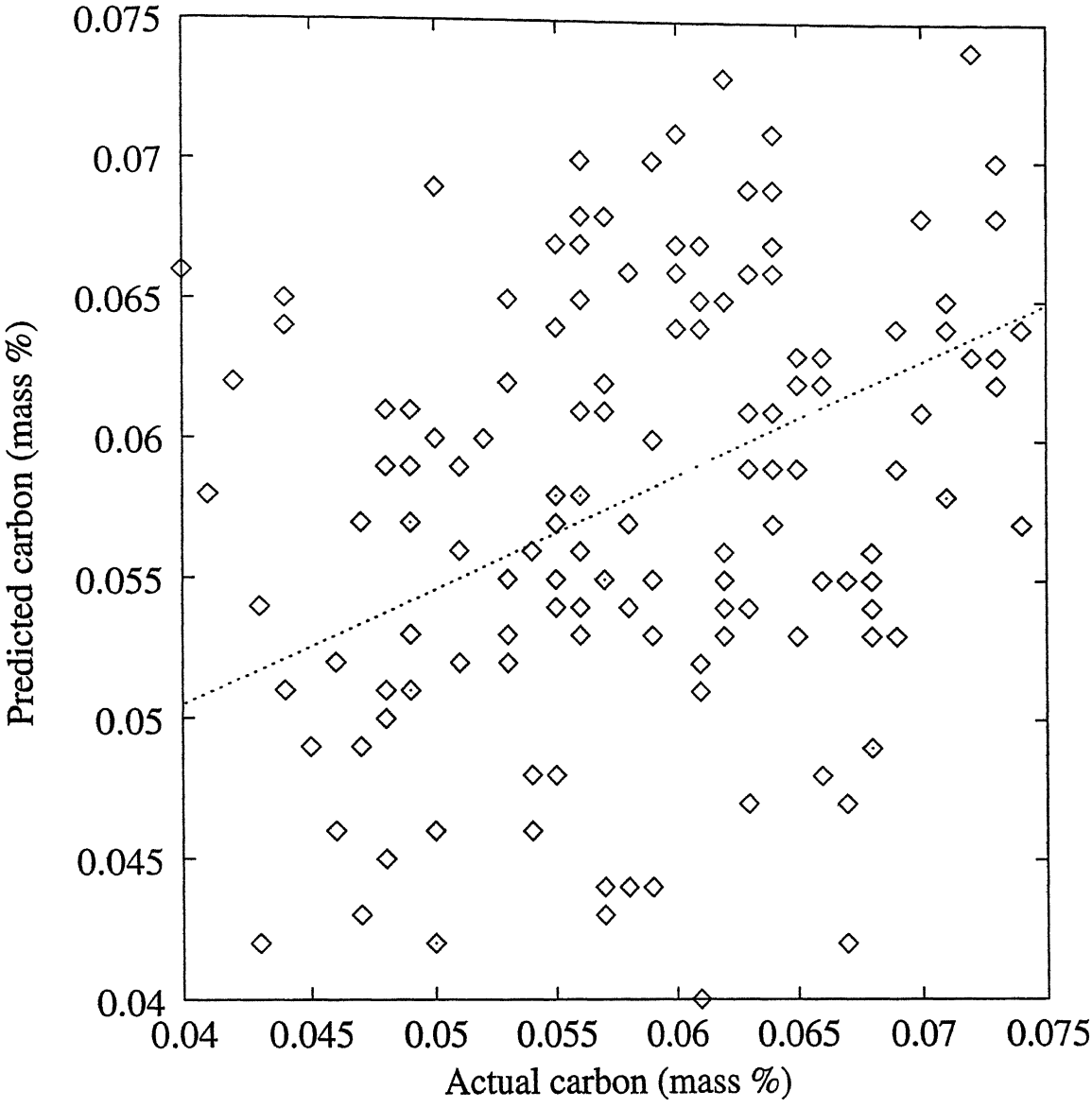

Figure 5.8: Data from Plant 1, Case Study 2(156 heats): Actual vs predicted carbon for model 5.5. Best fit line is y=0.412x+0.034. Statistics are n=156, R=0.37, std.error=0.008.

0.0000037), c_t (0.5438315) and constant(0.0317). From the statistis of regression it can be observed that σ=0.004 (0.00417)%C and R=0.66 (0.6571) (Table 5.1, model 5.1 (reg)), thus explaining 43.2% of variation. Fig. 5.9 shows the graph of actual versus predicted carbon. It can be observed that R increased from 0.59 in model 5.1 to 0.66 in model 5.1 (reg) i.e., an improvement of 12.3%. The value of σ also came down to 0.004% in model 5.1 (reg) from 0.007% in model 5.1, a decrease of 36.8% in standard error. For a typical heat with ore 1 = 3994, dolo1 = 413 and c_t = 0.052 (see model 5.1),

c'_t = 0.0317 + 0.5438315(0.052) - 0.0000009(3934) - 0.0000037(413)

= 0.055.

The actual carbon for this heat is 0.050.

Model 5.2 (reg)

Model 5.2 (reg) is regression performed on Non-Linear model (model 5.2). The respective coefficeints of operational variables by MLR acceped are Ore1 (-0.0000007), dolo1(-0.0000026), c_t (0.1644613) and μ_o (0.0521). From the statistis of regression (Table 5.1 (model 5.2 (reg))) it can be observed that σ=0.004 (0.00396)%C and R=0.69 (0.6847), thus explaining 46.9% of variation. Fig. 5.10 shows the graph of actual versus predicted carbon. It can be observed that R increased from 0.66 in model 5.2 to 0.69 in model 5.2 (reg) i.e., an improvement of 4.5%. σ also came down to 0.004% in model 5.2 (reg) from 0.024 in model 5.2 i.e., a reduction of 83.8% in standard error. For a typical heat with ore1 = 3994, dolo1 = 413 and c_t = 0.055 (see model 5.2),

c'_t=0.0521 + 0.1644613(0.055) − 0.0000007(3994) - 0.0000026(413)

= 0.057.

The actual carbon for this heat is 0.050.

Model 5.3 (reg)

Model 5.3 (reg) is regression model for Linear model (model 5.3). Operational parameters accepted in this model are Ore1 (-0.0000007), dolo1 (-0.0000022), O22 (-0.0000227), hlans2 (0.0000728), c_t (0.0843022) and μ_o (0.0623). From the statistis of regression (Table 5.1, model 5.3 (reg)) it can be observed that σ=0.004 (0.00418)%C and R=0.76 (0.7617),

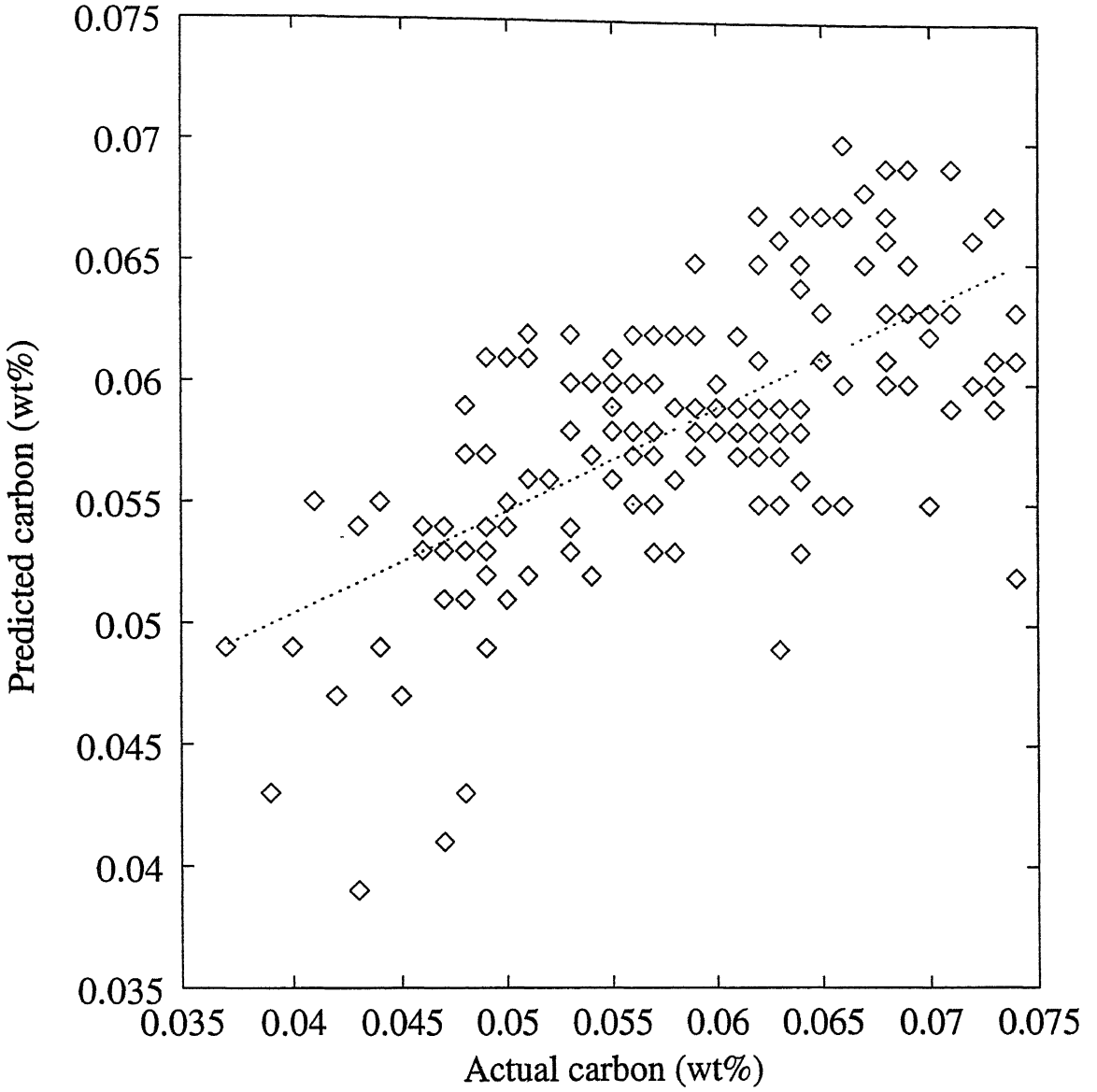

Figure 5.9: Data from Plant 1, Case Study 2(156 heats): Actual vs predicted carbon for model 5.1 (reg), best fit line is y=0.4294x+0.033. Statistics are n=156, R=0.66, std. error=0.004.

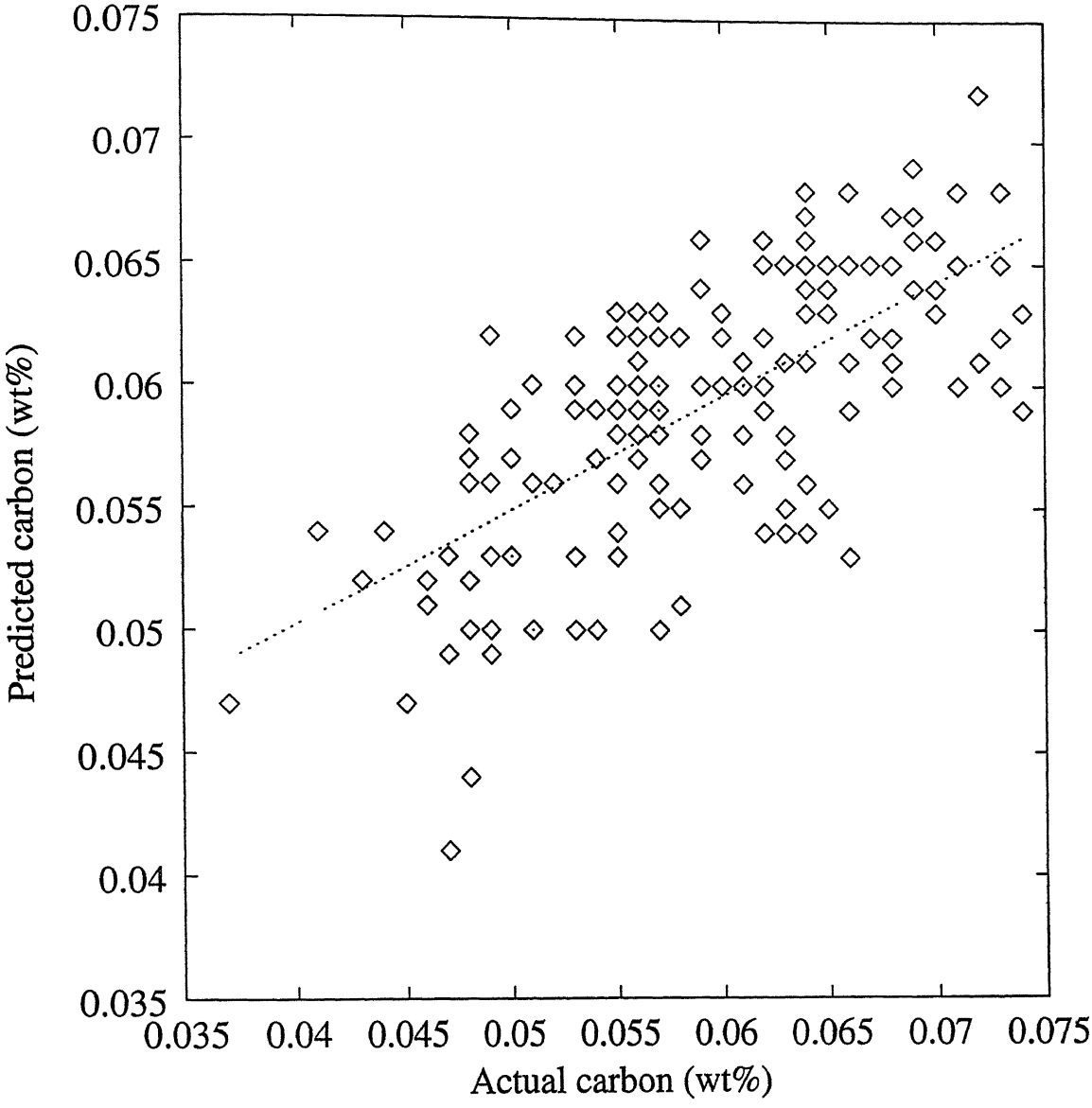

Figure 5.10: Data from Plant 1, Case Study 2(156 heats): Actual vs predicted carbon for model 5.2 (reg), best fit line is y=0.4980x+0.0315. Statistics are n=156, R=0.69, std. error=0.004.

thus explaining 58% of variation. Fig. 5.11 shows the graph of actual vs predicted carbon. It can be observed that R increased from 0.5 in model 5.3 to 0.76 in model 5.3 (reg) i.e., an improvement of 54.3%. The value of σ also came down to 0.004% in model 5.3 (reg) from 0.04% in model 5.3 i.e., a reduction of 100% in standard error. For a typical heat with ore1 = 3394, dolo1 = 413, 022 =2464, hlans2 = 187, we get

c_t' = 0.0623 + 0.0843022 (0.517) - 0.0000007(3994) - 0.0000022(413) - 0.0000227(2464) + 0.0000728(187)

= 0.059.

The actual carbon for this heat is 0.050.

Model 5.3 (a) (reg)

In this model sublance phosphorus and manganese are also considered as parameters in MLR. From statistics of regression (Table 5.1, model 5.3 (a) (reg)), it can be observed that R=0.82 and σ=0.004. Though there is no improvement in σ value from model 5.3 (reg) to model 5.3 (a) (reg), there is 7.7% improvement in R value. Thus if sublance phosphorus and manganese are available, this model gives better results. Fig. 5.12 shows graph of actual vs predicted carbon. Variables used in this model are ore1(-0.0000008219), T_o(0.0001869125), c_o(0.1146421219), Mn_o (0.0843178237), p_o(-1.0100703893), O22(-0.0000249837) and constant (-0.2346). For a typical heat with ore1=3994, T_o =1607, c_o = 0.326, Mn_o=0.517, p_o=0.027, O22=2464

c_t'=-0.2346-0.0000008219(3994)+0.0001869125(1607)+0.1146421219(0.326)+ 0.0843178237(0.517)-1.0100703893(0.027)-0.0000249837(2464)

=0.055.

Actual end point carbon for this heat is 0.050.

Model 5.4 (reg, method 1, Case Study 1)

Model 5.4(reg, method 1, Case Study 1) is regression model for model 5.4 (method 1, Case Study 1). The operational variables effecting the end point carbon content and statistics of regression are presented in Table 5.1, Model 5.4(reg, method 1, Case Study 1). Variables used in this model are hot ratio (0.0027146), Ore1 (-0.0000014), c_t(0.6304038), Dolo1(-

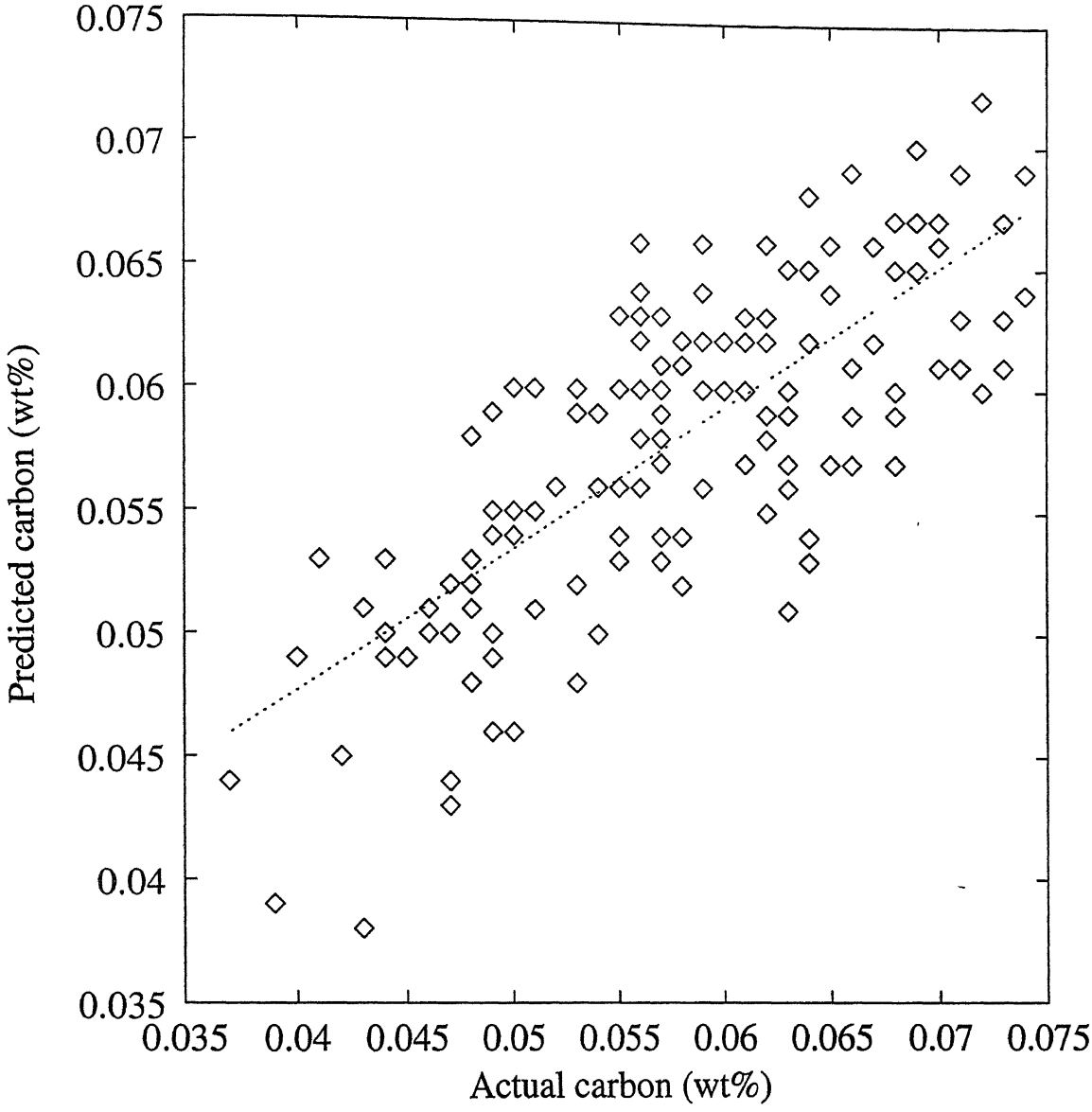

Figure 5.11: Data from Plant 1, Case Study 2(156 heats): Actual vs predicted carbon for model 5.3 (reg), best fit line is y=0.5796x+0.0245. Statistics are n=156, R=0.76, std. error=0.004.

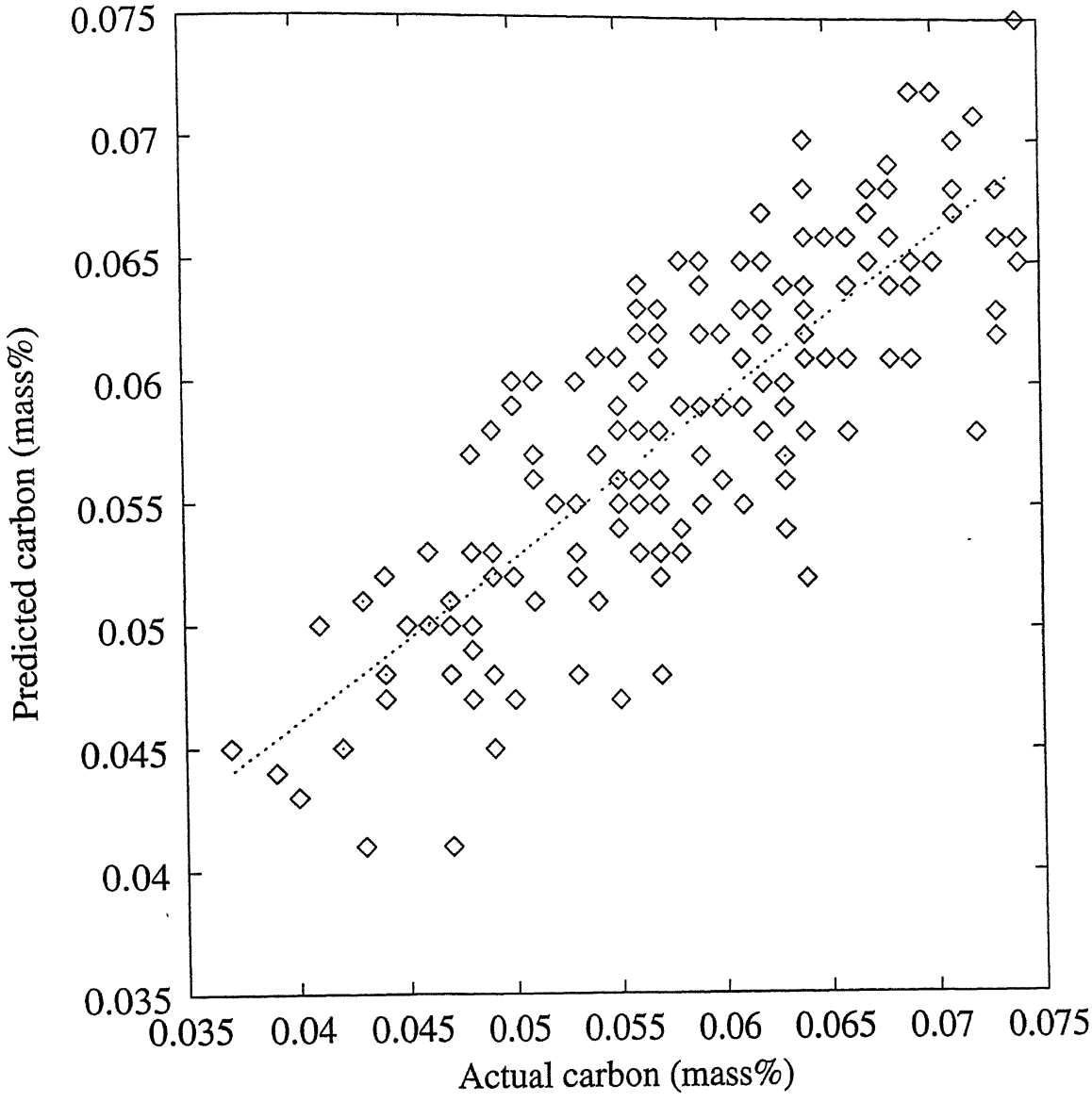

Figure 5.12: Data from Plant 1, Case Study 2(156 heats): Actual vs predicted carbon for model 5.3 (a) (reg), best fit line is y=0.6708x+0.0192. Statistics are n=156, R=0.82, std. error=0.004.

0.0000029), Ore2(-0.0000063), T_o(-0.0000870) and Constant(0.1542). Fig. 5.13 shows the graph of actual vs predicted carbon. It can be observed that R increased from 0.55 in model 5.4 (reg) to 0.67 in model 5.4 i.e., an improvement of 20%. The value of σ also came down to 0.005 in model 5.4 (reg, method 1, Case Study 1) from 0.008 in model 5.4 (method 1, Case Study 1) i.e., a reduction of 33.6%.

Model 5.4 (reg, method 1, Case Study 2)

Model 5.4 (reg, method 1, Case Study 2) is regression model for model 5.4 (method 1, Case Study 2). Variables accepted in this model are Ore1 (-0.0000009), Dolo1(-0.0000036), c_t(0.5167197) and Constant(0.0334) . Statistics of regression are presented in Table 5.1, model 5.4 (reg, method 1, Case Study 2). Fig. 5.14 shows the graph of actual vs predicted carbon. It can be observed that R increased from 0.60 in model 5.4 (method 1, Case Study 2) to 0.66 in model 5.4 (reg, method 1, Case Study 2) i.e., an improvement of 9.7%. The value of σ also came down to 0.004 in model 5.4 (reg, method 1,Case Study 2) from 0.007 in model 5.4 (method 1,Case Study 2) i.e., a reduction of 41% .

Model 5.4 (reg, method 2, Case Study 1)

Model 5.4 (reg, method 2, Case Study 1) is regression model for model 5.4 (method 2, Case Study 1). Variables accepted in this model are hot ratio (0.0018181), Ore1 (-0.0000010), Dolo1(-0.0000027), c_t(0.5188709), Ore2(-0.0000069) and Constant(0.0249). Statistics of regression are presented in Table 5.1, model 5.4 (reg, method 2, Case Study 1). Fig. 5.15 shows the graph of actual vs predicted carbon. It can be observed that R increased from 0.62 in model 5.4 (method2, Case Study 1) to 0.69 in model 5.4 (reg, method 2, Case Study 1) i.e., an improvement of 11.4%. The value of σ also came down to 0.005 in model 5.4 (reg, method 2, Case Study 1) from 0.010 in model 5.4 (method 2, Case Study 1) i.e., a reduction of 50%.

Model 5.4 (reg, method 2, Case Study 2)

Model 5.4 (reg, method 2, Case Study 2) is regression model for model 5.4 (method 2, Case Study 2). Variables accepted in this model are Ore1 (-0.0000008), Dolo1(-0.0000028),

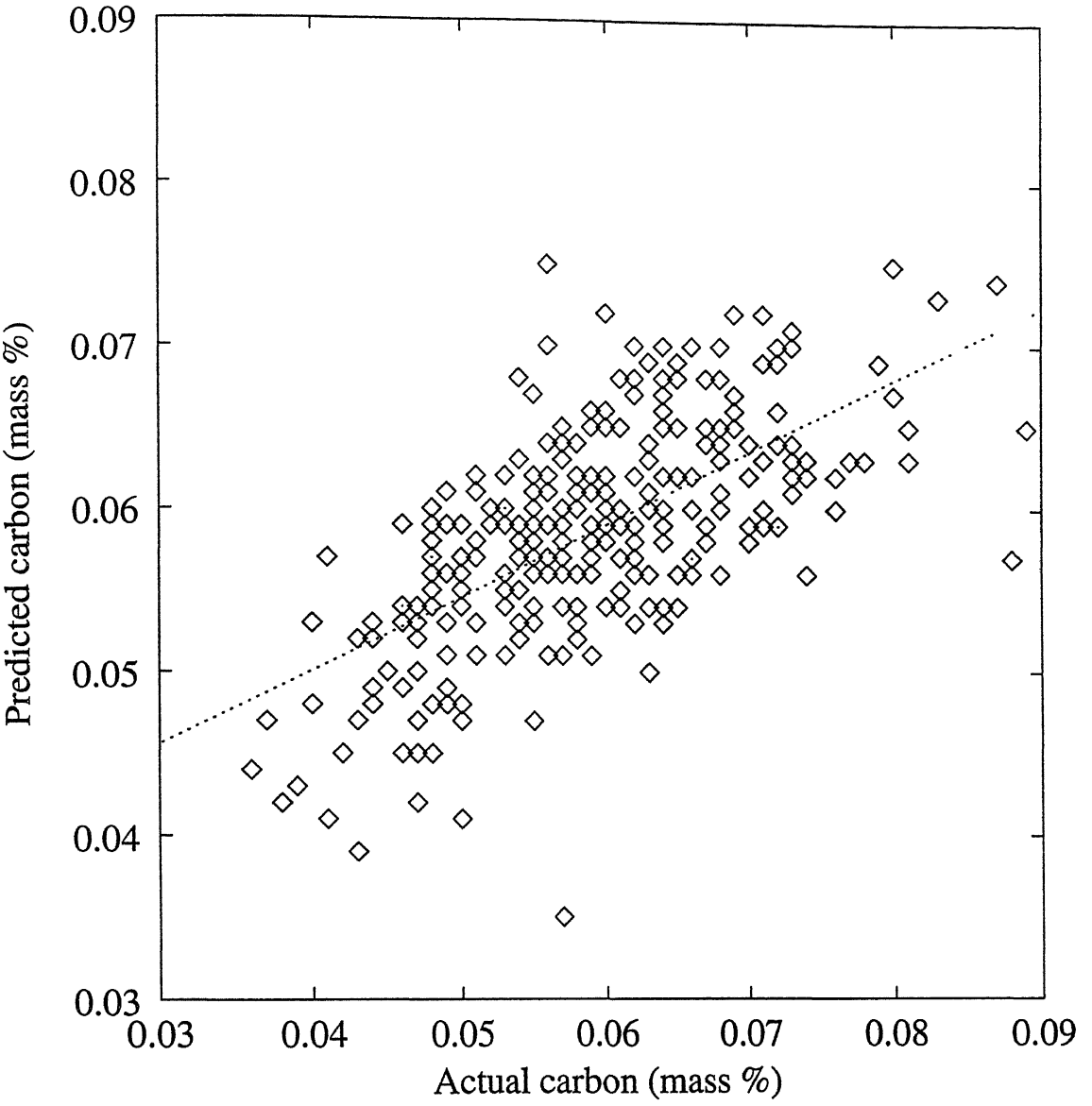

Figure 5.13: Data from Plant 1, Case Study 1(273 heats): Actual vs Predicted for model 5.4 (reg, method1, Case Study 1), best fit lie is given by y=0.4469x+0.0322. Statistics are n=273, R=0.67, std. error=0.005.

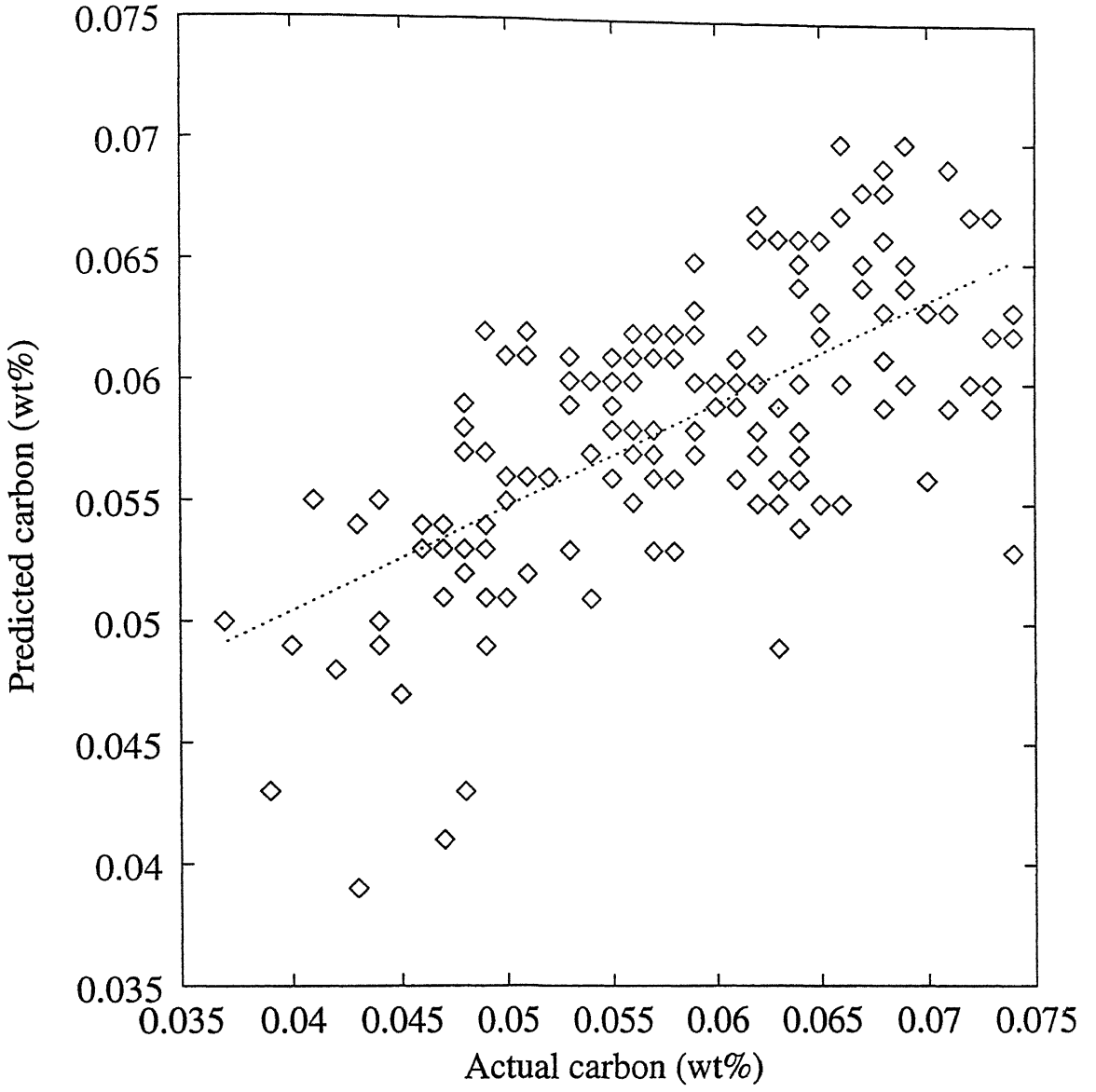

Figure 5.14: Data from Plant 1, Case Study 2(156 heats): Actual vs Predicted for Model 5.4 (reg, method 1, Case Study 2), best fit line is given by y=0.4333x+0.0331. Statistics are n=156, R=0.66, std. error=0.004.

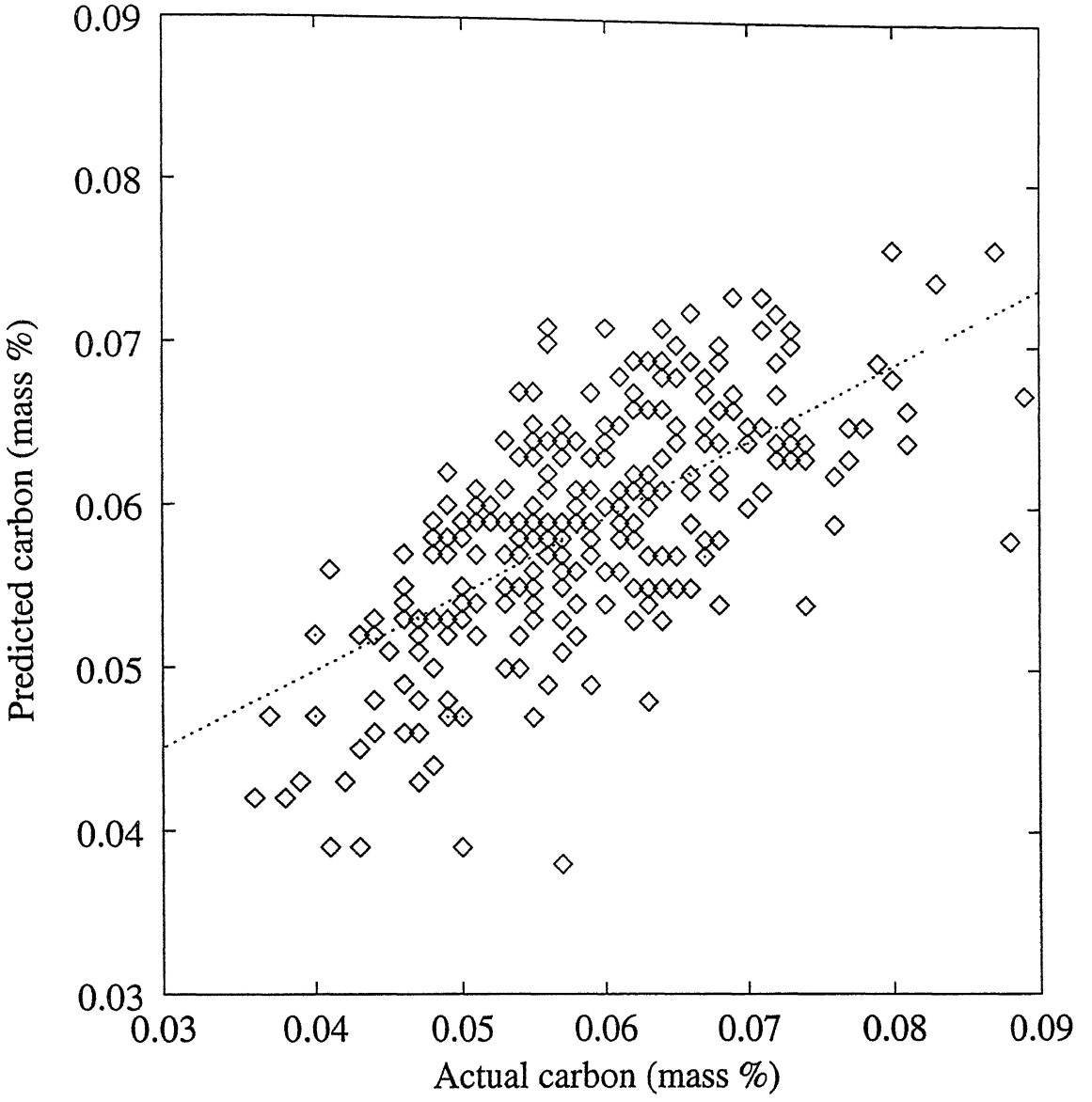

Figure 5.15: Data from Plant 1, Case Study 1(273 heats): Actual vs Predicted for model 5.4 (reg, method 2, Case Study 1), best fit line is given by y=0.0308x+0.4751. Statistics are n=273, R=0.69, std. error=0.005.

c_t(0.4660043) and Constant(0.0352). Statistics of regression are presented in Table 5.1 (Model 5.4 (reg, method 2, Case Study 2)). Fig. 5.16 shows the graph of actual vs predicted carbon. It can be observed from statistics of regression that R increased from 0.67 in model 5.4 (method 2, Case Study 2) to 0.71 in model 5.4 (reg, method 2, Case Study 2) i.e., an improvement of 5.5%. The value of σ also came down to 0.004% in model 5.4 (reg, method 2, Case Study 2) from 0.008% in model 5.4 (method 2, Case Study 2)i.e., a reduction of 50%.

Model 5.5 (reg)

Model 5.5 (reg) is regression model for model 5.5. Variables accepted in this model are Dolo1(-0.0000043), T_o(0.0002185), c_t(0.5238060), Dolo2(-0.0000053), hlans2(0.0001689) and Constant(-0.3487). Statistics of regression are presented in Table 5.1, model 5.5 (reg). Fig. 5.17 shows the graph of actual vs predicted carbon. It can be observed from statistics of regression that R value increased from 0.37 in model 5.5 to 0.74 in model 5.5 (reg) i.e., an increase of 101%. The value of σ also came down to 0.004 in model 5.5 (reg) from 0.009 in model 5.5 i.e., a reduction of 51.7%. For a typical heat with dolo1 = 413, T_o= 1607, dolo2 = 1501, hlans2 = 187, c_t = 0.068

c_t' = -0.3487 + 0.5238060(0.068) - 0.0000043(413) + 0.0002185(1607) - 0.0000053(1501) + 0.0001689(187)

= 0.060.

The actual carbon for this heat is 0.050.

5.2.1.7 Comparison of various models of carbon prediction for Plant 1

On comparing models 5.1 and 5.2, it can be observed that R value increased from 0.59 in model 5.1 to 0.66 in model 5.2. But the value of σ also increased from 0.007 in model 5.1 to 0.025 model 5.2, by 73%. On comparing model 5.1 (reg) and model 5.2 (reg), latter is able to predict better in terms of R and σ (see table 5.1). This may be due to the fact that Q_{eff} has been neglected in model 5.1. Also, by incorporating the operational variables like ore1, dolo1 in model 5.2 is able to give a better prediction.

On Comparing models 5.2 and 5.3 it would be observed that, prediction is poorer

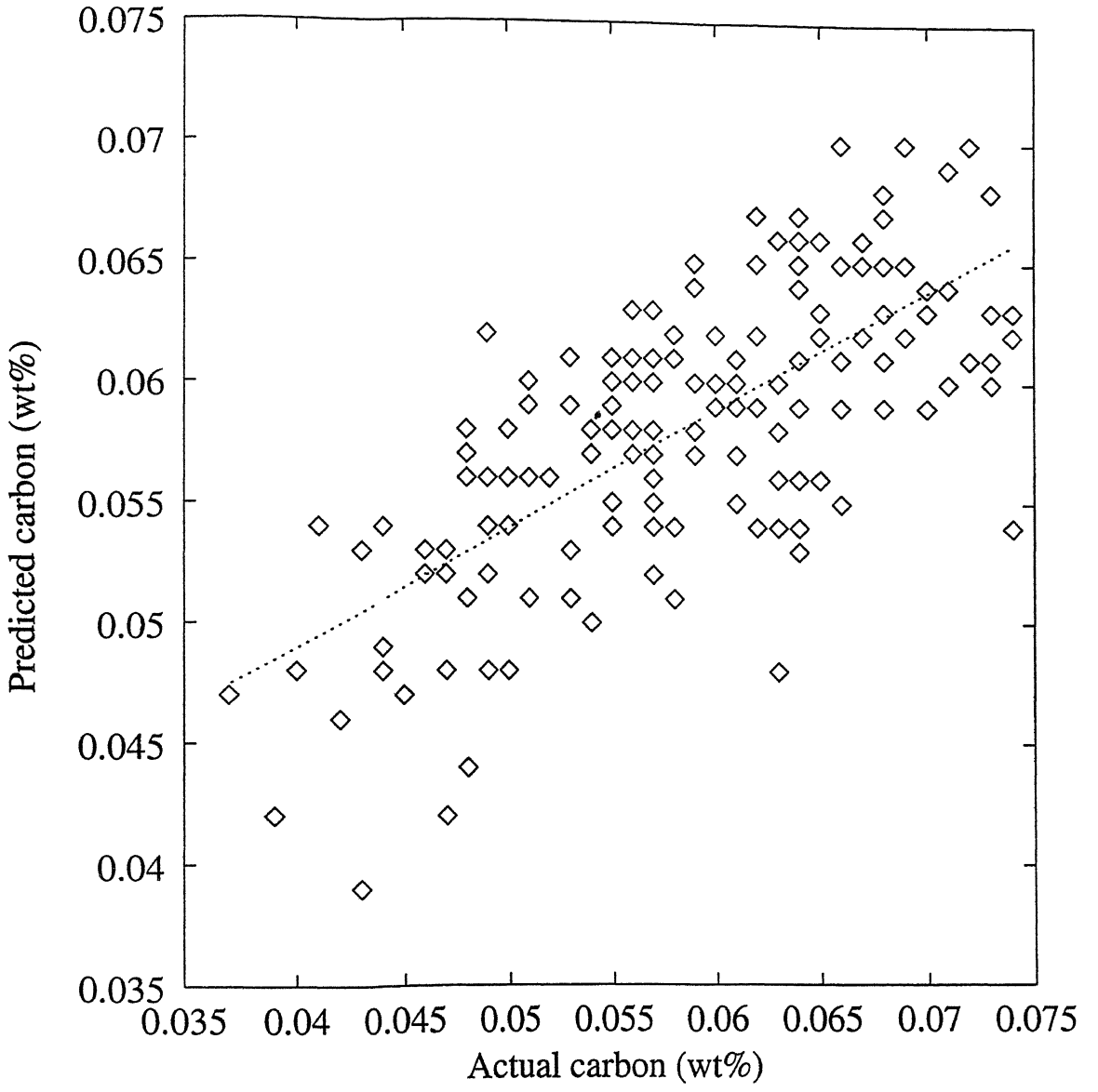

Figure 5.16: Data from Plant 1, Case Study 2(156 heats): Actual vs Predicted carbon for model 5.4 (reg, method 2, Case Study 2), best fit line is given by y=0.4962x+0.0291. Statistics are n=156, R=0.71, std. error=0.004.

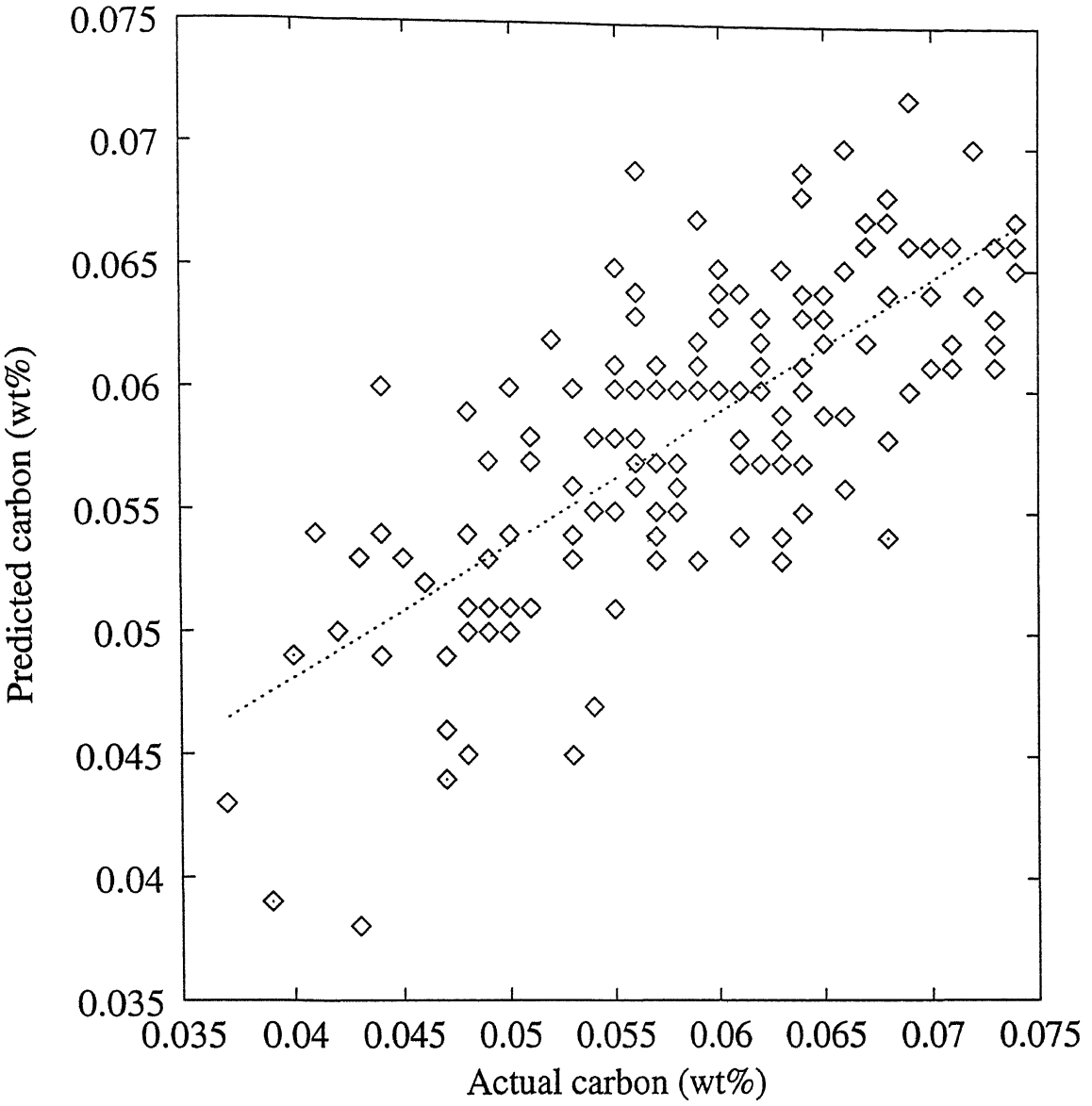

Figure 5.17: Data from Plant 1, Case Study 2(156 heats): Actual vs predicted for model 5.5 (reg), best fit line is y=0.55x+0.0261. Statistics are n=156, R=0.74, std. error=0.004.

for model 5.3. By incorporating operational variables like orel, dolo1, hlans2, O22 and sublance carbon c_o in model 5.3, prediction improved (see Table 5.1, model 5.2 (reg) and model 5.3 (reg)).

It can be observed from results of GA-decarb models that predictions for Case Study 2 are better than Case Study 1. This is because data set of Case Study 1 contains some heats in which ore 2 was added instead of dolo2. On Comparing model 5.4 (method 1, Case Study 2) and model 5.4 (method 2, Case Study 2) it can be seen that latter is able to predict better. This is because η is allowed to vary as a function of gas evolution in method 2. There is 8.34% improvement in R and 12.34% improvement in σ from model 5.4 (method 1, Case Study 1) to model 5.4 (method1, Case Study 2). Among GA-decarb models (see Table 5.1), model 5.4 (reg, method 2, Case Study 2) is giving best predictions with R=0.71 and σ =0.004%. Carefully observing the operational variables used in model 5.4 (reg, method 2, Case Study 2) and 5.3 (reg), lance height is used in model 5.3 (reg), which is missing in model 5.4(reg, method 2, Case Study 2). The possible reason for lower R value in model 5.4 (reg, method 2, Case Study 2) when compared to that of model 5.3 (reg) could be exclusion of lance height. The is also supported by the fact that stirring energy transfered to the metal ($Q_{eff}^{'}$) varies with lance height[1], and in GA-decarb models Q_{eff} is assumed to be constant. This is also the case with the other GA-decarb models. Variation of η and mass transfer coefficient (K') are discussed latter.

It can be observed that η value obtained from model 5.4, Case Study 2 is 2.477 where as that from model 5.5 is 2.91. It conforms that η value does change during the process. It is further observed that prediction is better with model 5.5 (reg) than with model 5.4 (reg, method 2, Case Study 2), with R 0.74 and nearly same σ value. Hence, it confirms that K' is proportional to stirring energy, which decreases as a function of time.

5.2.2 Temperature prediction models

Temperature models are given by eq. (3.15)

$$T = \mu_o + \sum_{i=1}^{n-1} \mu_i \cdot X_i \tag{5.8}$$

[1]See appendix 1

where T is predicted temperature and μ_i 's are coefficients of operational variables X_i. These models are developed using multiple linear regression (MLR). Temperature prediction models are tuned for Case Study 2 (156 data sets).

Model 5.6

Fig 5.18 shows graph of actual versus predicted temperature. From the statistics of regression (Table 5.2) it can be observed that $\sigma = 5\,^{\circ}C$ and R=0.90 (0.9027).Thus, this model is able to correlate 81% of variation in the data. Operational variables used and their coefficients are hot ratio(1.6089489), T_o(0.8260166), O22(0.0349623), slag2(-0.0051884), dolo2(-0.0105275) and constant(265.4443). For a typical heat with hot ratio = 5.2098, 022 = 2464, T_o= 1607, slg2 = 1508, dolo2 = 1501

T = 265.4443 + 1.6089489(5.2098) + 0.8260166(1607) + 0.349623(2464) - 0.0051884(1508) - 0.0105275(1501)

= 1663^{o}C.

The actual temperature for this heat is 1662 ^{o}C.

5.2.3 Dissolved oxygen prediction models

Dissolved oxygen models are given by eq. (3.15)

$$[O] = \mu_o + \sum_{i=1}^{n-1} \mu_i \cdot X_i \tag{5.9}$$

where μ_i 's are coefficients of operational variables X_i. These models are developed using MLR. Dissolved oxygen models are tuned for Case Study 2 (156 heats).

Model 5.7

Table 5.3, model 5.7 shows the statistics of regression for actual versus predicted dissolved oxygen. Fig 5.19 shows graph of actual versus predicted dissolved oxygen. From statistics of regression it can be observed that σ=37 ppm and R=0.83 (0.8267). Thus this model explains 68.3% variation in data. Operational variables used are basicity(12.3357568),

Table 5.2 Summary of results for temperature prediction obtained for Plant 1

S. No	Model No	Model equation	Parameters used	Parameters optimized	Statistics of regression (y=mx+c)			Remarks
					Dependent variable	Independent variable	Statistics	
18	5.6	$T = \mu_o + \sum_{i=1}^{n-1} \mu_i \cdot X_i$	hot ratio O22,T_o dolo2 slag2	μ_i	T (1663)	T_{act} (1662)	m=0.8146 c=307.76 R=0.90 σ=5 F=677.6145	Case study 2

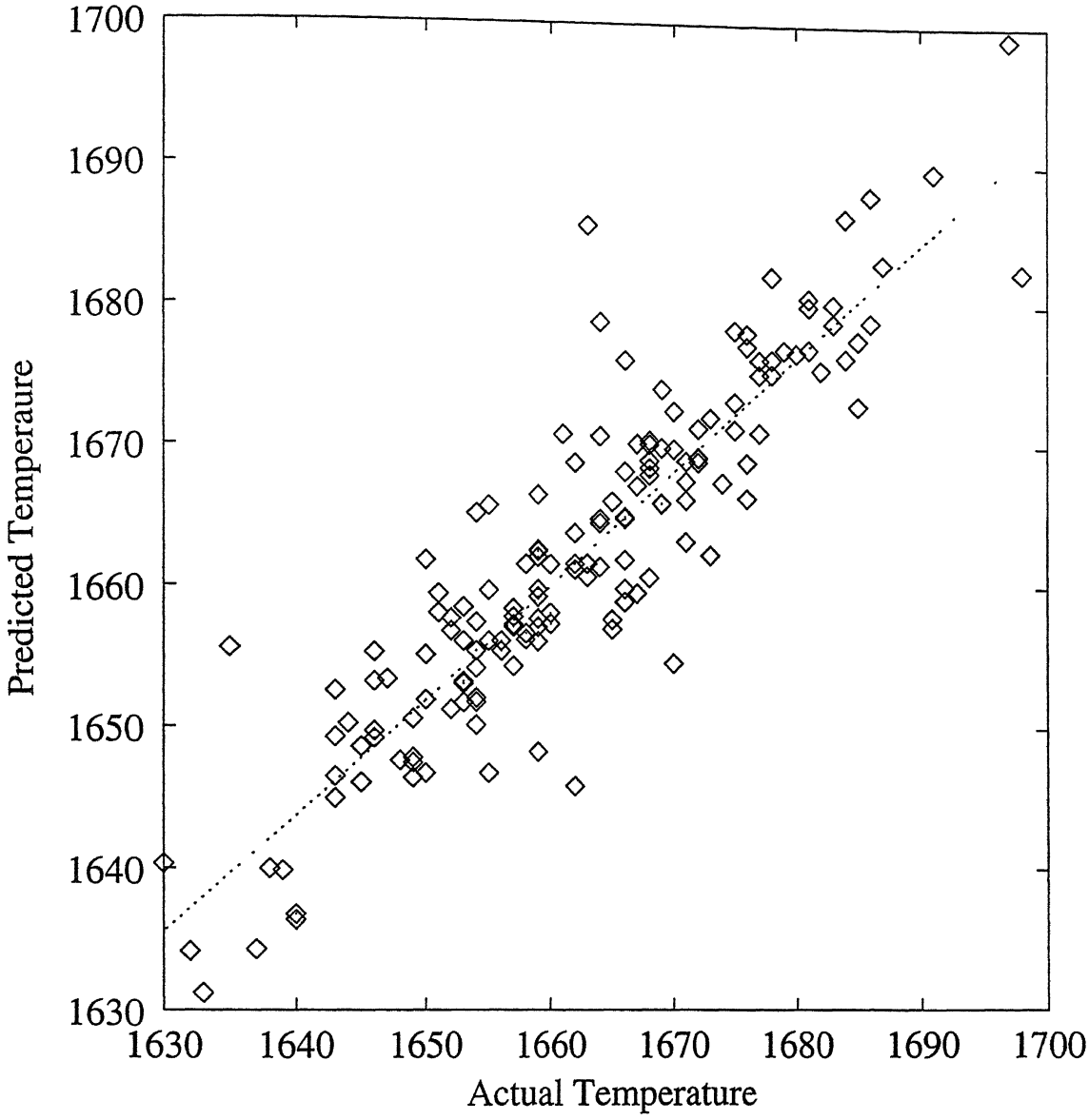

Figure 5.18: Data from Plant 1, Case Study 2(156 heats): Actual vs Predicted temperature for model 5.6, best fit line is y=0.8146x+307.76. Statistics are n=156, R=0.90, std. error=5.

c_o(-895.1580774), O22(0.2812597) and constant(123.6482). For a typical heat with basicity=5.443, c_o =0.326, O22=2464

$[O]$ = 123.6482+12.3357568(5.443)-895.1580774(0.326)+0.2812597(2464)

=592 ppm.

The actual dissolved oxygen content for this heat is 413 ppm.

In order to improve the prediction, lance height during the second blow (hlans2) and end point temperature (T) are also considered as independent variables. The results are as presented in model 5.8.

Model 5.8

From statistics of regression (Table 5.3, model 5.8) it can be observed that σ=34 ppm and R=0.87 (0.8724). Fig 5.20 shows graph of actual versus predicted dissolved oxygen. Thus this model explains 76% variation in data. It can be observed from model 5.7 and model 5.8 that prediction improved in terms of both R and σ. There is an improvement of 5.5%(approx) in R and 7.6% in σ in model 5.8 from model 5.7. Operational variables used and their coefficients are basicity(12.9760397), c_o(-875.4523083), O22(0.1364417), T_o(-2.9485933), dolo2(0.0428712), hlans2(-0.4622155), T(3.3075463) and constant(-300.6208). For a typical heat with basicity = 5.443, T_o= 1607, 022 = 2464, c_1= 0.517, dolo2 = 1501, hlans2 = 187, T = 1663 (see model 5.6)

[O] = -300.6208 + 12.9760397(5.443) - 2.9485933(1607) - 875.4523083(0.517) + 0.1364417(2464) + 0.0428712(1501) - 0.4622155(187) + 3.3075463(1663)

= 394 ppm.

The actual dissolved oxygen content for this heat is 413 ppm.

5.2.4 Phosphorus prediction models

Phosphorus models have been discussed in section 2.3.5. Detailed study was done first on Plant 1 and the best model is then tuned for Plant 3 data. In case of Plant 2, phosphorus content of heats was not available.

Table 5.3 Summary of results obtained for Dissolved oxygen prediction for Plant 1

S. No	Model No	Model equation	Parameters used	Parameters optimized	Statistics of regression (y=mx+c)			Remarks
					Dependent variable	Independent variable	Statistics	
19	5.7	$[O] = \mu_o + \sum_{i=1}^{n-1} \mu_i \cdot X_i$	Basicity c_o O22	μ_i	$[O]$ (592)	$[O]_{act}$ (413)	m=0.6786 c=148.1316 R=0.83 σ=37 F=332.5555	Case study 2
20	5.8	$[O] = \mu_o + \sum_{i=1}^{n-1} \mu_i \cdot X_i$	Basicity O22, c_o T_o, dolo2 hlans2	μ_i	$[O]$ (394)	$[O]_{act}$ (413)	m=0.761 c=101.255 R=0.87 σ=34 F=490.34061	Case study 2

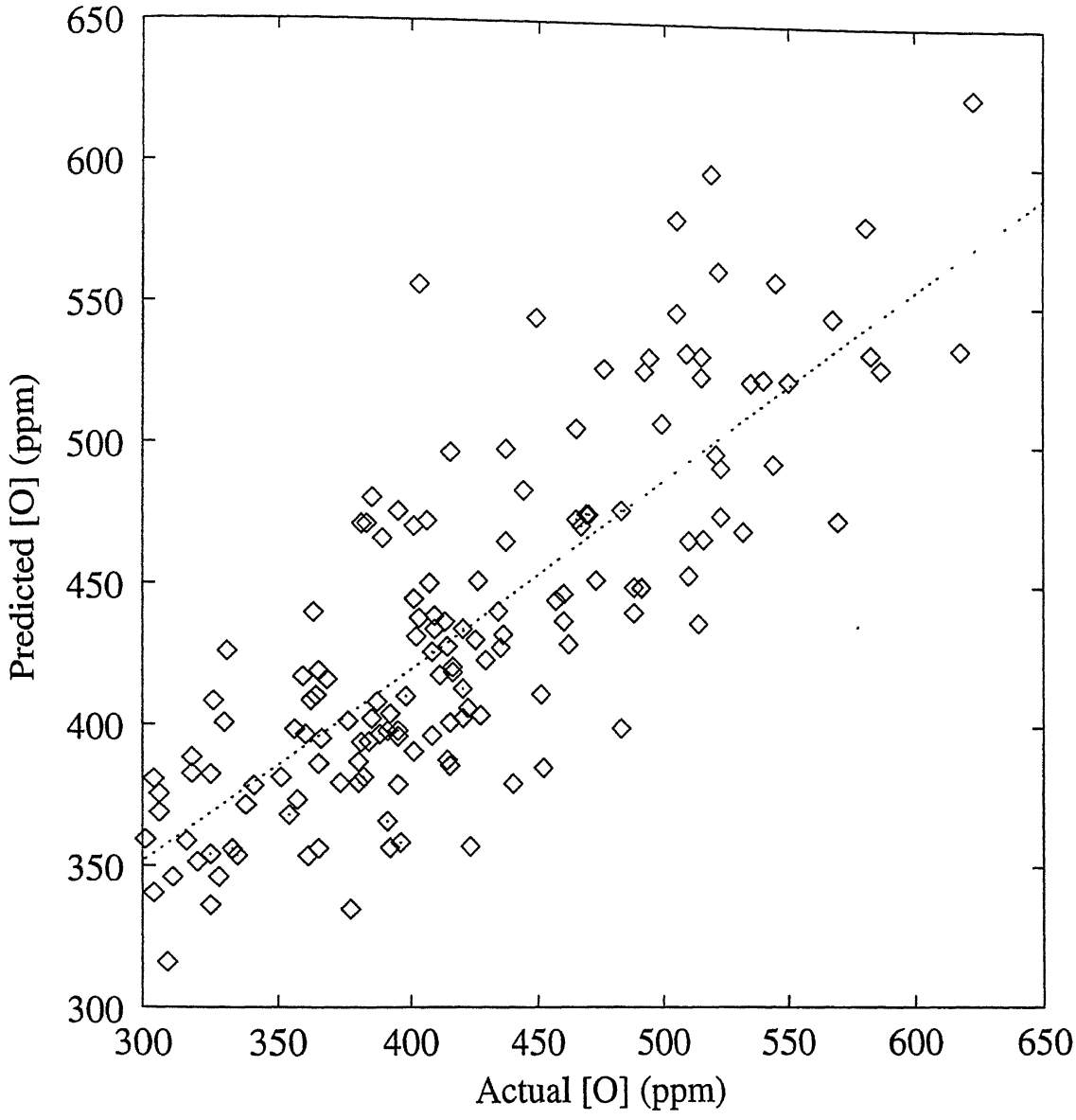

Figure 5.19: Data from Plant 1, Case Study 2(156 heats): Actual vs predicted [O] for model 5.7, best fit line is y=0.6786x+148.1316. Statistics are n=156, R=0.83, std. error=37.

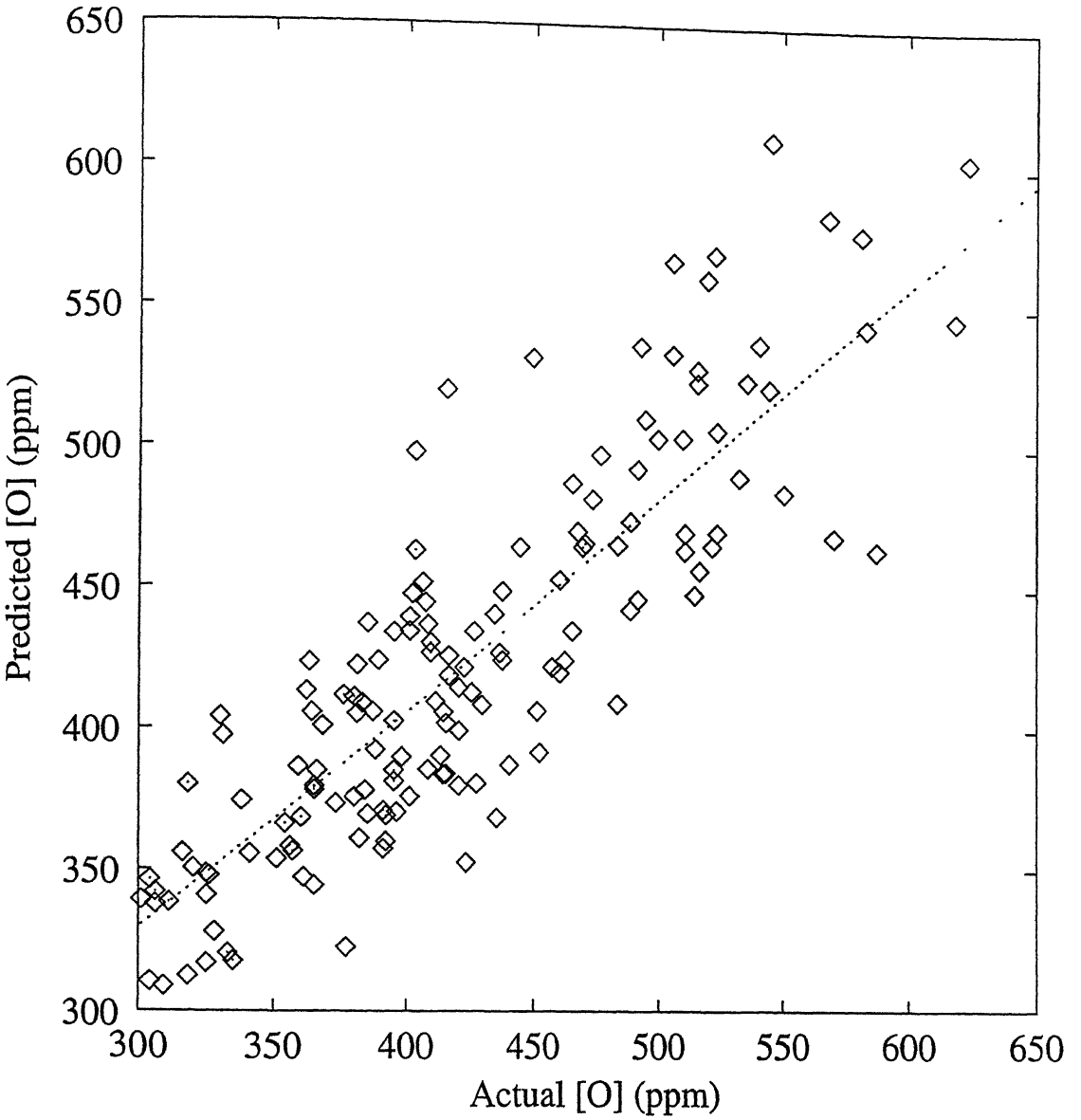

Figure 5.20: Data from Plant 1, Case Study 2(156 heats): Actual vs predicted [O] for model 5.8, best fit line is y=0.761x+101.255. Statistics are n=156, R=0.87, std, error=34.

5.2.4.1 Kinetic model of mass transfer

Kinetic model of mass transfer is given by eq. (3.21)

$$-\ln\frac{p_t - p_e}{p_o - p_e} = \mu_o + \sum_{i=1}^{n-1} \mu_i \cdot X_i \tag{5.10}$$

where μ_i 's are coefficients of operational variables X_i . These models are developed using MLR.

Model 5.9

In this model, equilibrium constant of phosphorus p_e is taken as 2. From statistics of regression (Table 5.4, model 5.9) it can be observed that σ=0.004 (0.00352)% and R=0.60 (0.6026). This model is able to explain 36.3% of the variation. Operational variables used and their coefficients are basicity(-0.0004353), dolo2(-0.0000018), c_o(-0.0099315), hlans2(0.0000365), O22(0.0000030) and constant(-0.0126). Fig. 5.21 shows graph of actual versus predicted phosphorus. For a heat with basicity=5.443, hlans2=187, O22=2464, c_o=0.326, dolo2=1501we obtain by substituting in eq. (5.10)

$-\ln(\frac{p_t-2}{p_o-2})$=-0.0126-0.0004353(5.443)-0.0000018(1501)-0.0099315(0.326)+ 0.0000365(187)+0.0000030(2464)=-6.69x10^{-3}

$\frac{p_t-2}{p_o-2} = 1.0067$

p_t =2+(0.027-2)(1.0067)

=0.014

Actual end point phosphorus value for this particular heat is 0.008.

Model 5.10

From statistics of regression on actual versus predicted phosphorus (Table 5.4, model 5.10) it can be observed that σ=0.003% and R=0.87. Fig 5.22 shows graph of actual versus predicted phosphorus. This model is able to explain 75.7% of the variation. It is observed from model 5.9 and 5.10 that by excluding the equilibrium factor of phosphorus from the dependent variable, prediction improved from 0.60 in model 5.9 to 0.87 in model 5.10 in terms of R and σ decreased to 0.0034 in model 5.10 from 0.0035 in model 5.9.

Table 5.4 Summary of results obtained for phosphorus prediction for Plant 1

S. No	Model No	Model equation	Parameters used	Parameters optimized	Statistics of regression (y=mx+c)			Remarks
					Dependent variable	Independent variable	Statistics	
21	5.9	$-\ln\frac{p_t-p_e}{p_o-p_e} = \mu_o + \sum_{i=1}^{n-1}\mu_i \cdot X_i$	basicity dolo2 c_o hlans2 O22	μ_i	p_t (0.014)	$p_{t_{act}}$ (0.008)	m=1.3253 c=0.0011 R=0.60 σ=0.004 F=87.8249	Case study 2
22	5.10	$-\ln\frac{p_t}{p_o} = \mu_o + \sum_{i=1}^{n-1}\mu_i \cdot X_i$	svol, Mn2 Ore1,slg2 hlans2 dolo2	μ_i	p_t (0.008)	$p_{t_{act}}$ (0.008)	m=0.9838 c=0.0002 R=0.87 σ=0.003 F=478.77301	Case study 2
23	5.11	$p'_t = \mu_o + \mu_1 p_o + \sum_{i=2}^{n-1}\mu_i \cdot X_i$	svol,T $htr * p$ slg2,Mn2 hlans2 p_o	μ_i	p'_t (0.009)	$p_{t_{act}}$ (0.008)	m=0.8792 c=0.0014 R=0.93 σ=0.0007 F=917.438	Case study 2

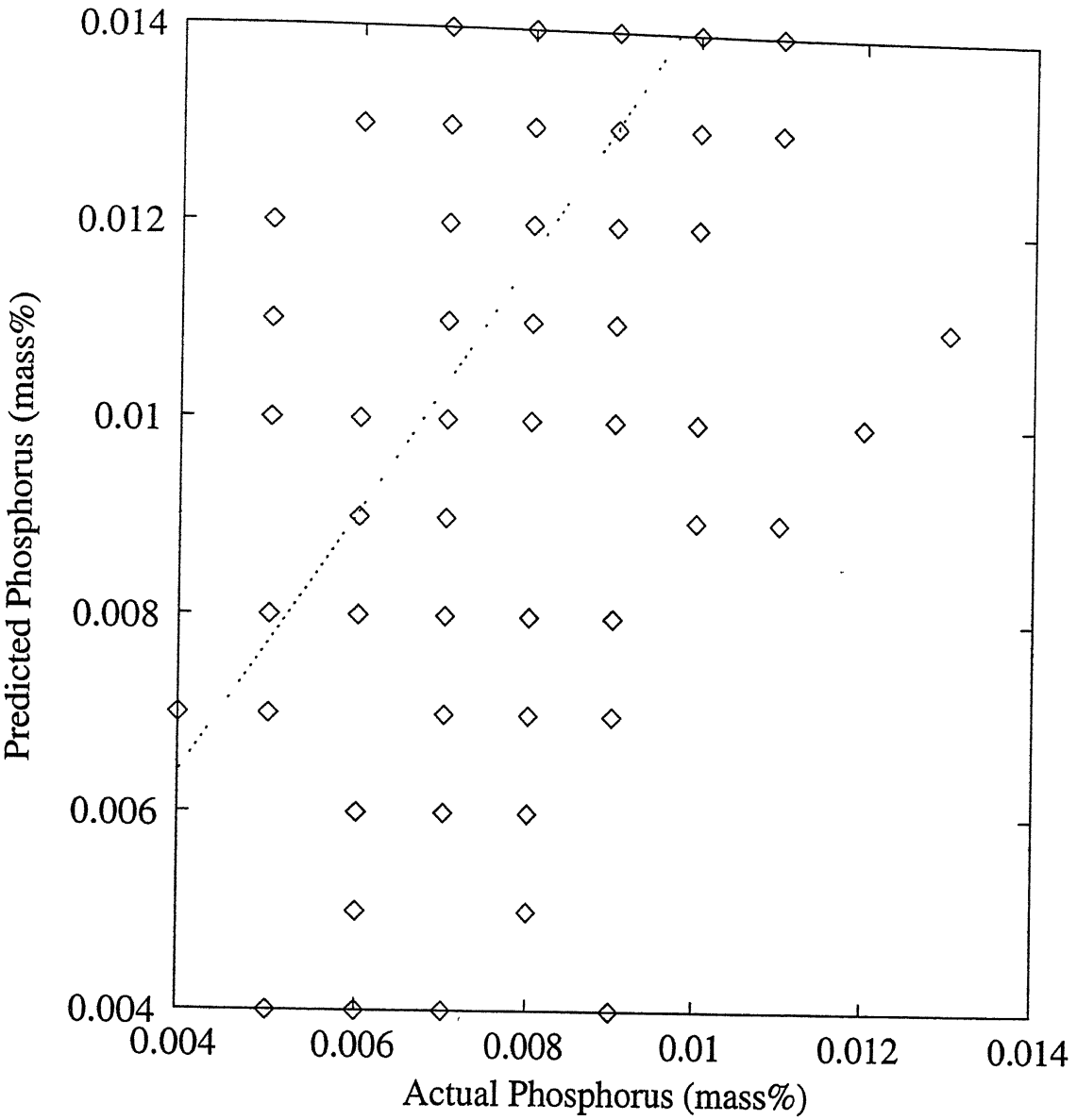

Figure 5.21: Data from Plant 1, Case Study 2(156 heats): Actual vs predicted phosphorus for model 5.9, best fit line is y=1.3253x+0.0011. Statistics are n=156, R=0.60, std. error=0.003. Each square may represent more than one heat.

Operational variables used and their coefficients are svol(0.0000181), Ore1(-0.0000140), slg2(0.0000968), hlans2(-0.0013645), dolo2(0.0001475), Mn2(-1.8107433) and constant(1.1448). For a typical heat with svol=17208.47, ore1=3994, slg2=1508, hlans2=187, dolo2=1501, Mn2=0.174 we obtain

$-\ln \frac{p_t}{p_o}$=1.1448+0.000018(17208.47)-0.0000140(3994)+0.0000968(1508)-0.0013645(187)+0.0001475(1501)-1.8107433(0.174)=1.1975

p_t =0.027(0.302) = 0.008.

Actual phosphorus for this heat is 0.008.

5.2.4.2 Regression model

Regression model is given by eq. (3.22)

$$p'_t = \mu_o + \mu_1 p_o + \sum_{i=2}^{n-1} \mu_i \cdot X_i \tag{5.11}$$

where, p'_t is the end point phosphorus value predicted from MLR, p_o is sublance phosphorus and μ_i 's are coefficients (to be determined by MLR) of operational variables X_i

Model 5.11

From statistics of regression on actual versus predicted phosphorus (Table 5.4, model 5.11)it can be observed that σ=0.0007% and R=0.93. Fig 5.23 shows graph of actual versus predicted phosphorus. This model is able to explain 85.6% of the variation. Operational variables used and their coefficients are svol(-0.0000002), $htr * p_o$(0.0032876), slg2(0.0000968), hlans2(-0.0013645), p_o(0.1063842), Mn2(0.0445678), T(0.0000339) and constant(1.1448). For a typical heat with slag mass = 17208.47, T = 1663 (see model 5.6), htr*p = 0.2917, slg2 = 1508, Mn2 =.172 , hlans2 = 187, p_o = 0.027

p'_t = -0.0533 - 0.0000002(17208.47) + 0.0032876(0.2917) + 0.1063842(0.027) - 0.0000004(1508) - 0.0000081(187) + 0.0000339(1663) + 0.0445678(0.172)

= 0.009.

Actual phosphorus for this heat is 0.008.

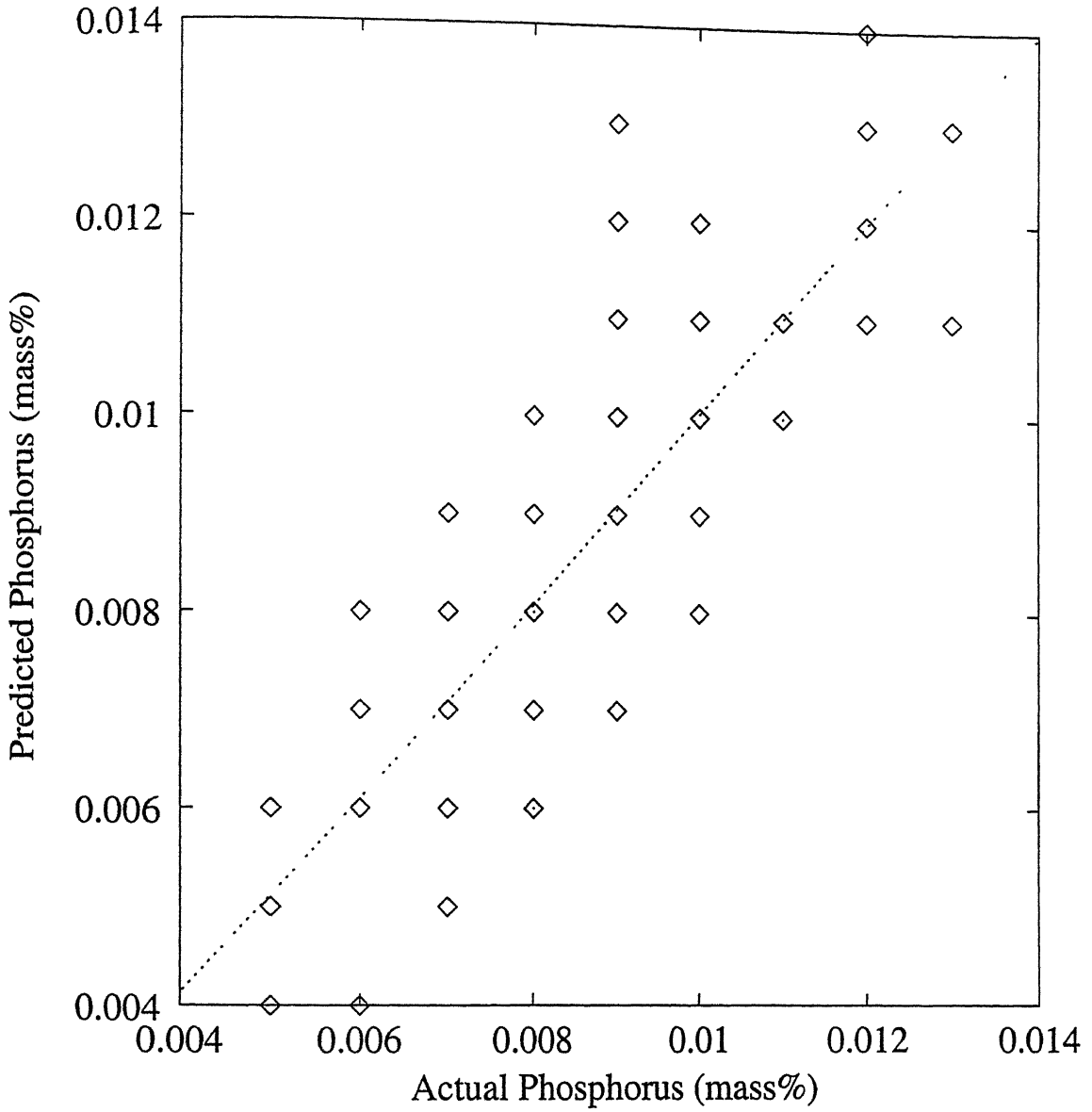

Figure 5.22: Data from Plant 1, Case Study 2(156 heats): Actual vs predicted phosphorus for model 5.10, best fit line is y=0.9838x+0.0002. Statistics are n=156, R=0.87, std. error=0.003. Each square may represent more than one heat.

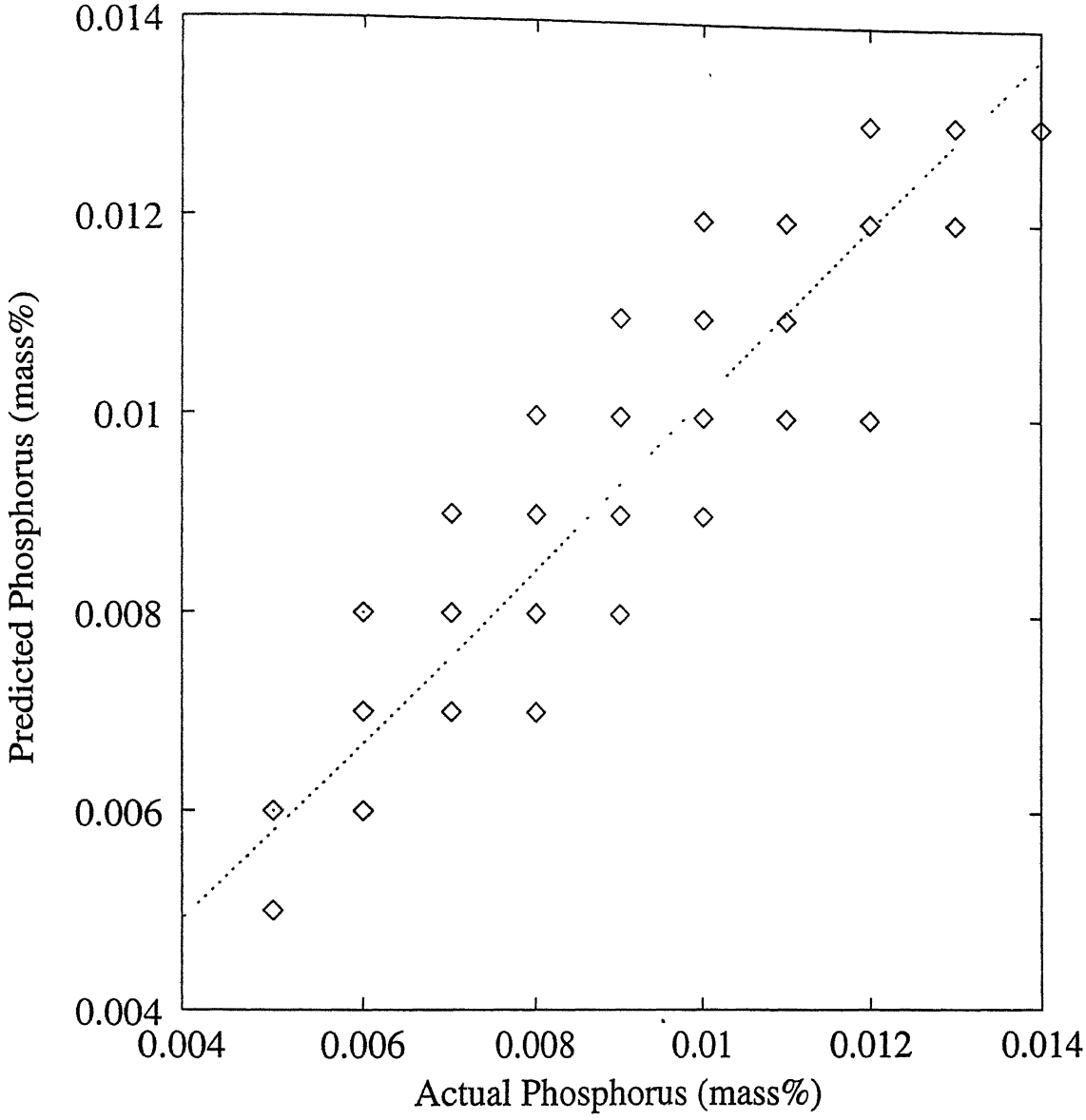

Figure 5.23: Data from Plant 1, Case Study 2(156 heats): Actual vs predicted phosphorus for model 5.11, best fit line is y=0.8792x+0.0014. Statistics are n=156, R=0.93, std. error=0.0007. Each square may represent more than one heat.

5.2.4.3 Discussion on phosphorus prediction results

It is observed that the best model for phosphorus prediction is model 5.11. Hence, this model is applied to Plant 3. In case of Plant 2, we did not have the data for measurement of phosphorus. Hence for only Plant 3 phosphorus model is developed.

5.2.5 Manganese prediction models

Manganese models developed in this work are discussed in section 3.9.2.

5.2.5.1 Kinetic model of mass transfer

Kinetic model of mass transfer is given by eq. (3.26)

$$-\ln \frac{Mn_t - Mn_e}{Mn_o - Mn_e} = \mu_o + \sum_{i=1}^{n-1} \mu_i \cdot X_i \tag{5.12}$$

where μ_i 's are coefficients of operational variables X_i.

Model 5.12

In this model, equilibrium constant of manganese Mn_e is taken as 0.005. Table 5.5, model 5.12 shows the statistics of regression for actual versus predicted manganese. Fig 5.24 shows graph of actual versus predicted manganese. From statistics of regression it can be observed that σ=0.007 (0.00699)% and R=0.96 (0.9608). This model is able to explain 92.2% of the variation. Operational variables used and their coefficients are T_o(-0.0027084), c_o(-0.8401064), O22 (0.0002366), hlans2 (-0.0011956), dolo2 (0.0001237), T (0.0035221), p_t(-43.9292138) and constant(-0.3590). For a typical heat with T_o=1607, c_o=0.326, O22=2464, hlans2=187, dolo2=1501, T=1662, p_t=0.008 we obtain

$-\ln \frac{Mn_t - 0.005}{Mn_o - 0\ 005}$=-0.359-0.0027084(1607)-0.8401064(0.326)+0.0002366(2464)-0.0011956(187)+ 0.0001237(1501)+0.003522(1662)-43.9292138(0.008)=1.062

Mn_t =(0.517-0.005)(0.3457)+0.005

= 0.182 %.

Actual manganese for this heat is 0.174 %.

5.2.4.3 Discussion on phosphorus prediction results

It is observed that the best model for phosphorus prediction is model 5.11. Hence, this model is applied to Plant 3. In case of Plant 2, we did not have the data for measurement of phosphorus. Hence for only Plant 3 phosphorus model is developed.

5.2.5 Manganese prediction models

Manganese models developed in this work are discussed in section 3.9.2.

5.2.5.1 Kinetic model of mass transfer

Kinetic model of mass transfer is given by eq. (3.26)

$$-\ln \frac{Mn_t - Mn_e}{Mn_o - Mn_e} = \mu_o + \sum_{i=1}^{n-1} \mu_i \cdot X_i \tag{5.12}$$

where μ_i 's are coefficients of operational variables X_i.

Model 5.12

In this model, equilibrium constant of manganese Mn_e is taken as 0.005. Table 5.5, model 5.12 shows the statistics of regression for actual versus predicted manganese. Fig 5.24 shows graph of actual versus predicted manganese. From statistics of regression it can be observed that σ=0.007 (0.00699)% and R=0.96 (0.9608). This model is able to explain 92.2% of the variation. Operational variables used and their coefficients are T_o(-0.0027084), c_o(-0.8401064), O22 (0.0002366), hlans2 (-0.0011956), dolo2 (0.0001237), T (0.0035221), p_t(-43.9292138) and constant(-0.3590). For a typical heat with T_o=1607, c_o=0.326, O22=2464, hlans2=187, dolo2=1501, T=1662, p_t=0.008 we obtain

$-\ln \frac{Mn_t-0.005}{Mn_o-0.005}$=-0.359-0.0027084(1607)-0.8401064(0.326)+0.0002366(2464)-0.0011956(187)+ 0.0001237(1501)+0.003522(1662)-43.9292138(0.008)=1.062

Mn_t =(0.517-0.005)(0.3457)+0.005

= 0.182 %.

Actual manganese for this heat is 0.174 %.

Table 5.5 Summary of results obtained for manganese prediction for Plant 1

S. No	Model No	Model equation	Parameters used	parameters optimized	Statistics of regression (y=mx+c)			Remarks
					Dependent variable	Independent variable	Statistics	
24	5.12	$-\ln\frac{Mn_t-Mn_e}{Mn_o-Mn_e} = \mu_o + \sum_{i=1}^{n-1}\mu_i \cdot X_i$	T_o,c_o T O22, p_t hlans2 dolo2	μ_i	Mn_t (0.182)	$Mn_{t_{act}}$ (0.174)	m=0.9419 c=0.0083 R=0.96 σ=0.007 F=1847.632	Case study 2
25	5.13	$Mn'_t = \mu_o + \mu_1 Mn_O + \sum_{i=2}^{n-1}\mu_i \cdot X_i$	T_o,c_o Mn_o O22 Ore1 dolo2	μ_i	Mn'_t (0.172)	$Mn_{t_{act}}$ (0.174)	m=0.8823 c=0.0204 R=0.94 σ=0.007 F=1144.241	Case study 2
26	5.14	$Mn'_t = \mu_o + \mu_1 Mn_O + \sum_{i=2}^{n-1}\mu_i \cdot X_i$	p_t, c_o O22,Mn_o hlans2 dolo2	μ_i	Mn'_t (0.218)	$Mn_{t_{act}}$ (0.174)	m=0.9237 c=0.0115 R=0.96 σ=0.0065 F=1827.27	Case study 2

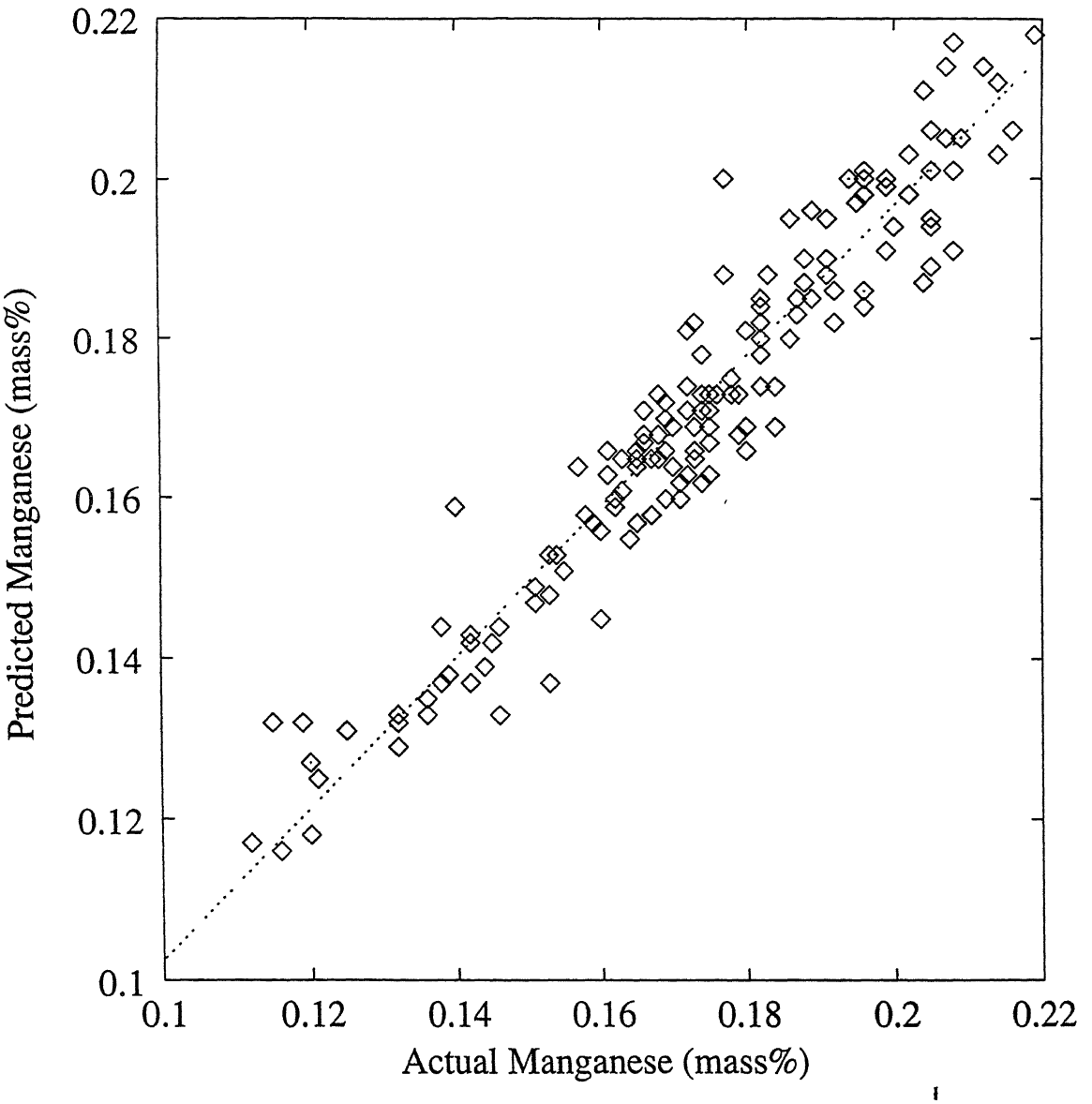

Figure 5.24: Data from Plant 1, Case Study 2(156 heats): Actual vs predicted manganese for model 5.12, best fit line is y=0.9419x+0.0083. Statistics are n=156, R=0.96, std. error=0.008.

5.2.5.2 Regression model

Regression model is given by eq. (3.27)

$$Mn'_t = \mu_o + \mu_1 Mn_o + \sum_{i=2}^{n-1} \mu_i \cdot X_i \tag{5.13}$$

where, Mn'_t is the end point manganese value predicted from MLR, Mn_o is the sublance manganese and μ_i 's are coefficients of operational variables X_i

Model 5.13

From statistics of regression on actual versus predicted manganese (Table 5.5, model 5.13) it can be observed that σ=0.007% and R=0.94. Fig 5.25 shows graph of actual versus predicted manganese. This model is able to explain 88.4% of the variation. Operational variables used and their coefficients are T_o(0.0003010), c_o(0.1810235), O22(-0.0000522), Ore1(-0.0000012), dolo2(-0.000014), Mn_o (0.4679948) and constant(-0.4030). For a typical heat with ore1 = 3994, T_o= 1607, c_o = 0.517, Mn_o = 0.326, 022 = 2464, dolo2 = 1501

$M'n_t$ = -0.4030 + 0.4679948 (0.0326) - 0.0000012(3994) + 0.0003010(1607) + 0.1810235(0.517) - 0.0000522(2464) - 0.0000140(1501)
= 0.172.

The actual manganese for this heat is 0.174.

Model 5.14

From statistics of regression on actual versus predicted manganese (Table 5.5, model 5.14) it can be observed that σ=0.0065% and R=0.96. Fig 5.26 shows graph of actual versus predicted manganese. This model is able to explain 92.2% of the variation. Operational variables used are p_t(4.993776), c_o(0.1076712), O22(-0.0000408), hlans2(0.0001395), dolo2(-0.0000106), Mn_o (0.4075651) and constant(0.0233). For a typical heat with c_o =0.326, O22=2464, hlans2=187, dolo2=1501, Mn_o=0.517, p_t=0.008

Mn'_t = 0.0233+0.1076712(0.326)-0.0000408(24640+0.0001395(187)-0.0000106(1501)+0.4075651(0.5170+4.993776(0.008)

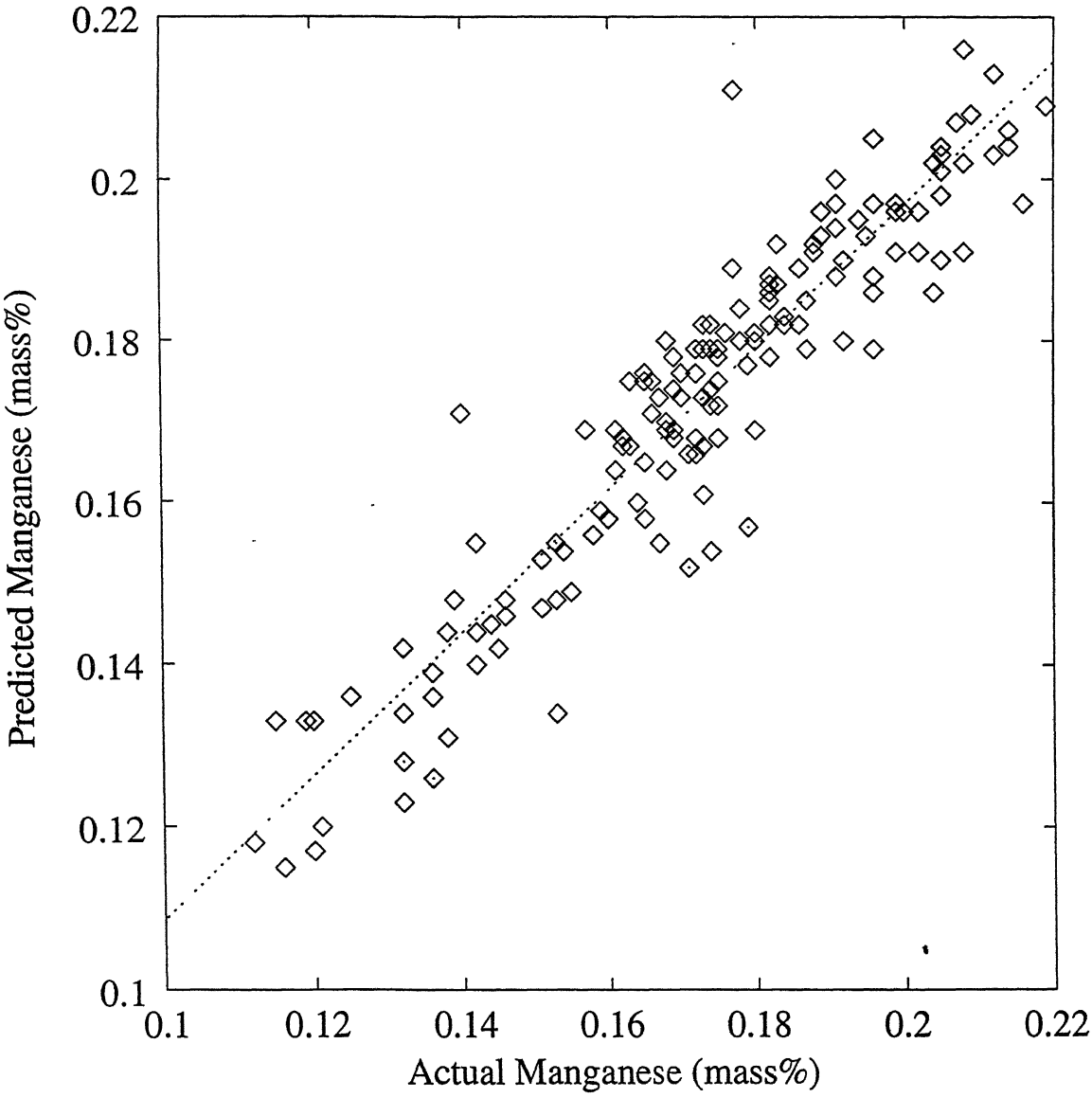

Figure 5.25: Data from Plant 1, Case Study 2(156 heats): Actual vs predicted manganese for model 5.13, best fit line is y=0.8823x+0.0204. Statistics are n=156, R=0.94, std. error=0.007.

=0.218

Actual manganese for this heat is 0.174.

5.2.5.3 Discussion on manganese prediction results

It is observed that prediction from model 5.14 is better than model 5.13 and model 5.12. It can be observed from results of model 5.12 and model 5.14 that although the R value is same, σ value is less in latter model (0.007, 0.0065). Hence this model is further tuned on Plant 3 data.

5.3 Results of Plant 2

5.3.1 End point carbon prediction models

5.3.1.1 GA-decarb models (model 5.4)

GA-decarb models tuned in this data in this section.

Model 5.4 (method 1)

Eq. (5.4) was optimized for 340 data sets. Optimized values of α_1 and η corresponding to minimum SSE are 0.0084 and 0.2910. Table 5.6, model 5.4 shows the statistics of regression performed on actual vs predicted carbon for Plant 2. From the statistics of regression it can be observed that σ=0.012 (0.0117)% and R= 0.61 (0.6129). Fig. 5.27 shows actual vs predicted graph.

Model 5.4 (method 2)

Eq. (5.5) was optimized for 340 data sets. Optimized values of α_1 and α_2 corresponding to minimum SSE are 0.017 and 0.0014. Table 5.6 (method 5.4, method 2) shows the statistics of regression performed on actual vs predicted carbon. It can be observed from the table that σ=0.014% and R=0.71 (0.7060). Fig. 5.28 shows graph of actual vs predicted carbon.

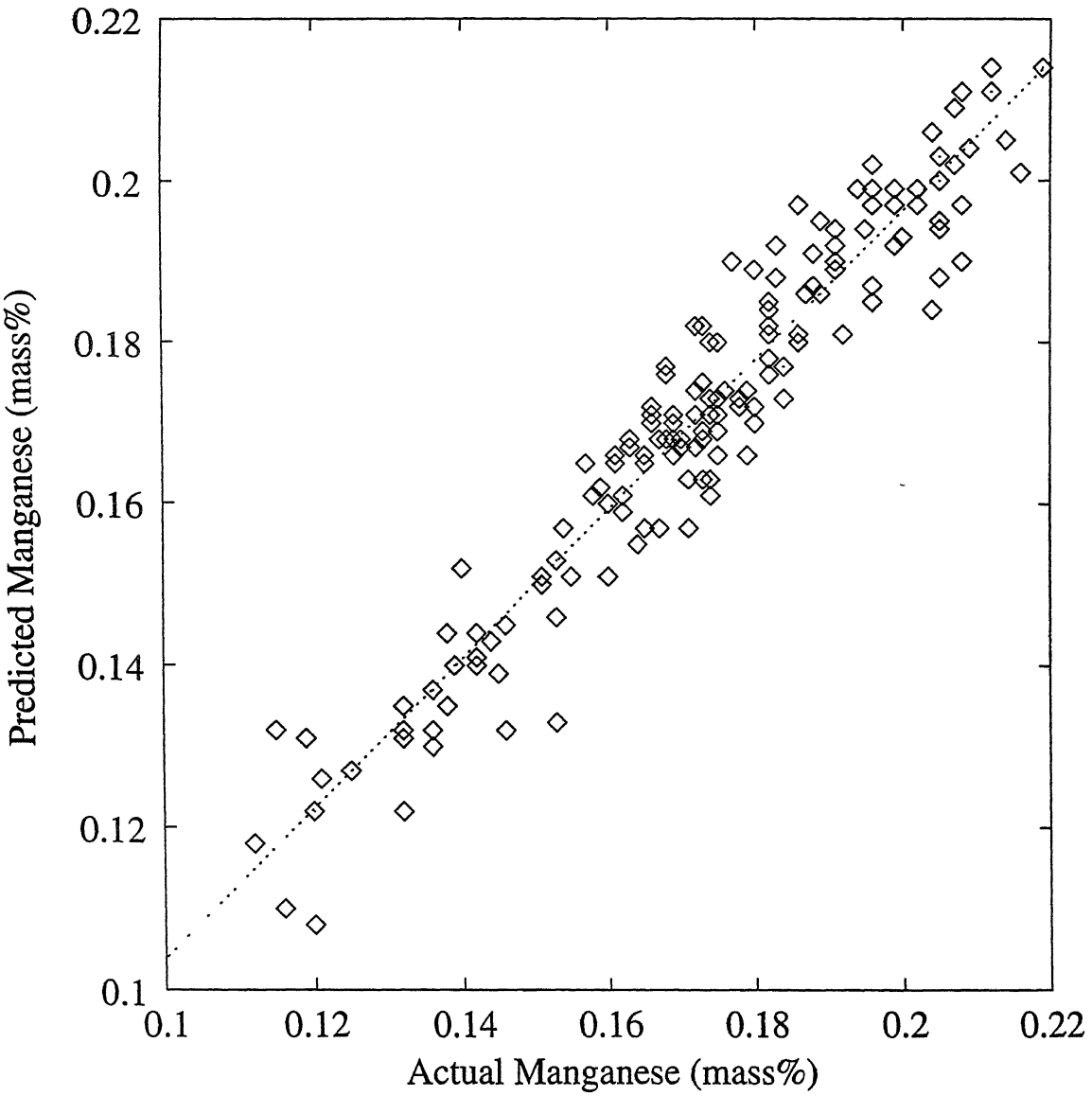

Figure 5.26: Data from Plant 1, Case Study 2(156 heats): Actual vs predicted manganese for model 5.14, best fit line is y=0.9237x+0.0115. Statistics are n=156, R=0.96, std. error=0.0065.

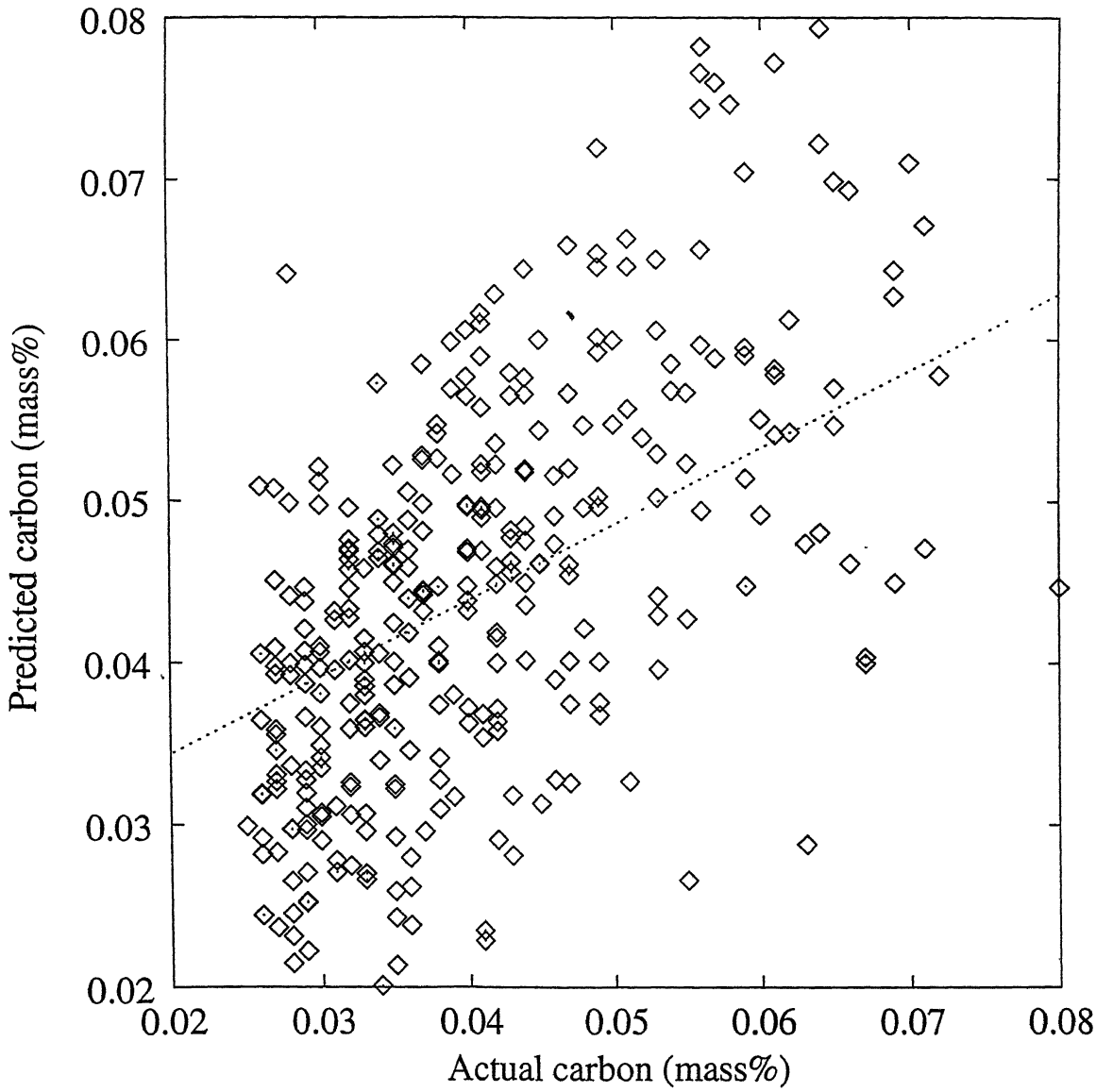

Figure 5.27: Data from Plant 2 (340 heats): Actual vs predicted carbon for model 5.4 (method 1), best fit line is y=0.4739x+0.0249. Statistics are n=340, R=0.61, std. error=0.012.

Table 5.6 Summary of results obtained for carbon prediction for Plant 2

S. No	Model No	Model equation	Parameters used	Parameters optimized	Statistics of regression (y=mx+c)			Remarks
					Dependent variable	Independent variable	Statistics	
1	5.4 (method 1)	$\Delta c = \Delta t \alpha_1 \epsilon^{\eta} c$ $\epsilon=(-\frac{dc}{dt}\beta_1 + Q_{eff})$	c_o, t	α_1 , η	c_t (0.027)	$c_{t_{act}}$ (0.029)	m=0.4739 c=0.0249 R=0.61 σ=0.012 F=203.319	Plant 2
2	5.4 (reg, method 1)	$c_t' = \mu_o + \mu_1 c_t + \sum_{i=2}^{n-1} \mu_i \cdot X_i$	Scrap chill scrap c_o, t	μ_i	c_t' (0.023)	$c_{t_{act}}$ (0.029)	m= 0.4130 c= 0.0246 R= 0.64 σ= 0.010 F= 233.16843	Plant 2
3	5.4 (method 2)	$\Delta c = \Delta t \alpha_1 \epsilon^{\alpha_2 \epsilon} c$ $\epsilon=(-\frac{dc}{dt}\beta_1 + Q_{eff})$	c_o , t	α_1 , α_2	c_t (0.023)	$c_{t_{act}}$ (0.029)	m=0.7433 c=0.0145 R=0.71. σ=0.014 F=335.862	Plant 2
4	5.4 (reg, method 2)	$c_t' = \mu_o + \mu_1 c_t + \sum_{i=2}^{n-1} \mu_i \cdot X_i$	Scrap chill scrap c_o, t	μ_i	c_t' (0.024)	$c_{t_{act}}$ (0.029)	m= 0.5064 c= 0.0201 R= 0.71 σ= 0.010 F= 333.916	Plant 2
5	5.3 (reg)	$c_t' = \mu_o + \mu_1 c_t + \sum_{i=2}^{n-1} \mu_i \cdot X_i$	$O22^2$,c_o^2 $O22 * c_o$ T_o,flux O22, c_o	μ_i	c_t' (0.028)	$c_{t_{act}}$ (0.029)	m=0.5498 c=0.0185 R=0.74 σ=0.005 F=389.423	Plant2

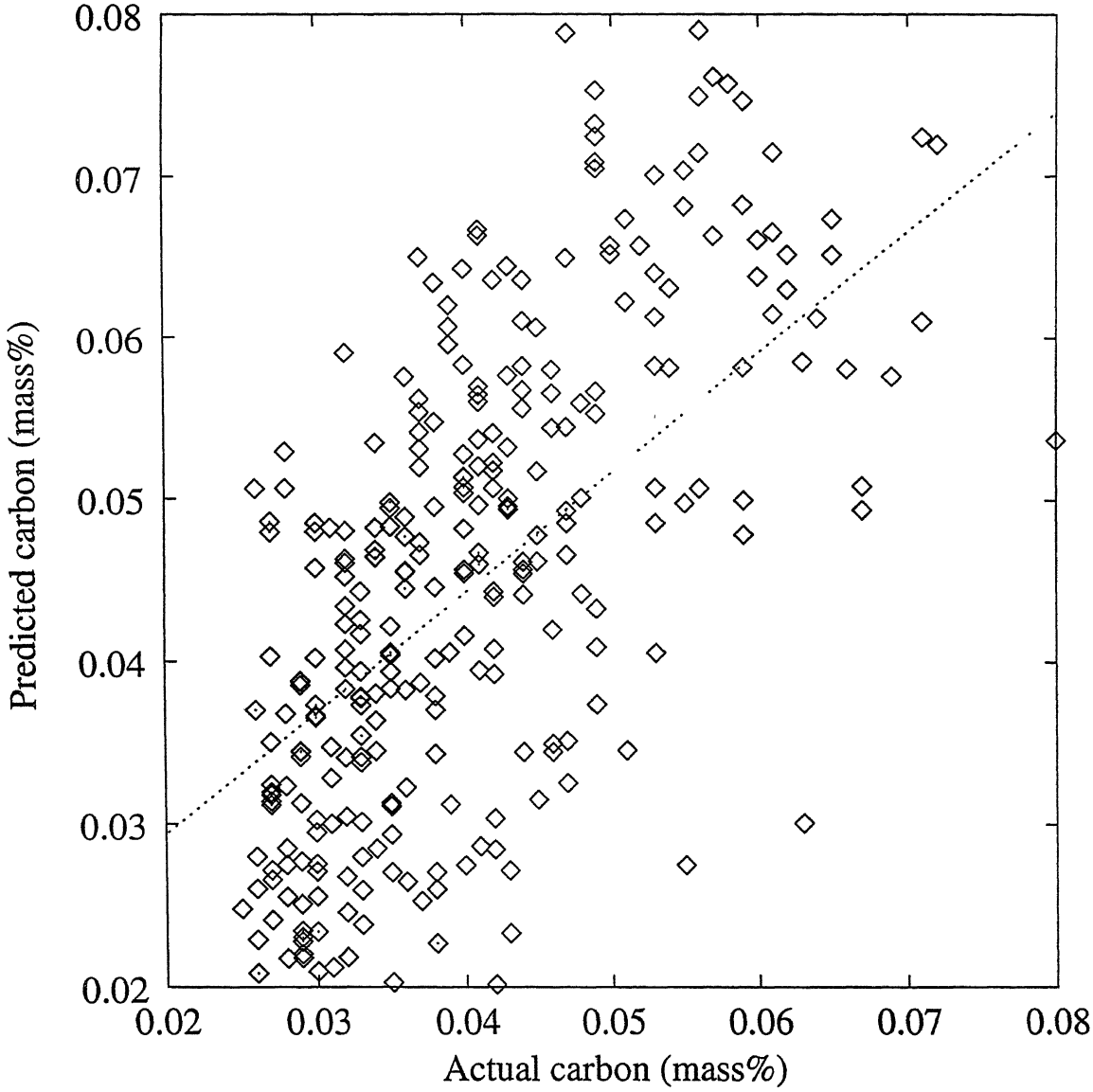

Figure 5.28: Data from Plant 2 (340 heats): Actual vs predicted carbon for model 5.4 (method 2), best fit line is y=0.7433x+0.0145. Statistics are n=340, R=0.71, std. error=0.014.

5.3.1.2 Regression models

Model 5.4 (reg, method 1)

Model 5.4 (reg, method 1) is regression model for model 5.4 (method 1). Variables accepted in this model are Scrap (-0.0000006), c_t(0.6997620), chill scrap(0.0000029) and Constant(0.0311). Statistics of regression are presented in Table 5.6 (method 5.4 (reg, method 1)). Fig. 5.29 shows the graph of actual vs predicted carbon. It can be observed that R increased from 0.61 in model 5.4 (method 1)to 0.64 in model 5.4 (reg, method 1) i.e., an improvement of 4.2%. σ also came down to 0.010 in model 5.4 (reg, method 1) from 0.012 in model 5.4 (method 1) i.e., a reduction of 13%.

Model 5.4 (reg, method 2)

Model 5.4 (reg, method 2) is regression model for model 5.4 (method 2). Variables accepted in this model are Scrap (-0.0000004), c_t(0.5904476), chill scrap(0.0000017) and Constant(0.0282). Statistics of regression are presented in Table 5.6 (model 5.4 (reg, method 2)). Fig. 5.30 shows the graph of actual vs predicted carbon. It can be observed that R value decreased slightly from 0.7060 in model 5.4 (method 2) to 0.7050 in model 5.4 (reg, method 2). σ also came down to 0.010 in model 5.4 (reg, method 2) from 0.014 in model 5.4 (method 2) i.e., a reduction of 30%.

Model 5.3 (reg)

Model 5.3 (reg) is developed based on 321 heats (with end point carbon (c_t) in the range 0.02-0.075) of Plant 2. First linear regression was performed to fit best fit line for model 5.3. Fig. 5.31 shows actual vs predicted carbon graph. But after observing the trend of results in Fig. 5.31, polynomial of $2nd$ order was tried. Then again multiple linear reression was performed to obtain a model with statistics R=0.81 and σ=0.011. After observing the parameters accepted, MLR is directly performed on the variables. The model so evolved is the one discussed here.

This model based on polynomial fit of $2nd$ order to the Linear model. Variables accepted in this model are O_{22}^2(0.0000000186), O_{22}(-0.0000421756), T_o(0.0000688766),

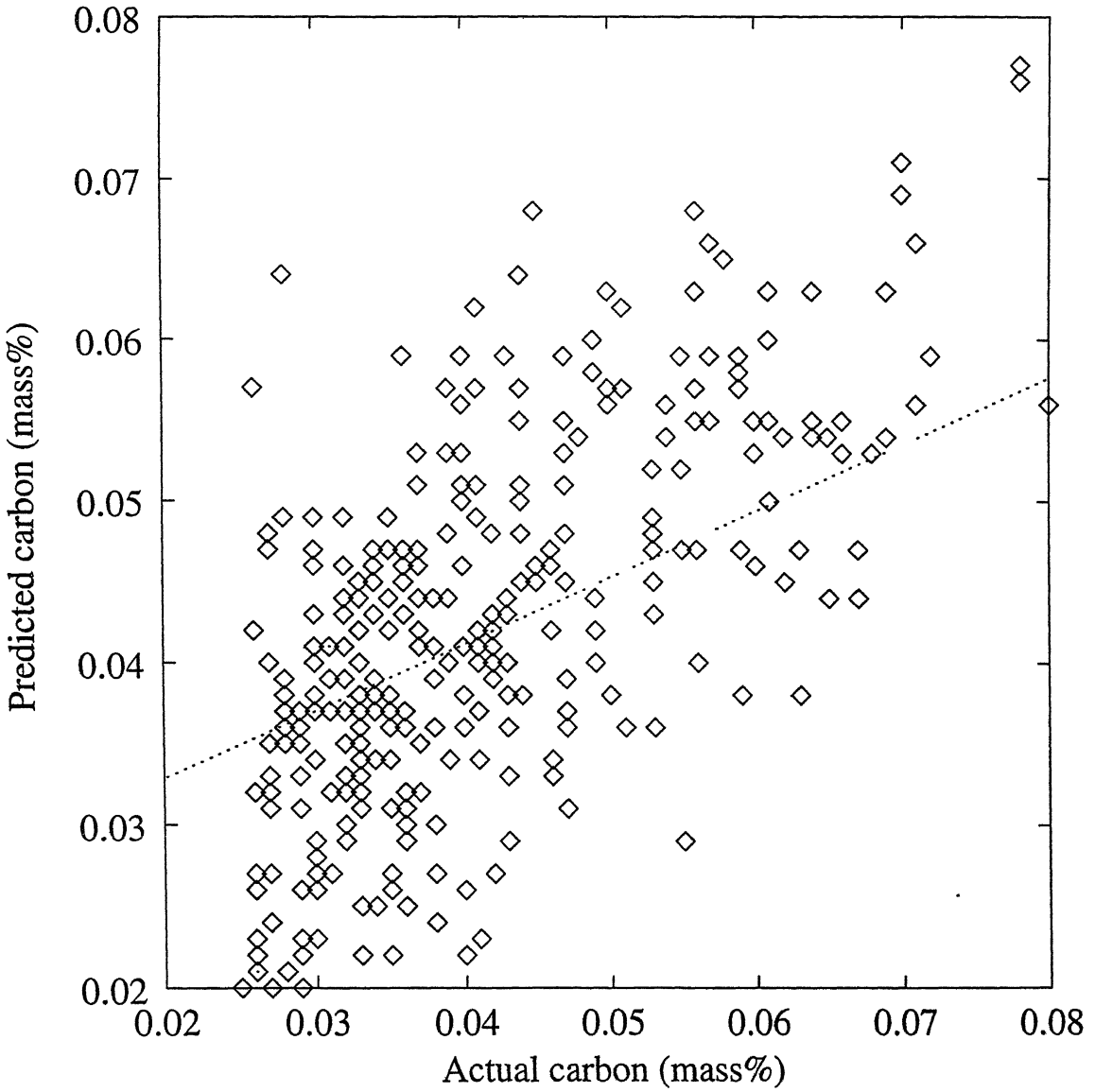

Figure 5.29: Data from Plant 2 (340 heats): Act vs predicted for model 5.4 (reg, method 1), best fit line is y=0.4130x+0.0246. Statistics are n=340, R=0.64, std. error=0.010.

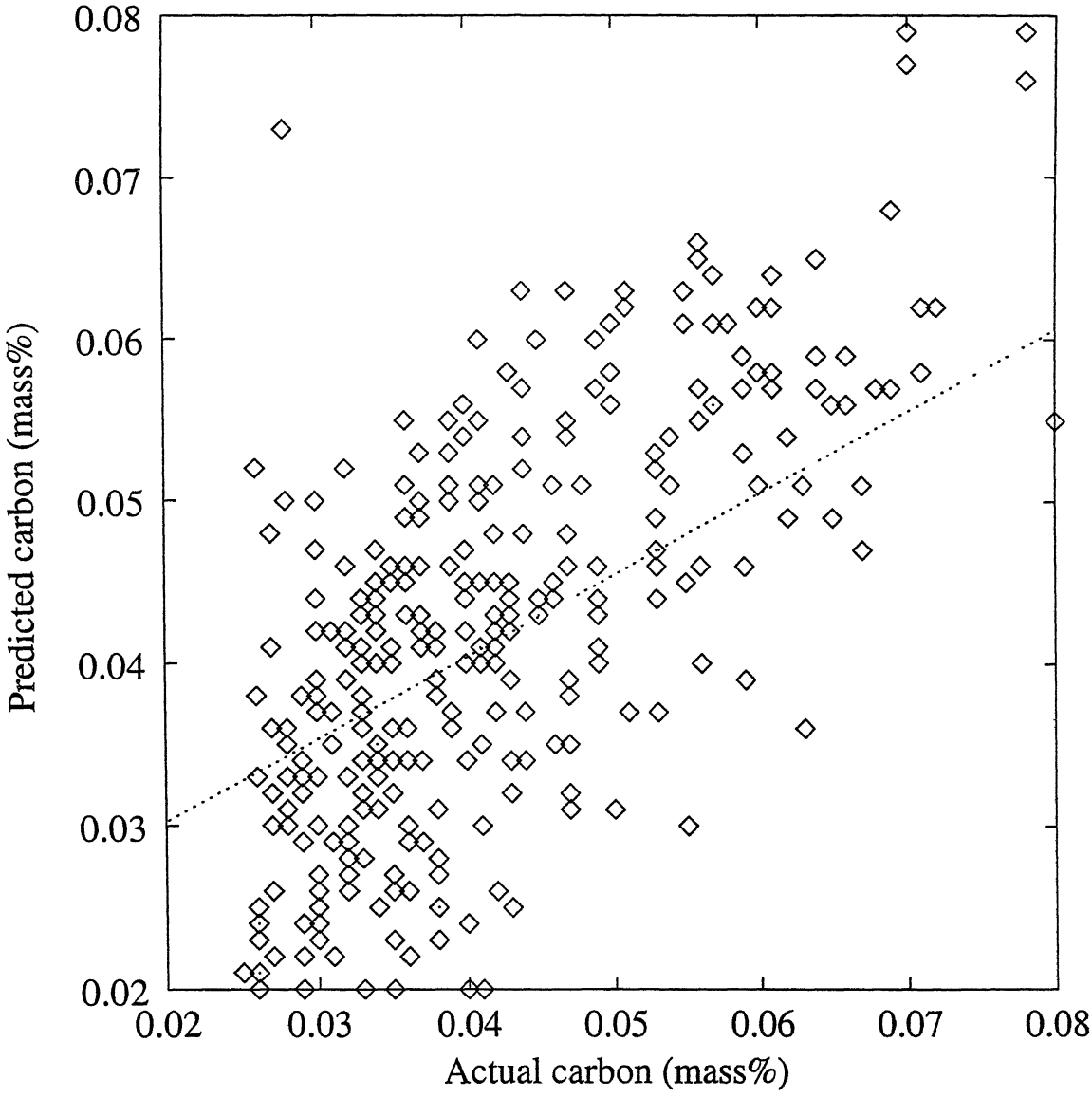

Figure 5.30: Data from Plant 2 (340 heats): Actual vs Predicted carbon for model 5.4 (reg, method 2), best fit line is y=0.5064x+0.0201. Statisatics are n=340, R=0.71, std. error=0.010.

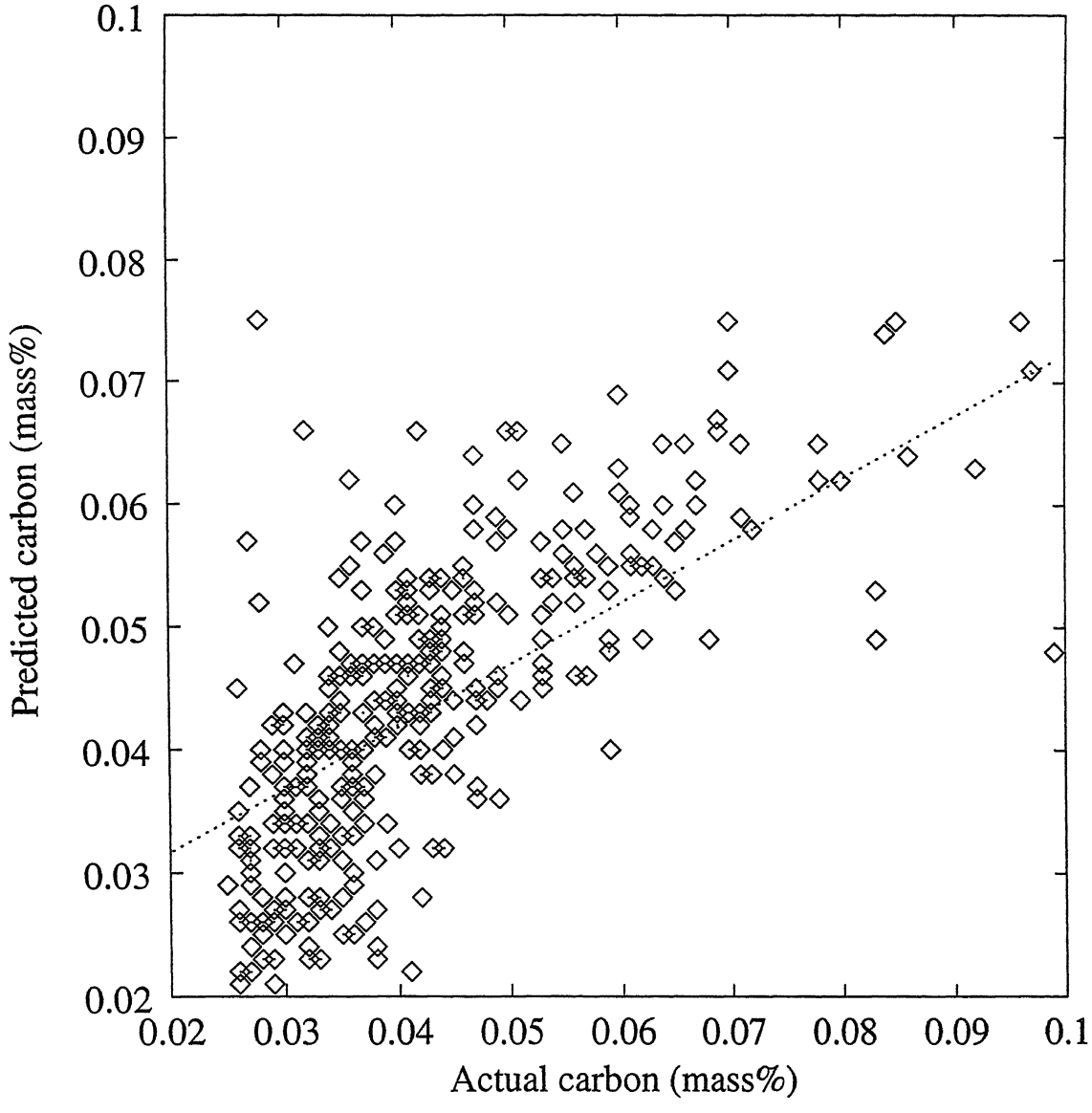

Figure 5.31: Data from Plant 2 (321 heats): Actual vs predicted carbon for model 5.3. Best fit line is y=0.5077x+0.0215. Statistics are n=339, R=0.71, std. error=0.010.

flux(-0.0000007942), c_o^2(0.0676718982), $O_{22} \cdot c_o$(-0.0000818279), c_o(0.1238672564) and constant(-0.05). Statistics of regression are presented in Table 5.6 (method 5.3 (reg)). Fig. 5.32 shows the graph of actual vs predicted carbon. It can be observed from the statistics that σ=0.006 (0.00554) and R=0.74 (0.7414). For a typical heat with $O22^2$=4524129, c_o^2=0.202, $O22 * c_o$ =957.150, O22=2127, c_o=0.450, T_o=1534, flux=12450

c_t'=-0.05+0.0000000186(4524129)-0.0000421756(2127)+0.0000688766(1534)-0.0000007942(12450)+0.0676718982(0.202)-0.0000818279(957.150)+0.1238672564(0.450)

=0.028.

Actual end point carbon value for this heat is 0.029.

5.3.1.3 Discussion on carbon prediction results

On Comparing results of prediction by model 5.4 (method 1) and model 5.4 (method 2), it can be observed that the latter model is giving better results with R of 0.71 and σ of 0.014. This is 15% improvement in R over that of model 5.4 (method 1). This improvement is because η is allowed to vary in method 2 of GA-decarb models. After performing MLR on the results obtained from GA-decarb models, value of σ decreased to 0.010 in model 5.4 (reg, method2) from 0.014 in model 5.4(method 2).

The best prediction for Plant 2 is given by model 5.3 (reg) with R of 0.7414 and σ of 0.00554%. This σ is 43% lower than the one obtained from model 5.4 (reg, method 2).

5.3.2 Temperature prediction results

Model 5.6

From the statistics of regression on actual versus predicted temperature(Table 5.7) it can be observed that $\sigma = 8\,^{\circ}C$ and R=0.72 (0.7241). Fig. 5.33 shows graph of actual versus predicted temperature. This model is able to correlate 52% of variation in the data. Operational variables used are O22(0.0230991), T_o(0.58), c_o(14.127787), flux(-0.0009627) and constant(714.4507). For a typical heat with O22=2127, c_o =0.450, T_o=1534, flux=12450

T =714.4507+0.0230991(2127)+0.58(1534)+14.127787(0.45)-0.0009627(12450)

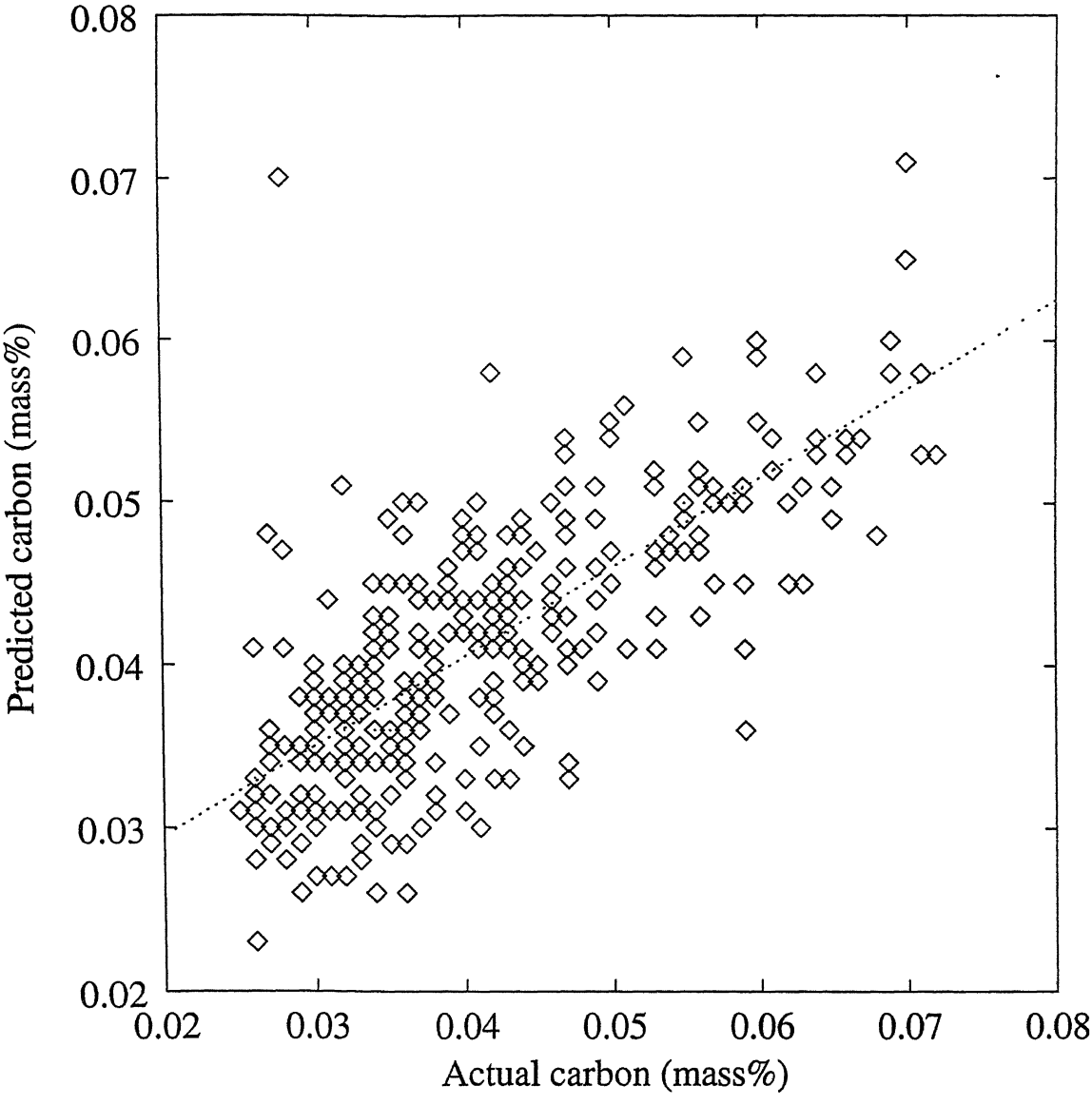

Figure 5.32: Data from Plant 2 (321 heats): Actual vs predicted carbon for model 5.3 (reg). Best fit line is y=0.5498x+0.0185. Statistics are n=321, R=0.74, std. error=0.005.

=1648.

Actual temperature for this heat is 1670.

5.3.3 Dissolved oxygen prediction results

Model 5.8

From the statistics of regression on actual versus predicted dissolved oxygen (Table 5.8) it can be observed that σ=139 ppm and R=0.82 (0.8181). Fig. 5.34 shows graph of actual versus predicted dissolved oxygen. This model is able to explain 67% of the variation. Operational variables used are T(8.7309033), c_o(-1542.8043187), O22(0.2338949), T_o(-7.1812861) and constant(-2002.4246). For a typical heat with T=1670, c_o =0.450, O22=2127, T_o =1534

$[O]$=-2002.4246+8.7309033(1670)-1542.8043187(0.45)+0.2338949(2127)-7.1812861(1534)

=1365 ppm.

Actual dissolved oxygen for this heat is 1432 ppm.

5.4 Results of Plant 3

The models developed for this Plant are tuned for a total of 297 heats .

5.4.1 End point carbon prediction models

5.4.1.1 GA-decarb models (model 5.4)

Ga-decarb models are presented in section 5.2.1.4. The result for method 1 of GA-decarb models is very poor and hence not presented here.

Model 5.4 (method 2)

This is GA-decab model developed as explained in eq. (5.5). Model is optimized for 297 data sets. Optimized values of α_1 and α_2 corresponding to minimum SSE are 0.0195 and

Table 5.7 Summary of results obtained for temperature prediction for Plant 2

S. No	Model No	Model equation	Parameters used	Parameters optimized	Statistics of regression (y=mx+c)			Remarks
					Dependent variable	Independent variable	Statistics	
6	5.6	$T = \mu_o + \sum_{i=1}^{n-1} \mu_i \cdot X_i$	O22 T_o c_o flux	μ_i	T (1648)	T_{act} (1670)	m=0.5269 c=786.211 R=0.72 σ=8.0 F=372.546	Plant 2

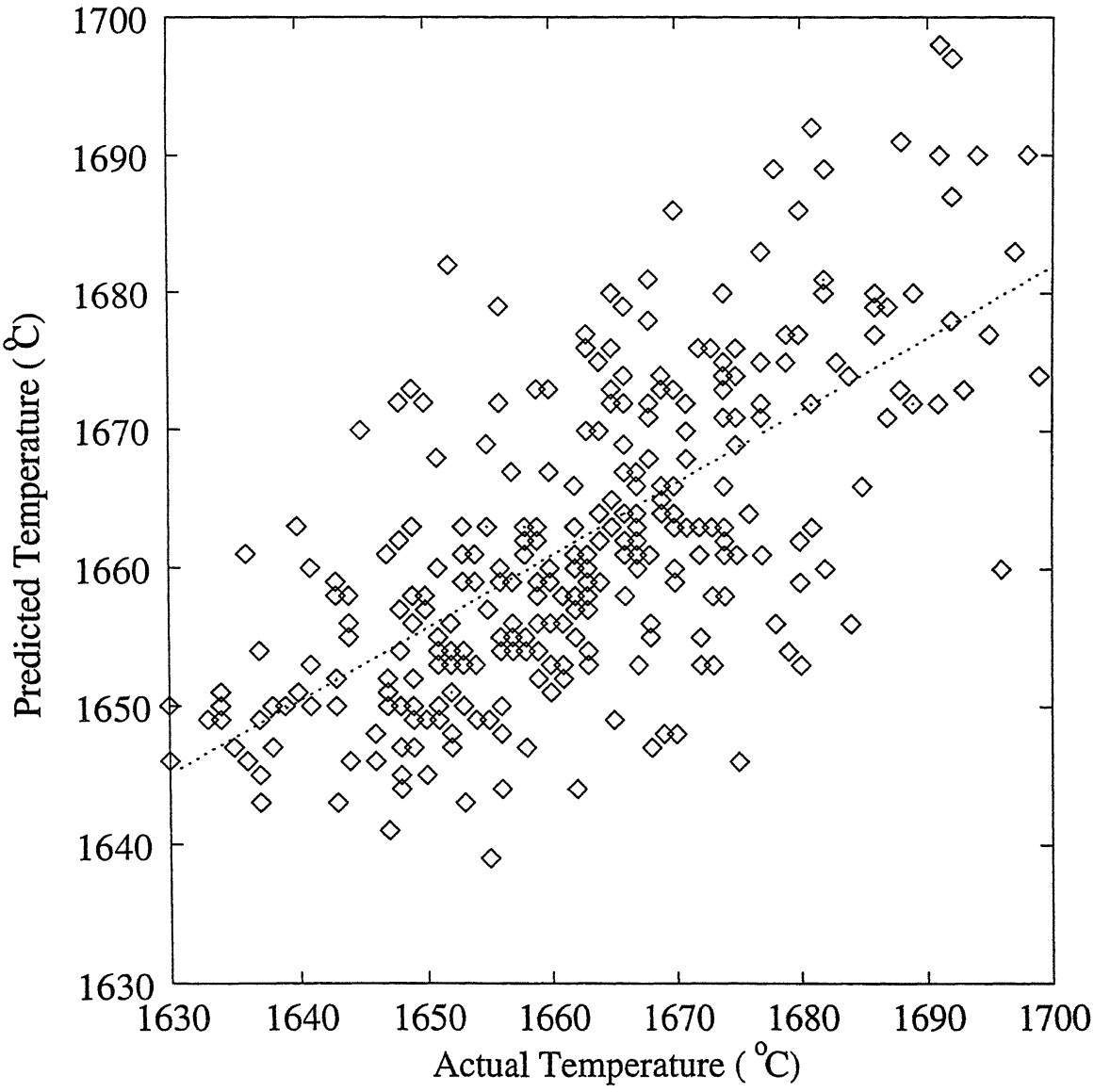

Figure 5.33: Data from Plant 2 (321 heats): Actual vs Predicted temperature for Model 5.6, best fit line is y=0.5269x+786.2107. Statistics are n=321, R=0.72, std. error=8.0.

Table 5.8 Summary of results obtained for Dissolved oxygen prediction for Plant 2

S. No	Model No	Model equation	Parameters used	Parameters optimized	Statistics of regression (y=mx+c)			Remarks
					Dependent variable	Independent variable	Statistics	
7	5.8	$[O] = \mu_o + \sum_{i=1}^{n-1} \mu_i \cdot X_i$	T T_o c_o O22	μ_i	$[O]$ (1365)	$[O]_{act}$ (1432)	m=0.6695 c=296.0932 R=0.82 σ=139 F=684.434	Plant 2

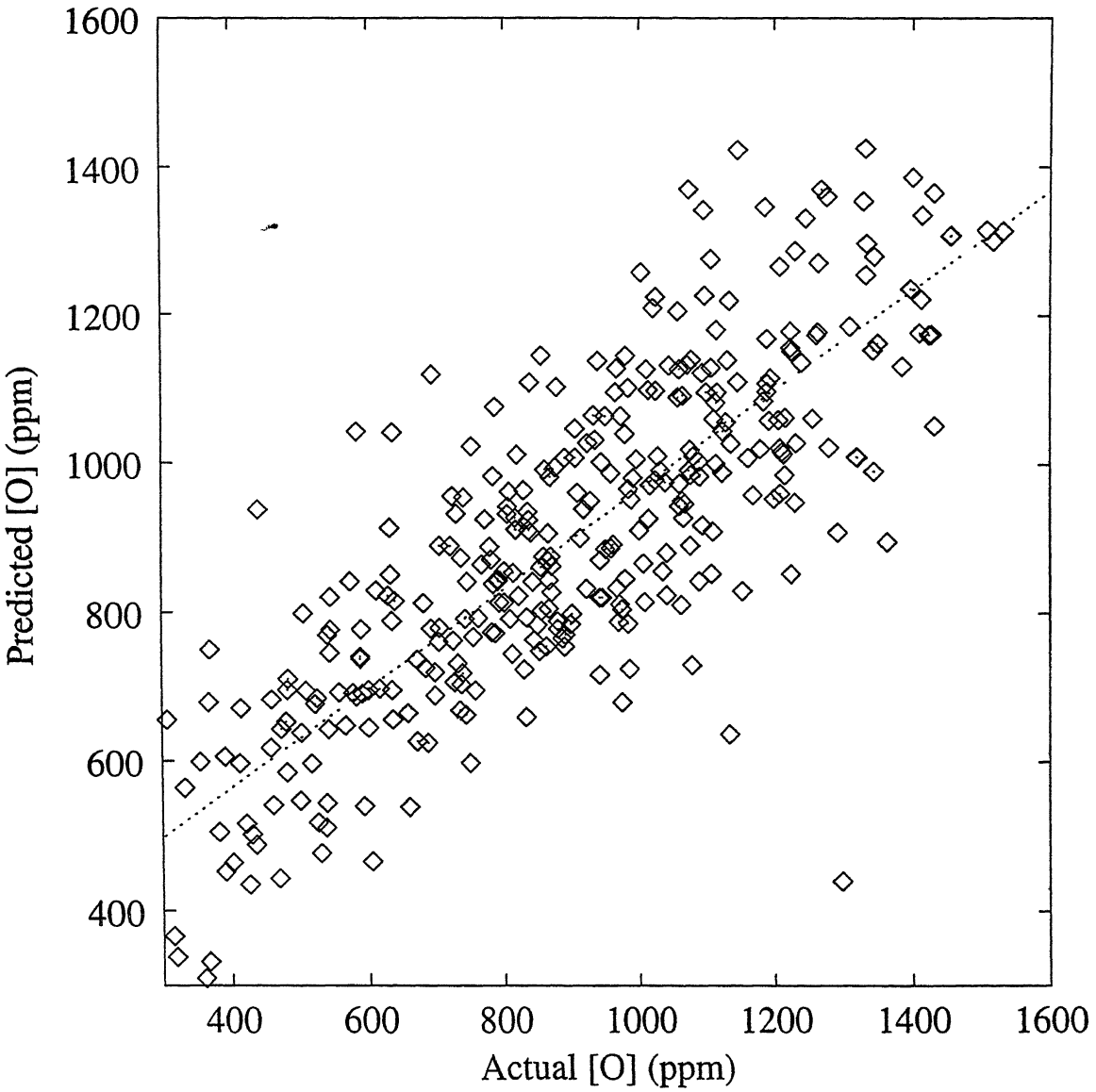

Figure 5.34: Data from Plant 2 (321 heats): Actual vs predicted [O] for model 5.8, best fit line is y=0.6695x+296.0932. Statistics are n=321, R=0.82, std. error=140.

0.00175. Table 5.9 shows the statistics of regression performed on actual vs predicted carbon for palnt 3. From the statistics of regression it can be observed that σ=0.016 and R=0.21 (see Table 5.9, model 5.4 (method 2)).

5.4.1.2 Regression models

Model 5.4 (reg, method 2)

Model 5.4 (reg, method 2) is regression model for model 5.4 (method 2). Variables accepted in this model are basicity (-0.0000010), c_t(0.3133347), T_o(-0.0001404), O22 (0.0000152) and constant (0.2630). Statistics of regression are presented in Table 5.9 (model 5.4 (reg, method 2)). Fig. 5.35 shows the graph of actual vs predicted carbon. It can be observed from statistics of regression that R value increased from 0.21 in model 5.4 (method 2)to 0.44 in model 5.4 (reg, method 2) i.e., an increase of 107%. σ also reduced to 0.004 in model 5.4 (reg, method 2) from 0.016 in model 5.4 (method 2) of Plant 3 i.e., a reduction of 76.3%.

Model 5.3 (reg)

Model 5.3 (reg) is tuned for 297 heats of Plant 3. Variables accepted in this model are basicity(-0.000011), T_o(-0.0001478), c_o(0.0232972), O22(-0.0000227) and constant(0.3038). Statistics of regression performed on actual and predicted carbon are presented in Table 5.9 (model 5.3 (reg)). From statistics of regression it can be observed that σ=0.003 (0.0034)% and R=0.39 (0.3783). Fig. 5.36 shows the graph of actual vs predicted carbon. For a typical heat with basicity=3.85, T_o=1629, c_o =0.549, O22=740

c_t = 0.3038-0.000011(3.85)-0.0001478(1629)+0.0232972(0.549)-0.0000227(740) =0.059.

Actual end point carbon for this heat is 0.050.

5.4.1.3 Discussion on carbon prediction results

From prediction statistics of model 5.4 (reg, method 2) and model 5.3 (reg) it can be observed that R value decreased from 0.44 in model 5.4 (reg, method 2) to 0.38 in model

Table 5.9 Summary of results obtained for carbon prediction for Plant 3

S. No	Model No	Model equation	Parameters used	Parameters optimized	Statistics of regression (y=mx+c)			Remarks
					Dependent variable	Independent variable	Statistics	
1	5.4 (method 2)	$\Delta c = \Delta t \alpha_1 \epsilon^{\alpha_2 \epsilon} c$ $\epsilon = (-\frac{dc}{dt}\beta_1 + Q_{eff})$	c_o , t	α_1 , α_2	c_t (0.034)	$c_{t_{act}}$ (0.050)	m=0.3621 c=0.0362 R=0.21 σ=0.016 F=13.912	Plant 3
2	5.4 (reg, method 2)	$c_t' = \mu_o + \mu_1 c_t + \sum_{i=2}^{n-1} \mu_i \cdot X_i$	basicity T_o,O22	μ_i	c_t' (0.052)	$c_{t_{act}}$ (0.050)	m= 0.1929 c= 0.0410 R= 0.44 σ= 0.004 F=70.494	Plant 3
3	5.3 (reg)	$c_t' = \mu_o + \mu_1 c_t + \sum_{i=2}^{n-1} \mu_i \cdot X_i$	basicity c_o T_o O22	μ_i	c_t' (0.059)	$c_{t_{act}}$ (0.050)	m=0.1435 c=0.0441 R=0.39 σ=0.003 F=49.772	Plant3

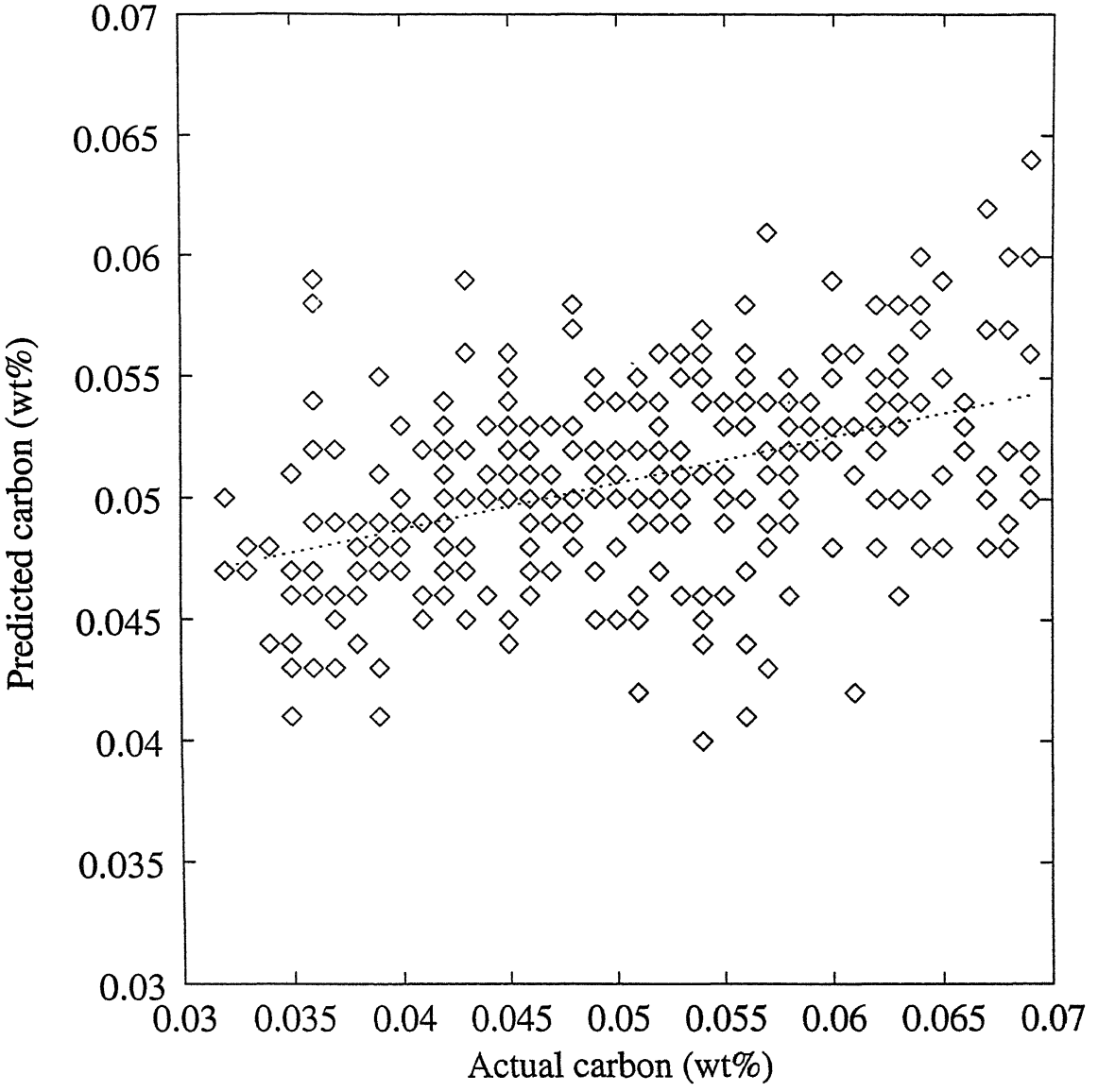

Figure 5.35: Data from Plant 3 (297 heats): Actual vs predicted carbon for model 5.4 (reg, method2), best fit line is y=0.1929x+0.041. Statistics are n=297, R=0.44, std. error=0.004.

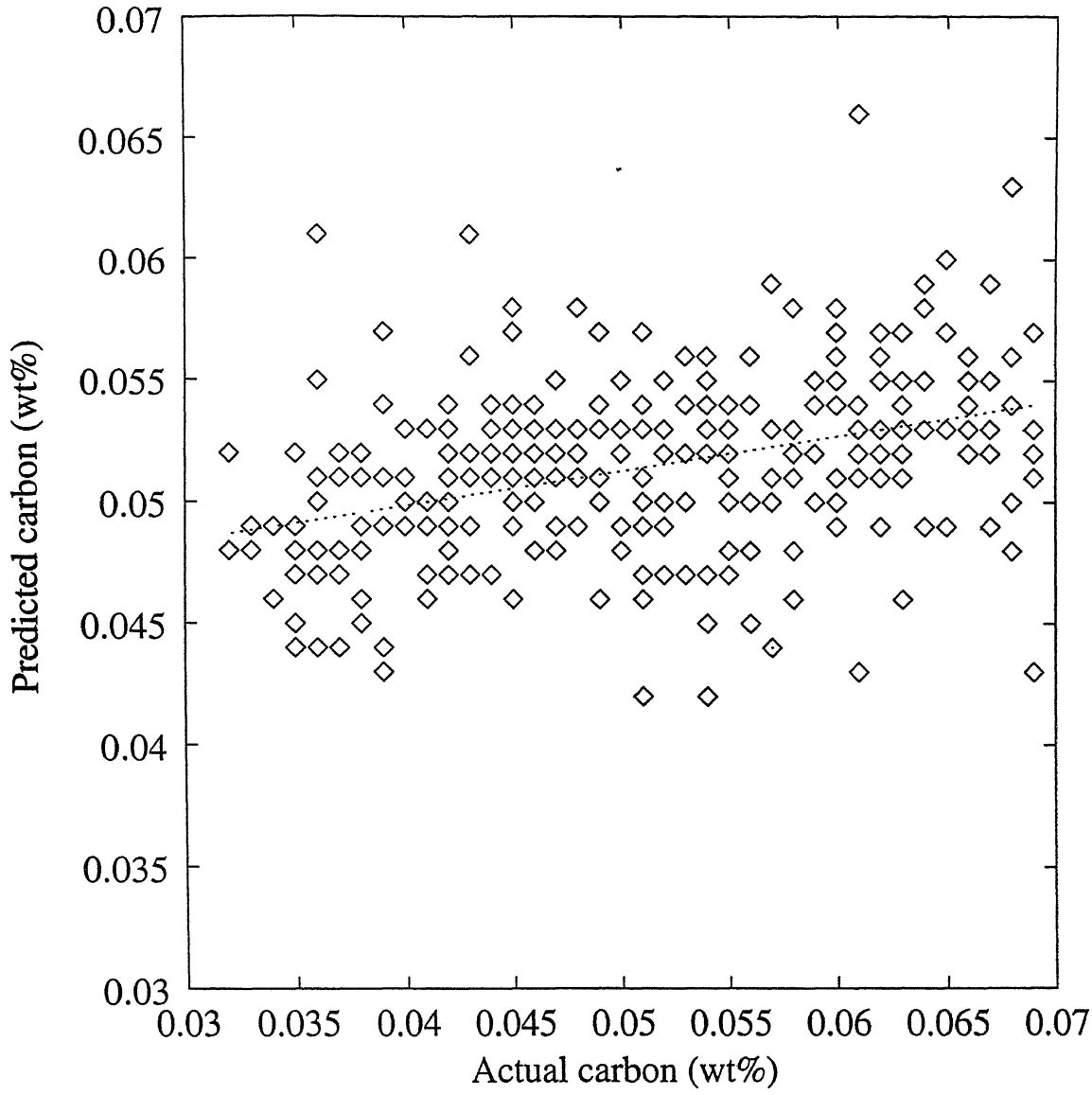

Figure 5.36: Data from Plant 3 (297 heats): Actual vs predicted carbon for model 5.3(reg), best fit line is y=0.1435x+0.0441. Statistics are n=297, R=0.39, std. error=0.003.

5.3 (reg). But σ value improved from 0.004 in model 5.4 (reg, method 2) to 0.003 in model 5.3 (reg).

5.4.2 Temperature prediction results

Model 5.6

From statistics of regression on actual versus predicted temperature (Table 5.10) it can be observed that $\sigma = 9\,^{\circ}C$ and R=0.73 (0.7310). Fig. 5.37 shows graph of actual versus predicted temperature. This model is able to correlate 59.6% of variation in the data. Operational variables used are raw dolo2(-0.0289692), T_o(0.8109563), O22(0.0982545), hlans2(0.6512143) and constant(215.8787). For a typical heat with raw dolo2=650, T_o =1629, O22=740, hlans2=148

T = 215.8787-0.0289692(650)+0.8109563(1629)+0.0982545(740)+
0.6512143(148)
=1687.
Actual temperature for this heat is 1702.

5.4.3 Dissolved oxygen prediction results

Oxygen models are developed for 297 heats.

Model 5.8

From statistics of regression on actual versus predicted dissolved oxygen (Table 5.11) it can be observed that σ=77 ppm and R=0.60 (0.5978). Fig. 5.38 shows graph of actual versus predicted dissolved oxygen. This model is able to explain 35% of the variation. Operational variables used are basicity(0.0175579), llife(0.2249089), raw dolo2(0.0847864), T_o(-0.9097412), T(5.2328732) and constant(-6928.4438). For a typical heat with basicity=3.85, llife=6, raw dolo2=650, T_o =1629, T=1702

$[O]$ = -6928.4438+0.0175579(3.85)+0.2249089(6)+0.0847864(650)-0.9097412(1629)+
5.2328732(1702)
=552.

Table 5.10 Summary of results obtained for temperature prediction for Plant 3

S. No	Model No	Model equation	Parameters used	Parameters optimized	Statistics of regression (y=mx+c)			Remarks
					Dependent variable	Independent variable	Statistics	
4	5.6	$T = \mu_o + \sum_{i=1}^{n-1} \mu_i \cdot X_i$	O22 T_o raw dolo2 hlans2	μ_i	T (1687)	T_{act} (1702)	m=0.5351 c=785.333 R=0.73 σ=9.0 F=342.074	Plant 3

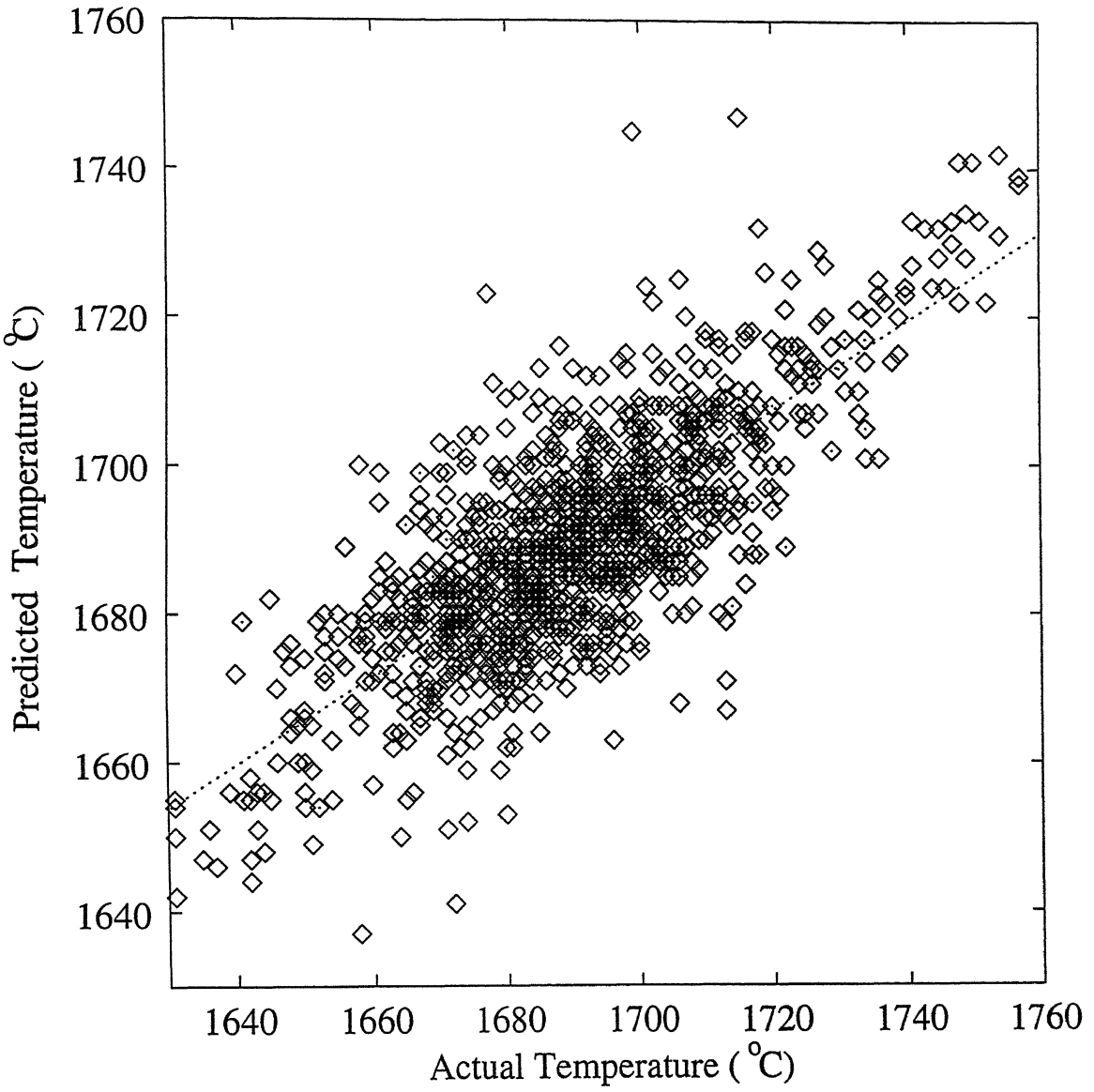

Figure 5.37: Data from Plant 3 (297 heats): Actual vs Predicted temperature for model 5.6, best fit line is y=0.5351x+785.333. Statistics are n=297, R=0.73, std. error=9.

Actual dissolved oxygen for this heat is 680.

5.4.4 Phosphorus prediction results

Phosphorus models are developed for 297 heats.

Model 5.11

From statistics of regression on actual versus predicted phosphorus (Table 5.12) it can be observed that σ=0.001% and R=0.81 (0.8113). Fig. 5.39 shows graph of actual versus predicted phosphorus. Using this model 75% of variation can be explained. Operational variables used are svol(-0.0000007), T_o(-0.0000237), c_o(-0.0016602), O22(-0.0000027), P1(0.2280134), Mn2(0.0237083), T(0.0000471) and constant (-0.0357). For a typical heat with svol=2871.444, O22=740, T_o =1629, c_o =0.549, P1=0.018, Mn2=0.120, T=1702

p'_t = -0.0357-0.0000007(2871.444)-0.0000237(1629)-0.0016602(0.549)-0.0000027(740)+ 0.2280134(0.018)+0.0237083(0.120)+0.0000471(1702)

=0.008

Actual phosphorus for this heat is 0.009.

5.4.5 Manganese prediction results

5.4.5.1 Regression model

Regression model is given by eq. (3.27)

$$Mn'_t = \mu_o + \mu_1 Mn_o + \sum_{i=2}^{n-1} \mu_i \cdot X_i \tag{5.14}$$

where, Mn'_t is the end point manganese value predicted from MLR, Mn_o is the sublance manganese and μ_i 's are coefficients of operational variables X_i

Model 5.13

From statistics of regression on actual versus predicted manganese (Table 5.13) it can be observed that σ=0.012% and R=0.83. Fig. 5.40 shows graph of actual versus predicted

Table 5.11 Summary of results obtained for Dissolved oxygen prediction for Plant 3

S. No	Model No	Model equation	Parameters used	Parameters optimized	Statistics of regression (y=mx+c)			Remarks
					Dependent variable	Independent variable	Statistics	
5	5.8	$[O] = \mu_o + \sum_{i=1}^{n-1} \mu_i \cdot X_i$	basicity T_o raw dolo2 llife T	μ_i	$[O]$ (552)	$[O]_{act}$ (680)	m=0.3571 c=387.1967 R=0.60 σ=77 F=165.1967	Plant 3

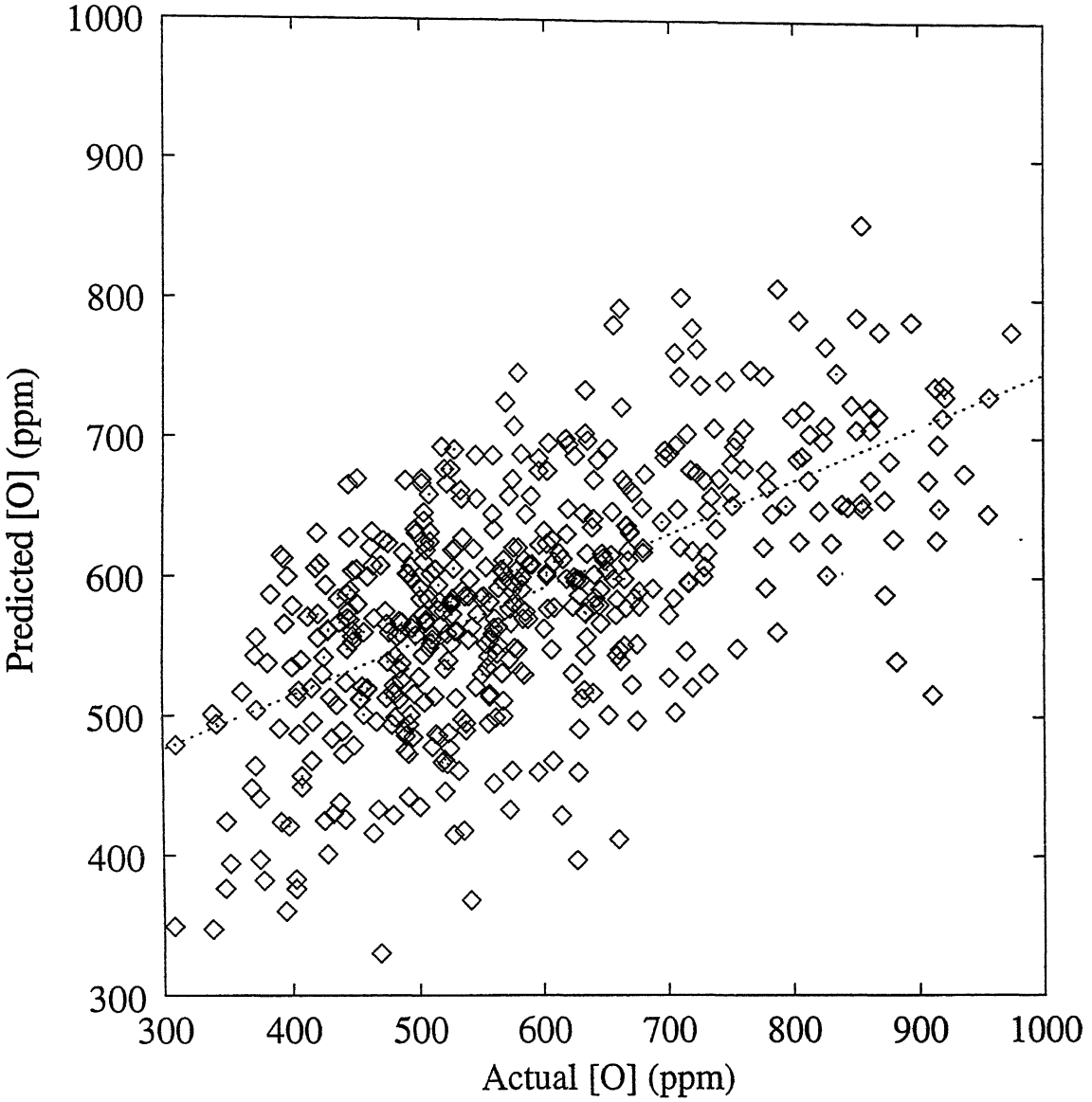

Figure 5.38: Data from Plant 3 (297 heats): Actual vs predicted [O] for model 5.8, best fit line is y=0.3571x+387.1967. Statistics are n=297, R=0.60, std. error=77.

Table 5.12 Summary of results obtained for phosphorus prediction for Plant 3

S. No	Model No	Model equation	Parameters used	Parameters optimized	Statistics of regression (y=mx+c)			Remarks
					Dependent variable	Independent variable	Statistics	
6	5.11	$p'_t = \mu_o + \mu_1 p_o + \sum_{i=2}^{n-1} \mu_i \cdot X_i$	svol,llife c_o, T_o O22, Mn2 T p_o	μ_i	p'_t (0.008)	p_t (0.009)	m=0.6823 c=0.0024 R=0.81 σ=0.001 F=574.0	Plant 3

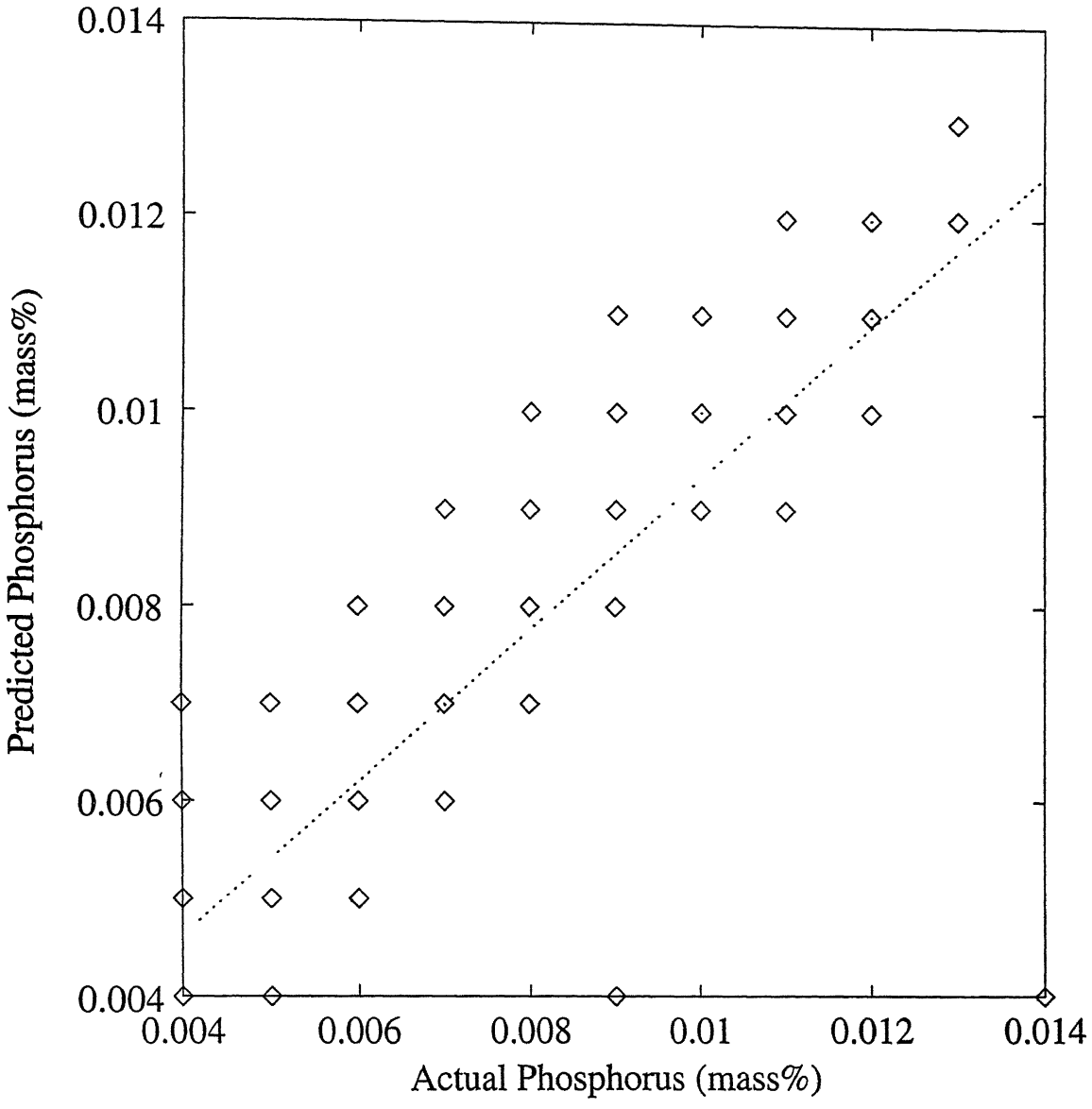

Figure 5.39: Data from Plant 3 (297 heats): Actual vs predicted phosphorus for model 5.11, best fit line is y=0.6823x+0.0024. Statistics are n=297, R=0.81, std. error=0.001. Each square may represent more than one heat.

manganese. Variables accepted in this model are Mn_o(0.4880717), O22(-0.0000294), raw dolo2(-0.0000091), hlans2(0.0006755) and constant(-0.0436). For a typical heat with Mn_o =0.19, O22=740, raw dolo2=650, hlans2=148

Mn'_t=-0.0436+0.4880717(0.19)-0.0000294(740)-0.0000091(650)+0.0006755(148) =0.121.

Actual manganese for this heat is 0.120.

5.5 Comparision of models developed for Plant 1, Plant 2 and Plant 3

In this section the best models tuned for Plants 1, 2 and 3 are compared to estimate the performance of each plant with respect to another.

5.5.1 Discussion on carbon prediction models

Models which are in common to all three plants are GA-decarb models (model 5.4) and model 5.3(reg). From model 5.4(reg, method1, Case Study 2) of Plant 1 and model 5.4 (reg, method 1) of Plant 2, it can be observed that the former is giving better prediction with σ=0.004%C. Among model 5.4 (reg, method 2, Case Study 2) of Plant 1, model 5.4 (reg, method 2) of Plant 2 and model 5.4 (reg, method 2) of Plant 3, Plant 1 has lowest value of σ (0.004), giving the best prediction.

From model 5.3 (reg) of Plants 1, 2 and 3 it can be observed that standard error σ is lowest (0.0034) in case of Plant 3. Best prediction is given by model 5.3 (reg) of Plant 1 with R value of 0.7617 and σ of 0.00418. Observing the parameters used in model 5.3 (reg), lance height is selected in Plant 1 and not in Plant 3. In case of Plant 2, lance height is not considered as it is kept constant for all the heats. Summary of best results for carbon prediction are summarized in Table 5.14, appendix 2, appendix 3 and appendix 4.

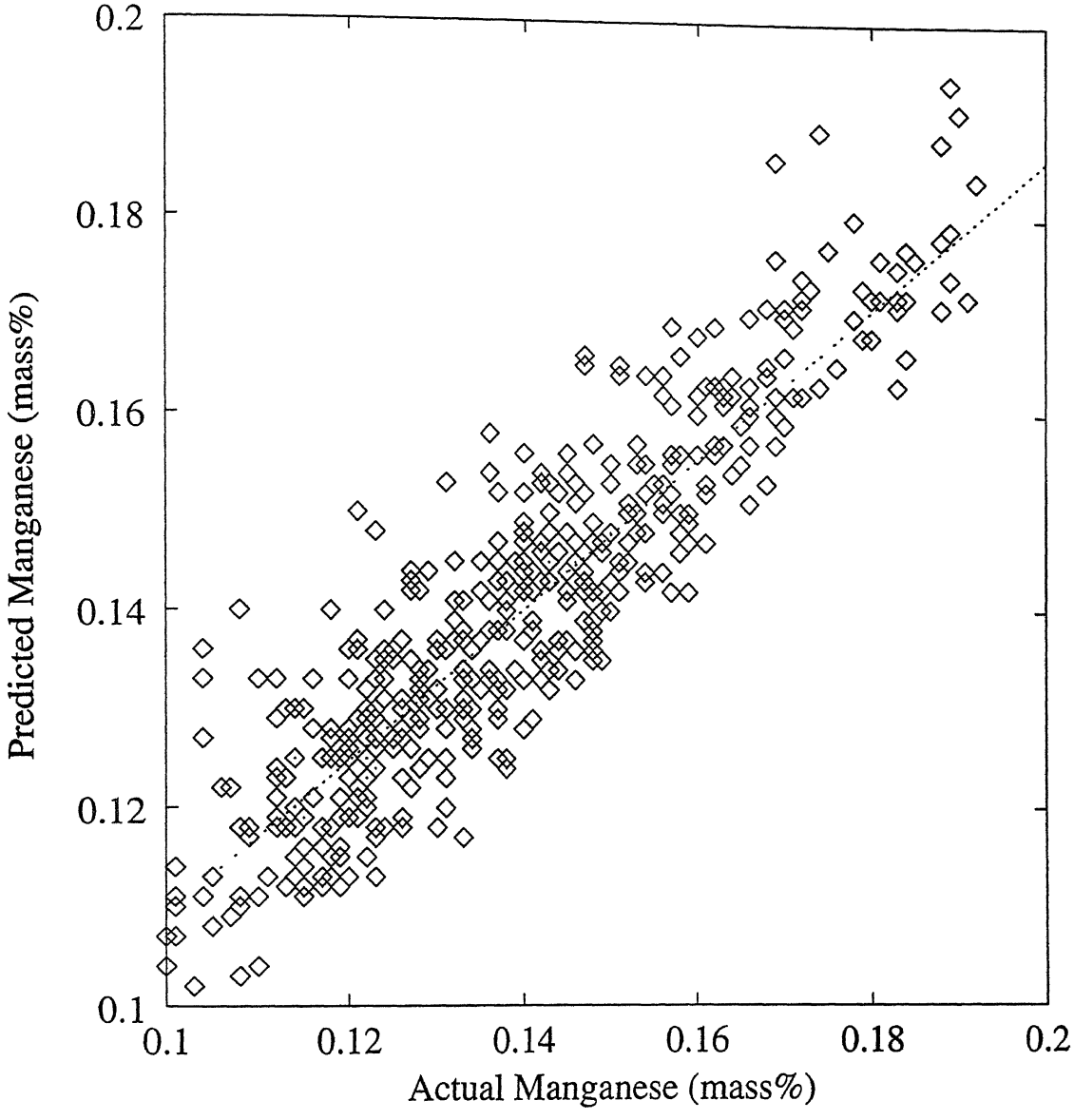

Figure 5.40: Data from Plant 3 (297 heats): Actual vs predicted manganese for model 5.13, best fit line is y=0.6848x+0.0456. Statistics are n=297, R=0.83, std. error=0.012.

Table 5.13 Summary of results obtained for manganese prediction for Plant 3

S. No	Model No	Model equation	Parameters used	parameters optimized	Statistics of regression (y=mx+c)			Remarks
					Dependent variable	Independent variable	Statistics	
7	5.13	$Mn'_t = \mu_o + \mu_1 Mn_o + \sum_{i=2}^{n-1} \mu_i \cdot X_i$	raw dolo2 Mn_o O22 hlans2	μ_i	Mn'_t (0.121)	Mn_t (0.120)	m=0.6848 c=0.0456 R=0.83 σ=0.012 F=647	Plant3

Table 5.14 Summary of best results for carbon prediction for Plant 1, Plant 2 and Plant 3

S. No	Model No	Model equation	Parameters used	Parameters optimized	Statistics of regression (y=mx+c)			Remarks
					Dependent variable	Independent variable	Statistics	
1	5.3 (reg)	$c'_t = \mu_o + \mu_1 c_t + \sum_{i=2}^{n-1} \mu_i \cdot X_i$	Ore1 O22 hlans2 dolo1 c_O	μ_i	c'_t	$c_{t_{act}}$	m=0.5796 c=0.0245 R=0.76 σ=0.004 F=212.882	Case study 2 Plant 1
2	5.3 (reg)	$c'_t = \mu_o + \mu_1 c_t + \sum_{i=2}^{n-1} \mu_i \cdot X_i$	$O22^2$,c_o^2 $O22 * c_o$ T_o,flux O22,c_o	μ_i	c'_t	$c_{t_{act}}$	m=0.5498 c=0.0185 R=0.74 σ=0.005 F=389.423	Plant2
3	5.4 (reg, method 2)	$c'_t = \mu_o + \mu_1 c_t + \sum_{i=2}^{n-1} \mu_i \cdot X_i$	basicity T_o,O22	μ_i	c'_t	$c_{t_{act}}$	m= 0.1929 c= 0.0410 R= 0.44 σ= 0.004 F=70.494	Plant 3

5.5.2 Discussion of temperature prediction models

From temperature models developed for Plants 1, 2 and 3 it can be observed that model 5.6 of Plant 1 is giving best prediction with R of 0.9027 and σ of 5.22 ^{o}C. The error of prediction in case of Plants 2 and 3 is 8 ^{o}C and 9 ^{o}C , respectively. Summary of best results for temperature prediction are summarized in Table 5.15, appendix 2, appendix 3 and appendix 4.

5.5.3 Discussion of dissolved oxygen prediction models

From dissolved oxygen models developed for Plants 1, 2 and 3 it can be observed that model 5.8 of Plant 1 is giving best prediction with R of 0.87 and σ of 34 ppm. Although R value is better for model 5.8 of Plant 2, σ is better for Plant 3. The accuracy of prediction in case of Plants 2 and 3 are 139 ppm and 77 ppm , respectively. Summary of best results for dissolved oxygen prediction are presented in Table 5.16, appendix 2, appendix 3 and appendix 4.

5.5.4 Discussion of phosphorus prediction models

No data was available for phosphorus prediction in case of Plant 2. Hence the models developed for Plants 1 and 3 are compared in this section. Comparing model 5.11 of Plants 1 and 3, Plant 1 is giving better prediction with R of 0.93 and σ of 0.0007%. In case of Plant 3, accuracy of phosphorus predicition is 0.001%. The best results for phosphorus prediction are summarized in Table 5.17, appendix 2, appendix 3 and appendix 4.

5.5.5 Discussion of manganese prediction models

No data was available for manganese prediction for the case of Plant 2. Hence the models developed for Plants 1 and 3 are compared in this section. Comparing model 5.13 of Plants 1 and 3, Plant 1 is giving better prediction with R of 0.96 and σ of 0.0065%. In case of Plant 3, accuracy of manganese predicition is 0.012%. The best results for manganese prediction are summarized in Table 5.18, appendix 2, appendix 3 and appendix 4.

Table 5.15 Summary of best results for temperature prediction for Plant 1, Plant 2 and Plant 3

S. No	Model No	Model equation	Parameters used	Parameters optimized	Statistics of regression (y=mx+c)			Remarks
					Dependent variable	Independent variable	Statistics	
1	5.6	$T = \mu_o + \sum_{i=1}^{n-1} \mu_i \cdot X_i$	hot ratio O22,T_o dolo2 slag2	μ_i	T	T_{act}	m=0.8146 c=307.76 R=0.90 σ=5 F=677.6145	Case study 2 Plant 1
2	5.6	$T = \mu_o + \sum_{i=1}^{n-1} \mu_i \cdot X_i$	O22 T_o c_o flux	μ_i	T	T_{act}	m=0.5269 c=786.211 R=0.72 σ=8 F=372.546	Plant 2
3	5.6	$T = \mu_o + \sum_{i=1}^{n-1} \mu_i \cdot X_i$	O22 T_o raw dolo2 hlans2	μ_i	T	T_{act}	m=0.5351 c=785.333 R=0.73 σ=9 F=342.074	Plant 3

Table 5.16 Summary of best results for Dissolved oxygen prediction for Plant 1, Plant 2 and Plant 3

S. No	Model No	Model equation	Parameters used	Parameters optimized	Statistics of regression (y=mx+c)			Remarks
					Dependent variable	Independent variable	Statistics	
1	5.8	$[O] = \mu_o + \sum_{i=1}^{n-1} \mu_i \cdot X_i$	Basicity O22, c_o T_o, dolo2 hlans2		$[O]$	$[O]_{act}$	m=0.761 c=101.255 R=0.87 σ=34 F=490.34061	Case study 2 Plant 1
2	5.8	$[O] = \mu_o + \sum_{i=1}^{n-1} \mu_i \cdot X_i$	T_{act} T_o c_o O22	μ_i	$[O]$	$[O]_{act}$	m=0.6695 c=296.0932 R=0.82 σ=139 F=684.434	Plant 2
3	5.8	$[O] = \mu_o + \sum_{i=1}^{n-1} \mu_i \cdot X_i$	basicity T_o raw dolo2 llife T_{act}	μ_i	$[O]$	$[O]_{act}$	m=0.3571 c=387.1967 R=0.60 σ=77 F=165.1967	Plant 3

Table 5.17 Summary of best results for phosphorus prediction for Plant 1 and Plant 3

S. No	Model No	Model equation	Parameters used	Parameters optimized	Statistics of regression (y=mx+c)			Remarks
					Dependent variable	Independent variable	Statistics	
1	5.11	$p'_t = \mu_o + \mu_1 p_o + \sum_{i=2}^{n-1} \mu_i \cdot X_i$	svol,T_{act} $htr * p$ slg2,Mn2 hlans2 p_o	μ_i	p'_t	$p_{t_{act}}$	m=0.8792 c=0.0014 R=0.93 σ=0.0007 F=917.438	Case study 2 Plant 1
2	5.11	$p'_t = \mu_o + \mu_1 p_o + \sum_{i=2}^{n-1} \mu_i \cdot X_i$	svol,llife c_o, T_o O22, Mn2 T_{act} p_o	μ_i	p'_t	p_t	m=0.6823 c=0.0024 R=0.81 σ=0.001 F=574.0	Plant 3

Table 5.18 Summary of best results for manganese prediction for Plant 1 and Plant 3

S No	Model No	Model equation	Parameters used	parameters optimized	Statistics of regression (y=mx+c)			Remarks
					Dependent variable	Independent variable	Statistics	
1	5.14	$Mn'_t = \mu_o + \mu_1 Mn_o + \sum_{i=2}^{n-1} \mu_i \cdot X_i$	p_t, c_o O22, Mn_o hlans2 dolo2	μ_i	Mn'_t	$Mn_{t_{act}}$	m=0.9237 c=0.0115 R=0.96 σ=0.0065 F=1827.27	Case study 2 Plant 1
2	5.13	$Mn'_t = \mu_o + \mu_1 Mn_o + \sum_{i=2}^{n-1} \mu_i \cdot X_i$	raw dolo2 Mn_o O22 hlans2	μ_i	Mn'_t	Mn_t	m=0.6848 c=0.0456 R=0.83 σ=0.012 F=647	Plant3

5.6 Evaluation of capacity mass transfer coefficient (K')

Capacity mass transfer coefficienthas been assumed , as suggested in literature[13], to depend on gas flow rate as follows

$$K' = \alpha_1 \left(-\frac{dc}{dt}\beta_1 + Q_{eff} \right)^{\eta} \tag{5.15}$$

where η is exponential factor. In the present work value of K' has been determined by two methods by using GA-decarb models for Plant 1, Plant 2 and Plant 3. The results are discussed for each plant followed by comparison of all three plants.

5.6.1 Capacity Mass transfer coefficient for Plant 1

GA-decarb model (Method 1)

In this method η in eq. (5.15) is assumed to be constant through out the process. Fig. 5.41 shows the variation of mass transfer coefficient with time. From model 5.4 (method 1, Case Study 1) and model 5.4 (method 1, Case Study 2) it can be observed that while α_1 values are very close to each other, the η values are different in both cases (although they are from same Plant) as seen from Table 5.19. This is because the data in Case Study 1 has some heats in which ore2 has also been added during second blow as coolant. Hence, there is combined effect of ore2 and dolo2 in optimizing the η value in Case Study 1, but in Case Study 2 only dolo2 plays role. Because of this difference in η, there is difference in the K'values as observed from Fig. 5.41(a) and 5.41(b) and the values in Fig. 5.41 (a) are slightly lower than in Fig. 5.41(b) in first 100 seconds. This may be attributed to higher slag volume in the former case due to ore addition.

GA-decarb model (Method 2)

In this method η is made to vary as a function of gas flow rate as

$$\eta = \alpha_2 \left(-\frac{dc}{dt}\beta_1 + Q_{eff} \right)$$

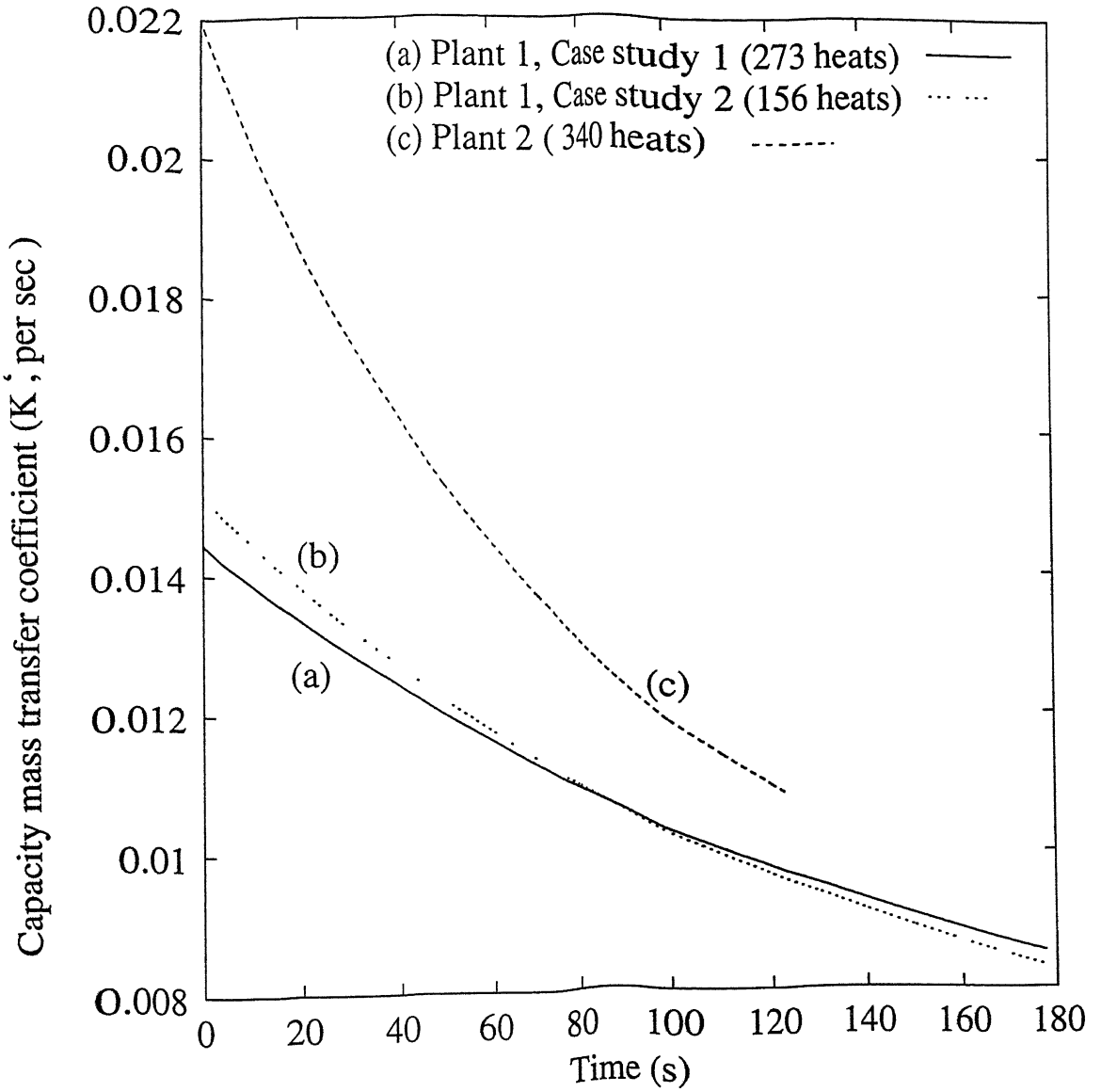

Graphs are drawn for heats with nearly same initial and final carbon values

(a) Co = 0.369 and Ct=0.044 (b) Co = 0.369 and Ct=0.044

(c) Co = 0.365 and Ct=0.043

Figure 5.41: Capacity mass transfer coefficient (K') vs time for method 1 of GA-decarb models.

Variation of η as a function of time is shown in Fig. 5.42. This graph is drawn for heat with c_o=0.369 and c_t=0.044. From Fig 5.42 (a) and 5.42 (b) it can be observed that the difference in η value between Case Study 1 and Case Study 2 is narrowing down towards the end of blow and the values in Case Study 1 are lower than in Case Study 2. Fig. 5.43 (a) shows the variation of mass transfer coefficient, K' with time. From Fig. 5.43(a) and (b) it can be observed that $K'$is almost the same for model 5.4 (method 2, Case Study 1) and model 5.4 (method 2, Case Study 2). It can also be observed that mass transfer coefficient decreases almost linearly with time but at a very slow rate. This is because gas evolution rate decreases with time.

5.6.2 Capacity Mass transfer coefficient for Plant 2

Method 1

Fig. 5.41 (c) shows the variation of mass transfer coefficient K' with time for model 5.4 (method 1) of Plant 2.

Method 2

Variation of η with time is shown in Fig. 5.42 (b) and Fig. 5.43 (c) shows the variation of mass transfer coefficient (K') with time. It can be observed that, similar to plant 1, K' almost linearly decreases with time.

5.6.3 Capacity Mass transfer coefficient for Plant 3

Since the results of method 1 were very poor, only method 2 is studied for variation of mass transfer coefficient. Variations of η and capacity mass transfer coefficient (K') for Plant 3 can be observed from Fig. 5.42 (c) and Fig. 5.43 (d), respectively. It can be seen that, similar to plants 1 and 2, K' almost linearly decreases with time.

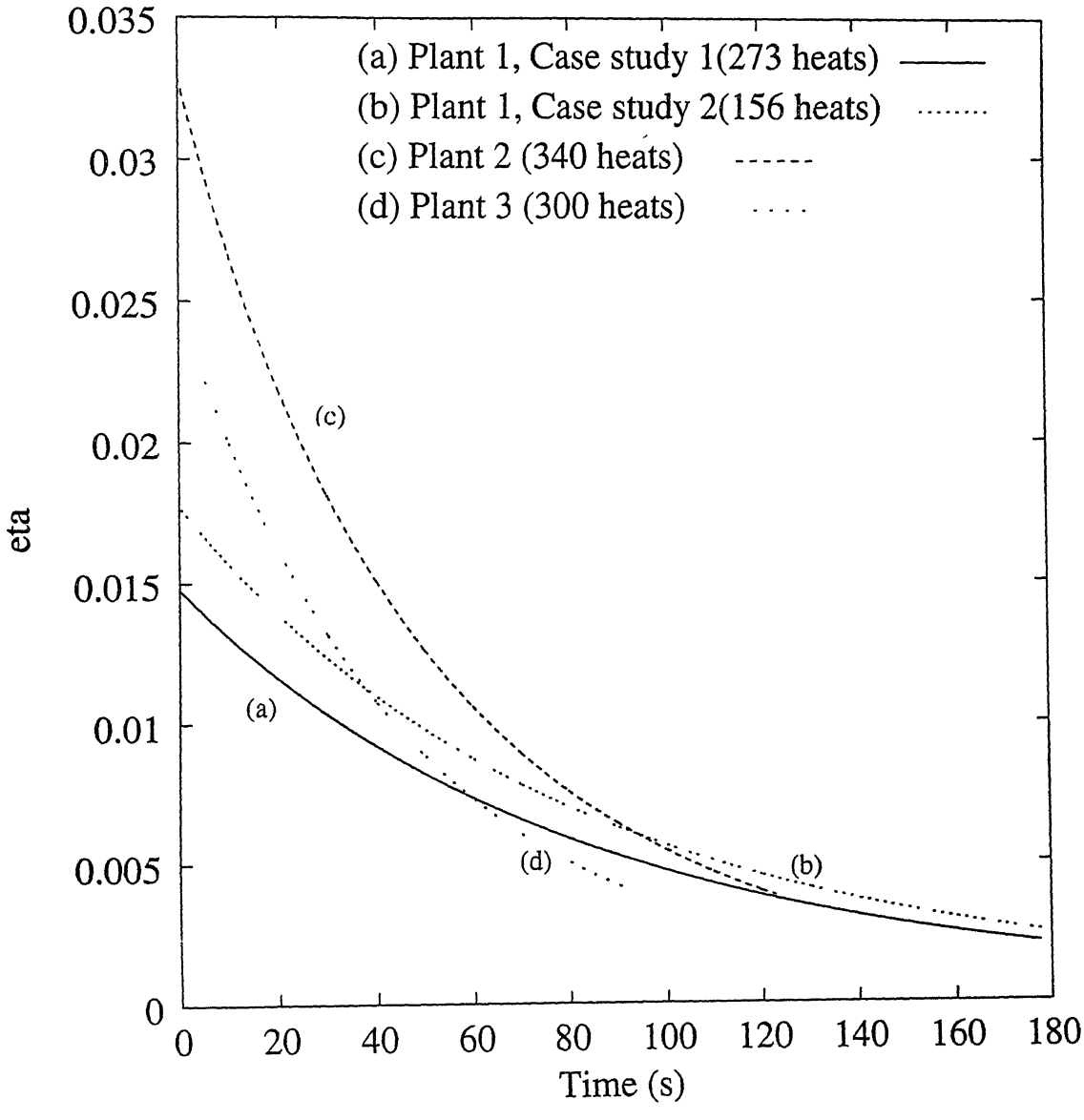

Graphs are drawn for heats with nearly same initial and final carbon vlaues

(a) Co=0.369 Ct=0.044 (b) Co=0.369 Ct=0.044

(c) Co=0.365 Ct=0.043 (d) Co=0.369 Ct=0.046

Figure 5.42: Variation of η with time for method 2 of GA-decarb models.

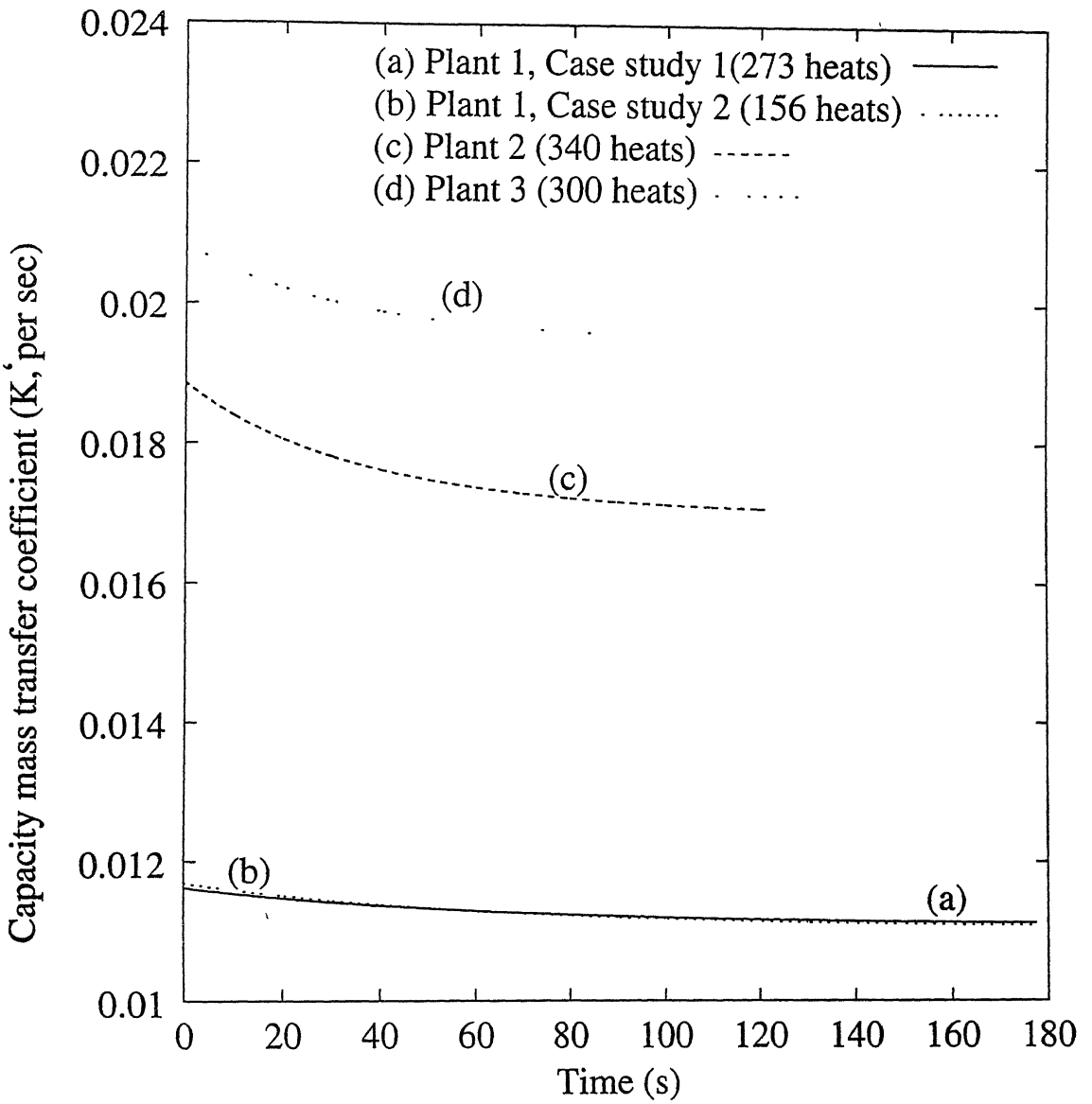

Graphs are drawn for heats with nearly same initial and final carbon values

(a) Co = 0.369 and Ct=0.044 (b) Co = 0.369 and Ct=0.044
(c) Co = 0.365 and Ct=0.043 (d) Co = 0.369 and Ct=0.046

Figure 5.43: Variation of capacity mass transfer coefficient, K' with time for method 2 of GA-decarb models.

5.6.4 Comparision of capacity mass transfer coefficients for Plant 1, Plant 2 and Plant 3

It can be observed from model 5.4 (method 1, Case Study 2) of Plant 1 and model 5.4 (method 1) of Plant 2 that α_1 and η values are larger in the latter model with 0.0084 and 0.291, respectively. Because of the larger values of α_1 and η, K' has greater magnitude as shown in Fig. 5.41(c). This indicates that agitation of bath is higher in case of Plant 2 (200 tn converter) than in Plant 1 (300 tn converter). This may be due to low lance height or less number of nozzles.

After about 100 s, η reaches to almost same value for Plant 1, Plant 2 and Plant 3 as shown in Fig. 5.42. The mass transfer coefficient in Fig. 5.43 (a) and (b) decreases very slowly with time. Hence, it can be concluded that lance height variation is properly adjusted in these cases. But in case of Fig. 5.43 (c) and (d), there is small amount of variation in K', indicating that lance height variation is not adjusted properly. This is specially true in the case of Plant 2 as in this case lance height is kept constant through out the blow. The values of K' and η at time t=40s are shown in Table 5.20.The higher value of $K'$for Plant 3 is because of larger values of α_1 and α_2 (Table 5.19) with 0.0195 and 0.0175, respectively. Hence, it is observed from Fig. 5.43 that K' increases from Plant 1 to Plant 3 (decreasing converter capacity). This indicates that in a 100 ton converter of Plant 3 bath is more agitated than in 200 ton converter of Plant 2 and 300 ton converter of Plant 1. This aspect is clear from Fig. 5.42. From this frigure it can also be observed that there is a sharp drop in η value in of Plant 2 and Plant 3 where as in Plant 1 the drop is more steady. This may be partially attributed to the changes in foaming nature of slag in the initial stages. After about 120 s, η attains nearly the same value in Plant 1, Plant 2 and Plant 3 (Fig. 5.42). From Fig. 5.43, the value of K' is highest in the smallest converter (100 t) and smallest in 300 t converter.

Table 5.19: Comparison of parameters in capacity mass trasfer coefficient

Method	Parameter	Plant 1		Plant 2	Plant 3
		Case study 1	Case study 2		
1	η	0.2267	0.2477	0.2524	-
	α_1	0.00677	0.0065	0.009	-
2	α_1	0.00677	0.0065	0.017	0.0195
	α_2	0.00063	0.00075	0.0014	0.00175

Table 5.20: Capacity mass transfer coefficient (K')and η at time t=40s.

Parameter	Plant 1		Plant 2	Plant 3
	Case Study 1	Case Study 2		
η	0.0092	0.011	0.015	0.011
K'	0.01136	0.01138	0.0176	0.0198

Chapter 6

Conclusions and Suggestions for Further work

6.1 Conclusions

1. Models are developed for prediction of end point carbon, temperature, phosphorus, manganese and dissolved oxygen for three plants Plant 1, Plant 2 and Plant 3. Best models for end point carbon prediction are as summarized below and corresponding results are shown in appendix 2, appendix 3 and appendix 4

Plant	Model No	Model equation	Parameters used	Statistics	Remarks
1	5.3 (reg)	$c_t' = \mu_o + \mu_1 c_t + \sum_{i=2}^{n-1} \mu_i \cdot X_i$	Ore1 O22 hlans2 dolo1 c_O	m=0.5796 c=0.0245 R=0.76 (0.7617) σ=0.004 (0.0041) F=212.882	Case study 2 appendix 2

Plant	Model No	Model equation	Parameters used	Statistics	Remarks
2	5.3 (reg)	$c'_t = \mu_o + \mu_1 c_t + \sum_{i=2}^{n-1} \mu_i \cdot X_i$	$O22^2$,c_o^2 $O22 * c_o$ T_o,flux O22,c_o	m=0.5498 c=0.0185 R=0.74 (0.7414) σ=0.005 (0.0055) F=389.423	appendix 3
3	5.4 (reg, met-hod 2)	$c'_t = \mu_o + \mu_1 c_t + \sum_{i=2}^{n-1} \mu_i \cdot X_i$	basicity T_o,O22	m= 0.1929 c= 0.0410 R= 0.44 (0.4374) σ=0.004 (0.0038) F=70.494	appendix 4

Best models for temperature prediction are as summarized below

Plant	Model No	Model equation	Parameters used	Statistics	Remarks
1	5.6	$T = \mu_o + \sum_{i=1}^{n-1} \mu_i \cdot X_i$	hot ratio O22,T_o dolo2 slag2	m=0.8146 c=307.76 R=0.90 (0.9027) σ=5 F=677.6145	Case study 2 appendix 2

Plant	Model No	Model equation	Parameters used	Statistics	Remarks
2	5.6	$T = \mu_o + \sum_{i=1}^{n-1} \mu_i \cdot X_i$	O22 T_o c_o flux	m=0.5269 c=786.211 R=0.72 (0.7241) σ=8 F=372.546	appendix 3
3	5.6	$T = \mu_o + \sum_{i=1}^{n-1} \mu_i \cdot X_i$	O22 T_o raw dolo2 hlans2	m=0.5351 c=785.333 R=0.73 (0.7310) σ=9 F=342.074	appendix 4

Best models for phosphorus prediction are as summarized below

Plant	Model No	Model equation	Parameters used	Statistics	Remarks
1	5.11	$p'_t = \mu_o + \mu_1 p_o + \sum_{i=2}^{n-1} \mu_i \cdot X_i$	svol,T_{act} $htr * p$ slg2,Mn2 hlans2 p_o	m=0.8792 c=0.0014 R=0.93 (0.9253) σ=0.0007 F=917.438	Case study 2 appendix 2
3	5.11	$p'_t = \mu_o + \mu_1 p_o + \sum_{i=2}^{n-1} \mu_i \cdot X_i$	svol,llife c_o, T_o O22, Mn2 T_{act} p_o	m=0.6823 c=0.0024 R=0.81 (0.8113) σ=0.001 F=574.0	appendix 3

Best models for manganese prediction are as summarized below

Plant	Model No	Model equation	Parameters used	Statistics	Remarks
1	5.14	$Mn'_t = \mu_o + \mu_1 Mn_O + \sum_{i=2}^{n-1} \mu_i \cdot X_i$	p_t, c_o O22, Mn_o hlans2 dolo2	m=0.9237 c=0.0115 R=0.96 (0.9603) σ=0.0065 F=1827.27	Case study 2 appendix 2
3	5.13	$Mn'_t = \mu_o + \mu_1 Mn_o + \sum_{i=2}^{n-1} \mu_i \cdot X_i$	raw dolo2 Mn_o O22 hlans2	m=0.6848 c=0.0456 R=0.83 (0.8274) σ=0.012 F=647	appendix 3

Best models for dissolved oxygen prediction are as summarized below

Plant	Model No	Model equation	Parameters used	Statistics	Remarks
1	5.8	$[O] = \mu_o + \sum_{i=1}^{n-1} \mu_i \cdot X_i$	Basicity O22, c_o T_o, dolo2 hlans2	m=0.761 c=101.255 R=0.87 (0.8724) σ=34 F=490.34061	Case study 2 appendix 2

Plant	Model No	Model equation	Parameters used	Statistics	Remarks
2	5.8	$[O] = \mu_o +$ $\sum_{i=1}^{n-1} \mu_i \cdot X_i$	T_{act} T_o c_o O22	m=0.6695 c=296.0932 R=0.82 (0.8182) σ=140 F=684.434	appendix 3
3	5.8	$[O] = \mu_o +$ $\sum_{i=1}^{n-1} \mu_i \cdot X_i$	basicity T_o raw dolo2 llife T_{act}	m=0.3571 c=387.1967 R=0.60 (0.5978) σ=77 F=165.1967	appendix 4

2. If the data for phosphorus and manganese are available at sublance point then the best model for prediction of end point carbon is model 5.3 (a) (reg) given by

$$c_t' = -8.219 * 10^{-7} * ore1 + 1.869 * 10^{-4} * T_o + 114.642 * 10^{-3} * c_o$$
$$84.317 * 10^{-3} * Mn_o - 1.01 * p_o - 2.498 * 10^{-5} * O22 - 0.2346$$

with R=0.82, σ =0.004%, F=308.958. This emphasises the point that during second blow carbon, manganese and phosphorus are simultaniosly removed and hence the variables phosphorus and manganese affect oxygen distribution significantly which, in turn, affects the kinetics of oxidation of carbon as well.

3. It is concluded from GA-decarb models that capacity mass transfer coefficient depends on stirring energy and the value of η decreases as a function of time in the range 0.005 to 0.032. However, by properly adjusting lance height, mass transfer can be controlled such that the variation is reduced and becomes nearly constant.

4. Capacity mass transfer coefficient ranges from 0.0116408- 0.0110834 for Plant 1,

0.0188207 - 0.0170647 for Plant 2 and 0.0208267-0.0195667 (1/s)for Plant 3. The capacity mass transfer coefficient is highest for the smallest converter Plant 3 and least for largest converter Plant 1.

6. It can be observed from GA-decarb models that capacity mass transfer coefficient decreases with time very slowly as shown in method 2, indicating that bath agitation is somewhat steady. More over GA-decarb models did not take into account the oxygen consumed for phosphorus and manganese removal. Hence, linear models are performing better.

6.2 Suggestions for further work

1. The effect of lance height variation can be studied by incorporating the variation of effective gas flow rate (Q_{eff}) and this effect can be included in GA-decarb models.
2. A dynamic model can be made if waste gas analysis is available as a function of time.
3. These models can be further tuned by using artificial intelligence techniques such as neural nets and fuzzy logic.
4. The effect of lance nozzle design and blowing patterns for same converter need to be studied.
5. Effect of droplet decarburization on slag foaming and post combustion can be incorporated.
6. The dynamic effects of coolants added during the blow can be incorporated.
7. A window based control model can be developed.
8. Effects of heat loss and lining life and wear pattern can be incorporated by time series analysis, if data for sequential heats is available.

Appendix 1

Specific stirring energy E^{o}_{b} (W/m^3) can be calculated from the expression given below.

$$E_b^o = \left(\frac{Q_b T_l}{V}\right)\left\{\ln\left(1+\frac{\rho g h}{P}\right)+\left(1-\left(T_m/T_l\right)\right)\right\} \quad \text{.....(1)}$$

Where,

Q_b = gas flow rate = 3 m^3/min,
T_l = temperature of liquid metal
ρ = density of metal = 7000 kg /m^3,
V = volume of liquid metal = (300 . 1000) / 7000 = 42.86 m^3
G = acceleration due to gravity = 9.81 m/s^2,
H = bath depth = 1.8 m,
P = ambient pressure = 1.0135 x 10^5 Pa,
T_m = temperature of gas = 298 °K.

Upon inserting the values of different parameters in Eq.(1) we get,

$$E_b^o = \left(\frac{6.18x3x1873}{42.86}\right)\left[\ln\left\{1+\left(\frac{7000x9.81x1.80}{1.0135x10^5}\right)\right\}+\left(1-\frac{298}{1873}\right)\right]$$

= 884.87W /m^3.

Discussion:- It is assumed in the above calculation that bath depth does not change during bottom stirring owing to finite residence time of gas bubbles in liquid metal .Actually bath depth (or height) increases or bath level rises due to gas bubbles in metal (see Example 4).Further , according to Eq.(1) the specific stirring energy is directly proportional to gas flow rate Q_b.It also increases with bath height though not in direct proportion ,for example if the bath height is decreased to 1.42 m then corresponding stirring energy decreases to 818.27 W/m^3 only.

The total flow rate of oxygen is given by :-
= 976.53 m^3/ min,

Now the expression for specific energy received by metal from top of jet is ,

$$E^{o}_{t} = [\ 6.32 \times 10^{-7} . \cos \Phi . \ Q^{3}_{t} \ \ M\ ] \ / \ V n^{2} dt LH \qquad .....(2)$$

Where,

$\Phi = 14^{o}$, $Q_t = 976.53\ m^3/min$, M = 32, V = 42.86 m^3/min, n = 5 ,dt = 0.0466 m, lance height LH is 2 m,

Substituting these values in to Eq(2),

$E^{o}_{t} = 84265.16$ Watts /m^3.

Since only 10 % of the energy of jet is absorbed by bath the effective energy received is 8426.52 W/m^3.

Discussion:- Specific stirring energy received from top jet ,varies inversely with lance height and square of number of nozzles; thus four hole lance will deliver approximately 1.56 times more energy than a five hole lance. Due to this reason , to properly utilize the jet energy, lance height is decreased as number of nozzles increase. Further as the number of nozzles increases the chances of jet interference increases. To avoid this nozzle angle (Φ) is increased as the number of nozzles increases. Thus, nozzle design and blowing regime are inter-dependent.

$$(K_c) = 8.9 \times 10^{-4} \ (Q_{eff})^{0.3}$$

where total stirring energy is

$$Q_{eff} = 1227.4 + 8552.54 \text{ watts/m}^3$$

$$(K_c) = 8.9 \times 10^{-4} \times (9779.94)^{0.3}$$

$$= 0.014$$

Where $K_c = 0.014\ m^3/s$ (volumetric mass transfer coefficient) ,

Appendix 2

Input data for regression models of Plant 1

Heat no.	Svol	Htr*p0	Basicity	Hot ratio	Llife	Orel	Slag1	Dolo1	T1	C1	Mn1	P1	O22	Slag2	Dolo2	Hlans2
M9170	21850.768	0.287	3 746	4 563	86	5864	4021	0	1599	0.369	0 337	0.022	2220	0	1	192
M9172	18818 600	0.316	4.384	5 185	88	5407	3149	0	1600	0 464	0 315	0 027	2253	0	496	191
M9175	18249 875	0.246	4 531	4 107	90	5979	3124	0	1587	0 381	0 313	0 015	2022	0	331	189
M9177	17943.504	0.287	4 749	4 783	91	5445	3046	0	1596	0 390	0 334	0 021	2152	0	1281	184
M9181	16569 447	0.267	5 043	4.533	93	6233	2849	0	1578	0 449	0.314	0.020	2324	0	1188	188
M9182	15853 072	0.256	5 254	4 569	176	5710	2719	0	1618	0.235	0 304	0 020	1744	0	1027	216
M9184	17041 258	0.321	5 322	5 437	177	5008	3404	0	1612	0 470	0 352	0 030	2262	0	2805	211
M9187	18895.980	0.257	4.661	4 435	96	5384	3640	0	1584	0 457	0.327	0.019	2434	0	1506	193
M9189	16649 943	0.365	5.505	6 086	97	4529	2906	0	1610	0 455	0.351	0 025	2233	0	1190	189
M9190	17119.346	0 301	5 220	4.939	98	4960	2972	0	1557	0 537	0 310	0 012	2960	0	991	192
M9193	17575.758	0.283	4 876	4 568	99	7270	3000	0	1536	0 481	0.286	0.013	2720	0	238	191
M9195	22300.977	0.308	5 364	4 805	100	178	4446	994	1611	0 338	0 287	0 018	2310	0	737	194
M9198	17678 311	0.285	5.358	5 005	184	5045	3121	1002	1616	0 252	0 272	0 014	1583	0	531	209
M9199	17099 869	0.358	4 778	5 970	185	6986	2934	0	1607	0 304	0 298	0.018	1961	0	874	210
M9201	18163.229	0.326	4 436	5.178	186	5515	3115	0	1594	0 451	0.313	0.020	2088	0	633	208
M9203	18444.051	0.288	4.588	4 571	187	6812	3507	0	1596	0 391	0 306	0 015	2237	0	397	205
M9211	17044.051	0.292	4.788	4 942	191	5187	2891	0	1595	0.515	0.332	0 025	1995	139	778	208
M9219	17121.760	0.363	5 857	6 054	113	5224	2983	794	1620	0.376	0 335	0 029	2226	0	1409	181
M9220	17794 232	0.351	4 672	5 850	114	5247	3051	0	1616	0.486	0 326	0.030	2221	0	1163	185
M9221	16934.480	0.398	4.912	6.626	115	6131	2910	379	1614	0 470	0 331	0 031	2139	0	501	185
M9223	18860 088	0.316	4 664	5 182	117	5149	3172	393	1617	0.377	0.379	0 027	2081	0	500	188
M9224	18407.152	0.357	4.996	5 577	118	4483	3138	513	1620	0.399	0 367	0.026	2149	0	1098	186
M9229	18969 029	0.314	4.341	5 061	126	4940	3630	0	1597	0.308	0.299	0 021	2036	0	524	203
M9230	18932.014	0.366	4.253	5.903	122	7980	3126	0	1597	0.404	0.309	0.021	2270	0	1308	180
M9232	17560.676	0.336	4 620	5 689	123	8484	3022	375	1600	0.292	0 276	0.018	1925	0	1595	183
M9234	20911.473	0.268	3.777	4 326	124	5094	3448	0	1582	0 480	0 325	0 024	2227	0	1001	181
M9235	20754.508	0.280	3.736	4.446	125	5499	3415	0	1573	0 478	0.281	0 023	2275	0	1102	183
M9240	21144.637	0.267	3.873	4.532	131	5606	3900	0	1602	0.338	0.294	0.024	2119	0	1792	204
M9241	15024.931	0.339	5.177	5 551	128	3680	2635	0	1595	0.504	0.349	0 028	2192	0	244	186
M9262	21653.660	0.326	4.047	5.350	138	5184	3597	0	1610	0 384	0.329	0.018	2059	0	670	179
M9263	18781.199	0.309	4.325	5.066	143	4639	3214	0	1612	0.354	0.326	0 022	1771	999	1503	220
M9265	18205.326	0.278	4.624	4.720	144	6927	2176	0	1586	0 382	0.302	0.018	1892	2921	274	222
M9266	19377.572	0 301	4.652	5.186	140	4573	3763	0	1622	0 392	0 324	0 019	2014	0	497	186
M9272	18781.355	0.302	4.794	5.292	143	5004	3309	0	1605	0.470	0.329	0.019	2254	0	911	185
M9274	21137.574	0.331	4.137	5.615	144	5294	3941	0	1601	0 472	0 325	0 020	2419	0	371	185
M9278	18968.777	0.324	4.350	5 682	146	5936	3203	0	1607	0 504	0.330	0 019	2308	0	1217	190
M9279	18180 805	0.279	4.943	4.502	151	5054	3076	0	1546	0.712	0.315	0 011	2894	0	1004	213
M9288	15052.380	0.383	5.419	6 384	151	6520	2584	0	1596	0 442	0 323	0.024	2288	0	104	184
M9289	17932.418	0.297	4.499	4.948	156	4871	3023	0	1602	0.388	0.324	0 020	1987	0	656	219
M9290	16614.670	0.312	4 771	5 113	152	3212	2864	0	1609	0.440	0 320	0.025	2399	0	1278	192
M9294	14800.970	0 313	7 903	5 790	154	2752	2701	586	1612	0 442	0 327	0.030	2435	0	1944	188
M9296	14759.924	0.440	5 253	7 591	155	5431	3361	0	1585	0 522	0 333	0 023	2492	0	1269	185
M9300	17205.801	0.333	5.293	5.737	157	2785	5942	0	1623	0 407	0 349	0 030	2145	0	1295	192
M9305	18078.969	0.268	4.481	4 470	159	5944	3063	313	1607	0.470	0 348	0.026	2576	0	1146	187
M9315	16742.785	0.317	4.896	5 201	164	5477	2860	0	1603	0 427	0.318	0 022	2517	0	992	190
M9319	17208.471	0.292	5.443	5 210	166	3994	2980	413	1607	0 517	0 326	0.027	2464	1508	1501	187
M9322	17519.359	0.427	5.972	6 892	173	3322	0	2499	1643	0 361	0.257	0 025	2285	2193	1506	213
M9326	16437.508	0.350	6 704	5 741	175	3386	2996	992	1612	0 274	0.269	0.018	2004	0	707	210
M9331	18113.139	0.293	4 308	4.891	172	5818	3058	0	1584	0 451	0 315	0.022	2433	0	899	175
M9333	17910.824	0.302	4.364	4.955	173	6226	3004	322	1600	0.418	0 308	0 024	2338	0	1802	174
M9334	16327 057	0.314	4 893	5 707	179	4345	3388	368	1622	0 351	0 309	0 025	1699	0	610	211
M9335	15654 943	0.296	5.354	5.187	174	3949	2706	0	1592	0 425	0 324	0 023	2230	0	1197	179
M9336	17645.502	0.298	4.434	4.962	180	5238	2968	329	1619	0.343	0.326	0 024	1690	0	1294	217

Actual and Predicted end point parameters of Plant 1

Heat No.	Carbon (%)		Temperature (°C)		[O] (ppm)		Phosphorus (%)		Manganese (%)	
	Actual	Predicted	Actual	Predicted	Actual	Predicted	Actual	Predicted	Actual	Predicted
M9170	0.044	0.053	1675	1671.192	469	464.483	0.008	0.008	0.168	0.177
M9172	0.060	0.060	1668	1668.962	398	389.678	0.011	0.010	0.187	0.186
M9175	0.062	0.058	1654	1650.150	416	418.607	0.007	0.008	0.170	0.167
M9177	0.059	0.056	1653	1653.216	407	444.488	0.007	0.008	0.162	0.161
M9181	0.057	0.057	1643	1644.938	426	434.283	0.007	0.007	0.153	0.153
M9182	0.064	0.054	1651	1659.453	395	433.904	0.009	0.009	0.179	0.166
M9184	0.061	0.062	1646	1655.286	365	379.421	0.008	0.009	0.161	0.165
M9187	0.063	0.056	1644	1650.234	401	434.269	0.008	0.007	0.167	0.157
M9189	0.073	0.061	1664	1670.666	331	397.336	0.010	0.011	0.205	0.188
M9190	0.063	0.051	1643	1652.554	403	497.942	0.006	0.007	0.153	0.133
M9193	0.049	0.050	1632	1634.147	509	503.476	0.005	0.005	0.136	0.130
M9195	0.046	0.050	1679	1676.892	505	533.373	0.006	0.007	0.146	0.132
M9198	0.061	0.057	1651	1658.095	359	386.272	0.007	0.007	0.164	0.155
M9199	0.058	0.054	1650	1661.818	381	422.270	0.008	0.008	0.171	0.157
M9201	0.074	0.064	1652	1656.783	306	342.008	0.009	0.009	0.192	0.181
M9203	0.062	0.055	1654	1665.153	383	408.824	0.008	0.008	0.173	0.163
M9211	0.072	0.072	1653	1651.730	321	284.432	0.010	0.010	0.205	0.203
M9219	0.046	0.051	1684	1676.325	415	519.860	0.011	0.011	0.173	0.175
M9220	0.055	0.063	1677	1675.107	415	383.748	0.011	0.011	0.187	0.186
M9221	0.060	0.062	1683	1678.806	440	387.043	0.012	0.012	0.196	0.202
M9223	0.059	0.056	1681	1676.943	434	440.438	0.010	0.012	0.209	0.204
M9224	0.054	0.056	1677	1676.139	401	439.250	0.010	0.011	0.199	0.192
M9229	0.057	0.053	1657	1658.403	444	464.200	0.009	0.008	0.174	0.163
M9230	0.053	0.052	1655	1659.685	437	448.569	0.008	0.008	0.155	0.151
M9232	0.047	0.050	1650	1646.735	532	489.843	0.007	0.007	0.132	0.132
M9234	0.058	0.062	1643	1646.486	382	360.905	0.007	0.008	0.165	0.166
M9235	0.053	0.060	1639	1639.860	408	385.386	0.007	0.007	0.146	0.145
M9240	0.055	0.054	1652	1651.234	470	465.806	0.006	0.006	0.136	0.132
M9241	0.059	0.066	1669	1665.941	354	366.185	0.012	0.013	0.219	0.214
M9262	0.066	0.057	1672	1668.873	416	425.622	0.008	0.009	0.184	0.173
M9263	0.069	0.065	1645	1646.046	306	337.758	0.007	0.008	0.178	0.172
M9265	0.062	0.063	1633	1631.210	325	316.994	0.006	0.006	0.169	0.168
M9266	0.068	0.060	1664	1678.769	326	347.834	0.009	0.009	0.192	0.181
M9272	0.071	0.061	1671	1668.930	364	405.627	0.009	0.009	0.184	0.177
M9274	0.065	0.057	1685	1677.599	460	452.813	0.010	0.009	0.175	0.180
M9278	0.064	0.062	1669	1669.876	401	375.763	0.009	0.009	0.182	0.176
M9279	0.074	0.069	1630	1640.321	318	312.426	0.006	0.006	0.162	0.159
M9288	0.052	0.056	1685	1672.937	473	481.597	0.011	0.011	0.180	0.189
M9289	0.056	0.062	1659	1659.248	420	379.664	0.008	0.008	0.174	0.180
M9290	0.063	0.057	1675	1673.152	483	465.310	0.010	0.009	0.161	0.166
M9294	0.049	0.055	1677	1670.967	540	537.282	0.010	0.010	0.160	0.160
M9296	0.063	0.059	1668	1660.661	403	462.929	0.010	0.010	0.168	0.176
M9300	0.055	0.060	1680	1676.661	488	442.303	0.011	0.011	0.177	0.190
M9305	0.048	0.052	1676	1678.043	521	465.290	0.009	0.009	0.166	0.170
M9315	0.051	0.051	1682	1675.474	535	523.921	0.009	0.009	0.154	0.157
M9319	0.050	0.060	1662	1663.757	413	390.259	0.008	0.009	0.174	0.161

Appendix 3

Input data, Actual and Predicted end point parameters of Plant 2

Heat no.	$O22^2$	C^2_o	$O22*C_o$	O22	C_o	T1	Flux	Carbon (%)		Temperature (°C)		[O] (ppm)	
								Actual	Predicted	Actual	Predicted	Actual	Predicted
928262	4524129	0.202	957.150	2127	0.450	1534	12450	0.029	0.031	1670	1648	1432	1365
915062	1505529	0.023	185.277	1227	0.151	1589	12620	0.026	0.031	1679	1654	1517	1300
915063	2660161	0.052	371.868	1631	0.228	1553	12110	0.027	0.029	1662	1644	1401	1386
928270	2893401	0.047	369.117	1701	0.217	1566	14960	0.026	0.028	1660	1651	1457	1308
928271	3161284	0.094	545.846	1778	0.307	1564	14160	0.026	0.030	1673	1653	1508	1315
915074	1106704	0.042	216.712	1052	0.206	1605	10490	0.030	0.039	1667	1662	1200	954
915075	1784896	0.109	440.880	1336	0.330	1583	7000	0.040	0.043	1668	1661	878	996
928275	2951524	0.347	1011.90	1718	0.589	1593	9500	0.040	0.048	1686	1677	892	771
915078	4223025	0.192	900.090	2055	0.438	1548	13420	0.025	0.031	1680	1653	1330	1354
915079	3474496	0.038	363.480	1864	0.195	1561	13540	0.028	0.030	1661	1653	1333	1425
915081	1164241	0.102	344.201	1079	0.319	1601	10520	0.053	0.046	1664	1662	635	789
928279	2617924	0.429	1059.79	1618	0.655	1595	6910	0.071	0.058	1682	1680	413	597
915082	1868689	0.225	647.958	1367	0.474	1602	8670	0.065	0.051	1669	1674	480	653
928282	3024121	0.202	782.550	1739	0.450	1573	11040	0.029	0.038	1674	1663	1233	1029
915087	2768896	0.094	510.848	1664	0.307	1567	10200	0.032	0.034	1649	1656	1130	1057
928285	2418025	0.262	796.160	1555	0.512	1563	9500	0.044	0.046	1657	1655	794	814
915089	1923769	0.094	425 809	1387	0.307	1584	8350	0.033	0.039	1680	1662	1079	1141
915093	2924100	0.030	295.830	1710	0.173	1545	11630	0.035	0.029	1629	1641	1004	1258
915094	2292196	0.094	464.798	1514	0.307	1557	13180	0.030	0.032	1648	1644	1185	1085
915096	1560001	0.088	369.704	1249	0.296	1575	11480	0.042	0.038	1648	1650	838	911
928296	2013561	0.030	245.487	1419	0.173	1570	7430	0.032	0.033	1653	1653	1135	1220
928297	2876416	0.026	274.752	1696	0.162	1555	8570	0.029	0.032	1639	1650	1232	1287
928298	1382976	0.042	242.256	1176	0.206	1584	10120	0.035	0.036	1663	1654	1026	1099
928300	1962801	0.161	561.801	1401	0.401	1570	7940	0.049	0.044	1656	1655	705	890
915104	1887876	0.151	534.486	1374	0.389	1585	10740	0.037	0.042	1658	1661	972	812
928304	790321	0.068	232.029	889	0.261	1611	9500	0.049	0.049	1666	1664	692	779
915105	3659569	0.213	883.806	1913	0.462	1544	8410	0.035	0.036	1641	1653	1017	972
915106	1392400	0.062	295.000	1180	0.250	1594	10910	0.030	0.038	1680	1659	1190	1109
928309	783225	0.088	261.960	885	0.296	1619	7180	0.061	0.054	1668	1671	525	685
915109	1695204	0.042	268.212	1302	0.206	1585	8500	0.032	0.035	1664	1659	1108	1130
915110	1464100	0.042	249.260	1210	0.206	1589	9560	0.037	0.036	1666	1658	966	1097
915112	2528100	0.249	793.410	1590	0.499	1584	11110	0.042	0.044	1685	1666	837	936
915114	4186116	0.429	1340.13	2046	0.655	1531	7810	0.051	0.041	1634	1651	672	737
915117	5494336	0.034	431.296	2344	0.184	1527	12600	0.031	0.038	1618	1645	1147	1423
928317	2076481	0.109	475.530	1441	0.330	1572	10990	0.042	0.037	1648	1654	838	925
928318	2745649	0.088	490.472	1657	0.296	1595	11320	0.030	0.035	1677	1671	1195	1116
928319	3017169	0.030	300.501	1737	0.173	1554	12790	0.029	0.029	1644	1646	1247	1331
928320	1243225	0.094	342.305	1115	0.307	1623	8940	0.040	0.047	1679	1677	881	789
928321	2808976	0.081	475.984	1676	0.284	1558	7570	0.029	0.035	1651	1654	1265	1178
915125	1221025	0.094	339.235	1105	0.307	1598	9920	0.062	0.045	1648	1662	509	695
915126	3767481	0.394	1218.94	1941	0.628	1542	7810	0.034	0 043	1651	1655	1042	824
915131	2452356	0.213	723.492	1566	0.462	1576	11990	0.043	0.041	1656	1660	810	792
928334	2729104	0.125	584.808	1652	0.354	1572	13260	0.047	0.033	1650	1657	741	955
915135	2259009	0.142	566.631	1503	0.377	1579	7120	0.040	0.042	1670	1663	892	1009
915138	3359889	0.171	757.029	1833	0.413	1554	8420	0.027	0.036	1678	1656	1346	1280
915139	1758276	0.088	392.496	1326	0.296	1590	11330	0.034	0.038	1662	1661	1061	944
928345	4397409	0.523	1516.13	2097	0.723	1546	9810	0.046	0.043	1641	1660	750	598

Appendix 4

Input data for regression models of Plant3

eat No	Svol	Llife	T1	C1	P1	O22	Basicity	Raw dolo2	Mn1	Hlans2	C2(model 5 4 method 2)
1	3030 774	203	1638	0 433	0 020	580	7588 181	0	0 270	159	0 050
2	2580 609	217	1639	0 263	0 014	430	8081 661	0	0 250	163	0 053
3	2900 755	218	1655	0 253	0 018	450	7485 427	0	0 230	165	0 047
4	2500 608	219	1634	0.460	0.019	750	7798 069	520	0 280	165	0 028
5	2990 606	220	1660	0 249	0.017	370	9612.305	0	0 210	166	0 063
6	3160 753	221	1640	0 233	0 014	430	8101 852	0	0 230	163	0 047
7	2530.712	224	1619	0 418	0 019	560	6933 333	0	0 220	159	0 052
8	3171 053	225	1637	0.355	0 018	510	5790 616	0	0 220	158	0 053
9	3100 857	227	1618	0 550	0 021	660	6990 081	0	0.180	159	0 046
10	2790 886	232	1610	0.357	0 023	670	6137 085	0	0 220	169	0 029
11	3670 993	241	1603	0 416	0 016	560	7167 253	0	0 170	161	0 051
12	2871 444	6	1629	0 549	0 018	740	3850 853	650	0.190	159	0 034
13	3631.546	22	1639	0 419	0 023	650	4579 349	390	0 190	172	0 037
14	3711 411	24	1554	0 478	0 020	1600	5074 187	270	0 190	159	0.001
15	2340 585	26	1626	0 380	0 023	470	7675 214	0	0 270	161	0 066
16	2640 654	37	1618	0 242	0 016	620	7811.408	0	0 180	159	0 024
17	2150 418	50	1623	1 009	0 020	680	9772.999	620	0 210	161	0 075
18	3600.482	53	1625	0.308	0 018	490	14601 481	0	0.160	149	0 050
19	2110 524	54	1617	0.476	0.018	700	7733 225	600	0 260	161	0 035
20	3611 050	60	1608	0.408	0.014	650	6727.380	0	0 170	161	0 036
21	3030 847	61	1614	0 360	0 014	590	6944 022	0	0 180	159	0 040
22	2600 623	68	1630	0 251	0.016	370	7700 771	0	0 250	169	0 063
23	2020 475	73	1606	0.535	0.023	700	8173 829	360	0 210	161	0 039
24	2160 366	74	1633	0 373	0.021	520	11189 083	0	0 170	161	0 054
25	1900 429	76	1618	0.452	0 022	630	8353 333	410	0 200	161	0.043
26	2190 580	78	1626	0 352	0 020	490	7116.920	390	0 240	161	0 057
27	1860 666	79	1662	0 236	0 017	330	5358 119	300	0.230	159	0 069
28	1870 664	80	1630	0 283	0 015	450	5374.193	0	0 180	159	0 053
29	3690.677	81	1654	1 332	0 025	580	10537.635	620	0.190	159	0 139
30	3040 746	82	1624	0 292	0 013	420	8430 099	0	0 210	161	0 061
31	2560.616	86	1638	0.360	0.016	500	8062 198	500	0 230	159	0 056
32	2790.740	89	1666	0 328	0.016	530	7359 182	0	0.240	162	0 046
33	3030 760	112	1607	0.572	0.018	780	7666 010	610	0 220	159	0.031
34	1860 612	125	1649	0.436	0 014	730	5796 442	610	0 190	160	0.029
35	2960 642	126	1646	0.338	0 015	470	8972 861	390	0.200	161	0 058
36	3380 712	144	1625	0.264	0 013	450	9199 068	0	0 190	159	0 050
37	3650 957	173	1609	0 298	0 009	710	7405 517	650	0 120	159	0 021
38	3130 788	177	1648	0 480	0 017	870	7744.615	0	0 200	159	0 019
39	3651 101	211	1614	0 481	0 015	660	6451 571	660	0 170	162	0 041
40	2830.710	212	1615	0 600	0 015	810	7721 417	490	0.180	161	0.029
41	3210.794	217	1623	0.403	0 011	560	7755 954	610	0 160	159	0 050
42	3130 606	219	1608	0 492	0.009	700	10002 829	300	0.150	159	0 036
43	3140 808	222	1614	0.355	0.013	640	7522.093	260	0.160	159	0.033
44	3070 791	245	1598	0 597	0.021	760	7474.660	480	0 160	164	0 035
45	3270 874	246	1644	0 415	0.017	590	7285 948	490	0 170	160	0 046
46	2880.754	247	1608	0 296	0.009	530	7386.568	0	0.130	163	0.041
47	2190.508	248	1630	0 372	0.012	540	8245.828	880	0 150	161	0.050
48	3640.966	249	1604	0.496	0.015	660	7325 942	390	0 160	161	0 042
49	3681 071	250	1603	0 365	0.012	760	6647 993	640	0 130	152	0.022
50	2590 455	251	1633	0 249	0 011	560	10825 083	0	0 120	161	0 031
51	3631 201	3	1667	0.290	0 016	440	5902.852	440	0.220	159	0 056
52	3380 885	5	1617	0 462	0.014	660	7426 066	400	0.180	159	0 039
53	3631.109	7	1620	0 385	0 013	610	6382.691	350	0.160	159	0 040
54	2610 656	51	1655	0.456	0.022	540	7619.296	0	0 220	159	0.061
55	2840.732	59	1637	0 354	0 013	440	7570.300	0	0.170	161	0.069
56	3691.558	124	1566	0.238	0.010	1270	4569.123	0	0.150	159	0.002
57	3671 297	128	1682	0 191	0.022	400	5480 403	660	0.260	159	0.043
58	3693 073	131	1581	0.637	0.020	840	2319.993	0	0.120	155	0 027
59	3612 936	132	1624	0.683	0 022	850	2401.022	1170	0.140	159	0.028
60	3631.560	133	1606	0 767	0.025	1130	4532 051	920	0.180	159	0 011
61	3641 564	134	1619	0 724	0 021	980	4526.275	480	0.190	159	0 018
62	3631 305	135	1644	0.320	0 023	460	5417 624	890	0 220	159	0.058
63	3451.234	136	1665	0.269	0.020	410	5455 388	420	0 210	160	0.058
64	3661 504	137	1638	0.429	0.020	570	4719.848	230	0 190	158	0 051
65	3651.909	138	1653	0.383	0 017	520	3713 931	1010	0 180	159	0 055
66	2800 887	163	1618	0 600	0.018	780	6188.630	670	0 200	159	0 044
67	3320 896	165	1697	0.307	0.015	450	7223 286	0	0.230	158	0.032
68	3220 873	167	1628	0.487	0.014	630	7197.118	910	0.190	159	0.057
69	3641 355	168	1606	0.496	0.014	690	5217.162	230	0.140	159	0 046
70	3631.297	169	1618	0.616	0.014	710	5442.672	1050	0.160	159	0.037
71	3500.876	173	1622	0 483	0 014	620	7714 253	20	0.200	160	0.043
72	3200.814	174	1642	0.423	0.015	550	7600.355	640	0.210	161	0.048
73	2640.356	177	1621	0.349	0 015	480	13888.889	0	0.180	168	0.054
74	3320 779	178	1581	0.499	0.007	650	7879.155	0	0.160	161	0.058

Actual and Predicted end point parameters of Plant 3

Heat No.	Carbon (%)			Temperature (°C)		[O] (ppm)		Phosphorus (%)		Manganese (%)	
	Act.	Pred. (Model 5.3 reg)	Pred. (Model 5.4 reg method 2)	Act.	Pred.	Act.	Pred.	Act.	Pred.	Act.	Pred.
1	0.056	0.050	0.050	1718	1705	559	750	0.014	0.012	0.190	0.179
2	0.039	0.049	0.048	1710	1693	1169	719	0.012	0.010	0.170	0.176
3	0.043	0.047	0.045	1718	1710	814	736	0.013	0.011	0.160	0.167
4	0.055	0.047	0.046	1708	1707	697	753	0.012	0.011	0.180	0.178
5	0.054	0.045	0.046	1712	1707	651	738	0.011	0.010	0.160	0.160
6	0.055	0.048	0.046	1708	1694	701	709	0.010	0.010	0.170	0.166
7	0.066	0.054	0.054	1702	1687	669	677	0.012	0.011	0.160	0.155
8	0.053	0.052	0.052	1692	1696	635	589	0.009	0.009	0.150	0.156
9	0.062	0.055	0.053	1676	1696	519	544	0.009	0.009	0.150	0.132
10	0.058	0.052	0.050	1700	1697	560	663	0.014	0.012	0.180	0.158
11	0.054	0.056	0.055	1668	1676	524	522	0.008	0 007	0.120	0.132
12	0.050	0.055	0.052	1702	1694	680	620	0.009	0.008	0.120	0.129
13	0.067	0.052	0.050	1692	1710	495	553	0.010	0.009	0.140	0.143
14	0.069	0.043	0.064	1706	1729	579	702	0.012	0.008	0.150	0.107
15	0.062	0.053	0.055	1689	1686	516	571	0.012	0.012	0.190	0.183
16	0.050	0.048	0.045	1703	1692	755	657	0.010	0.009	0.120	0.133
17	0.043	0.061	0.059	1690	1686	911	674	0.009	0.008	0.130	0.142
18	0.057	0.044	0.043	1676	1679	498	632	0.009	0.008	0.130	0.121
19	0.047	0.052	0.050	1672	1683	661	549	0.009	0.008	0.150	0.166
20	0.069	0.053	0.052	1690	1689	446	584	0.008	0.007	0.120	0.129
21	0.065	0.053	0.051	1692	1686	464	593	0.008	0.008	0.140	0.134
22	0.066	0.052	0.052	1681	1684	523	536	0.010	0.010	0.190	0.182
23	0.049	0.054	0.052	1684	1681	629	613	0.012	0.010	0.140	0.144
24	0.052	0.047	0.047	1697	1696	679	679	0.012	0.010	0.130	0.133
25	0.042	0.052	0.051	1671	1683	733	542	0.012	0.009	0.130	0.141
26	0.063	0.053	0.053	1673	1676	487	522	0.011	0.010	0.170	0.164
27	0.046	0.050	0.051	1686	1691	715	519	0.012	0.010	0.170	0.164
28	0.046	0.053	0.052	1668	1685	628	429	0.010	0.008	0.140	0.138
29	0.061	0.066	0.073	1702	1700	560	729	0.014	0.008	0.130	0.134
30	0.062	0.052	0.052	1667	1679	457	484	0.009	0.007	0.150	0.155
31	0.055	0.050	0.050	1698	1682	575	670	0.011	0.009	0.160	0.157
32	0.056	0.045	0.044	1740	1725	655	810	0.012	0.011	0.170	0.167
33	0.050	0.053	0.051	1684	1682	656	633	0.009	0.008	0.150	0.143
34	0.041	0.047	0.046	1722	1711	921	764	0.010	0.009	0 130	0.130
35	0.068	0.048	0.048	1680	1690	457	584	0.008	0.008	0.140	0.145
36	0.060	0.049	0.048	1684	1681	566	599	0.009	0.008	0.140	0 143
37	0.043	0.049	0.047	1685	1675	718	649	0.006	0.005	0.090	0.096
38	0.039	0.043	0.043	1757	1741	1108	942	0.010	0.010	0.140	0.136
39	0.059	0.054	0.053	1675	1676	559	585	0.007	0.007	0.120	0.123
40	0.048	0.052	0.050	1688	1696	677	660	0.008	0.007	0.130	0.125
41	0.069	0.052	0.052	1659	1673	482	513	0.007	0.005	0.120	0.120
42	0.057	0.051	0.049	1681	1684	554	655	0.006	0.005	0.100	0.114
43	0.058	0.051	0.049	1675	1684	574	572	0.006	0.006	0.110	0.121
44	0.066	0.056	0.054	1675	1679	509	610	0.010	0.008	0.120	0.119
45	0.064	0.049	0.048	1678	1697	556	582	0.008	0.007	0.130	0.126

Bibliography

[1] Sateesh Kumar: End point carbon and Temperature prediction using Sublance measurements in Oxygen Steel Making Converters, M. Tech Thesis (1998), IIT, Kanpur.

[2] H.G.Lee and Y.K.Rao. Met Trans. B, Vol.13B, Sep 1982, p 403.

[3] P.A.Distin, G.D.Hallett and F.D.Richardson. J.Iron Steel Inst.(London), 1968, Vol.206, p.821

[4] K-C Chou, U.B Pal, R.G Reddy. ISIJ International, 1993, Vol.33, No. 8, p.862.

[5] D.A.Bensel, H.Henein and P H.Dauby Iron Steelmaking Trans. ISS/AIME, 1987, p.45.

[6] A Rist and J. Chipman: Rev. Met., Vol. 53, 1956, p.796.

[7] N.Bessho, S.Takeuchi, K.Nakanishi, T.Emi, S.Yamada, F.Sudo: Decarburization models and their application to the dynamic control of the basic oxygen processes., Mc. Master Symp. No. 9 on BOF end point determination, E.d. W. K. Lee May 81, Hamelton Canada, p 11-17.

[8] S.M.Byun, B.D You, M.S.Song, Y.K.Shin and S.D.Shin: The development of a ublance process model for BOF at POSCO, Personal communication.

[9] J Szegdi, .J Manak, P Tardy, J Mezei: Control of BOF steelmaking by a reaction-model on the reaction-kinetic laws of carbon oxidation., Personal communication.

[10] J Fukumi, Chihiro and T Hatanaka: Development of refining control in BOF based on exhaust gas information , Personal communication.

[11] K Iwamura, M Furusawa, M Miyamoto, M Hoteiya and H Tachibana: New end point Control System with Auto-parameter-tuning in BOF., ISS/AMIE, Steel making Conference Proceedings, 1995, p. 715.

[12] Dixit, Droplet decarburization model, B Tech Project (1998), IIT, Kanpur.

[13] Brahma Deo, Rob Boom 'Fundementals of Steel Making', Prentice Hall, 1993.

[14] K Bakajiva et al, Iron & Steel Institute, 153 (1946), p 115.

[15] Brahma Deo et al, Transactions of Indian Institute of Metals, Vol 41, No 5, october 1988, p 475

[16] Turkdogan E T, Trans ISI Japan 24, 1984, p 591-611.

[17] Wagner C, 'Metal, Trans 6B',1993. p 409-450.

[18] A. B. Snoeijer, R. Boer, T J.M. Böhmer, M Harting, R. Mostert, Temperature Control at BOS2 of Hoogovens Staal, Second Europian Oxygen Steelmaking Congress, Taranto, Italy, Oct 13-15, p 227-236

[19] K. J. Robertson, S R. Balajee, J M. Shearer and J. E. Bradly, 'The sublance dynamic control operation and its effect on the performance', I&SM, 1989, p 36-42.

[20] D.Bergman, P.Hahlin, 'Experiences of waste gas analysis based control system for LD-LBE process at SSAB Tunnplat AB. Second Europian Oxygen Steelmaking Congress, Taranto, Italy, Oct 13-15, p 303-312.

[21] David E. Goldberg,'Genetic Algorithms in Search, Optimization and Machine Learning', Addison-Wesley, 1989.

[22] Krishna Kumar, 'Micro-Genetic Algorithms for Stationary and Non-stationary Function Optimization', Intelligent Control and Adaptive Systems, vol.1196, SPIE - Proceedings, Philadephia, Pensylvania, 7-8 Novembar 1989.

[23] http://www.staff.uiuc.edu/~carroll.

A 130846

Date Slip

This book is to be returned on the date last stamped.